ABSTRACT

SZUCH, RYAN PAUL. Application of Ground-penetrating Radar to Map Stratigraphy of a Drained Carolina Bay and Aid Its Wetland Restoration. (Under the direction of Jeffrey G. White and Michael J. Vepraskas.)

Carolina Bays (bays) are a wetland type found along the Atlantic Coastal Plain that occur as oval-shaped depressions. Knowledge of bay stratigraphy might improve inconclusive theories on bay formation and aid attempts at wetland restoration of drained bays. Ground-penetrating radar (GPR) provides high-resolution and continuous profiles of the subsurface but has seldom been used for large-scale investigations or in Carolina Bays.

A GPR survey was performed at Juniper Bay, a 300 ha drained bay in Robeson County, North Carolina. The survey included 23.2 km of GPR transects and soil borings at 174 locations. The broad objective of the survey was to map Juniper Bay's stratigraphy, particularly to determine the depth, extent, and continuity of clayey horizons likely to act as aquitards.

To prevent ambiguity in identifying the ground surface on GPR transects, a “lift-test” was developed that delineated the surface. Spatial variation in wave velocity was addressed using a "reflector-interface matching" technique to determine velocity at multiple locations and at various depths within the bay. A linear calibration equation relating travel time of GPR waves to depth of soil interface was developed. The average deviation between observed and predicted depth to clayey horizons was 0.25 m (16% error). Error was mainly attributed to the survey's large scale, subsurface complexity, presence of organic soils, and depth of the horizons. The lift-test improved accuracy by 10%, and the use of multiple calibration points limited extrapolation of the calibration equation. These calibration

methods should prove valuable for future study of GPR accuracy on large-scale, complex sites.

Information obtained during the GPR survey and associated coring was used to describe Juniper Bay's stratigraphy and develop theories on its formation. The bay's stratigraphy consists of alternating layers of sands and clays. Clayey layers appear continuous over much of the bay except where truncated by features that seem to be paleochannels. Historic geomorphic events at Juniper Bay have varied spatially and temporally but have included repeated lacustrine deposition, fluvial deposition, and fluvial incision. The original bay probably expanded and incorporated a smaller bay and fluvial feature. Future GPR work and integration of geologic and hydrologic studies may aid our assessment of Juniper Bay's stratigraphy and evolution.

Many bays have been drained for conversion to agriculture. Clayey subsurface strata commonly occurs in bays and act as aquitards, restricting vertical water flow. Modification to drainage systems could lead to restoration of wetland conditions. The North Carolina Department of Transportation (NCDOT) intends to restore Juniper Bay for wetland mitigation credit. Ground-penetrating radar interpretation found that clayey aquitards underlay most of the bay at an average depth of 1.64 m. An anomalous GPR reflection in the southeast corner of the bay was interpreted as a fluvial deposit that does not contain aquitards until 3 to 5 m. NCDOT should consider alternative restoration plans for this area. By comparing the depths of aquitards and drainage ditches, several areas were identified as likely locations of ditch-induced aquitard discontinuity. NCDOT should fill or line suspect ditches to prevent potential water losses. Hypothetical proposals by professional firms indicated that GPR could provide large volumes of data with cost and time efficiency.

Ground-penetrating radar surveys are suggested as a useful tool for determining suitability of potential wetland restoration sites.

APPLICATION OF GROUND-PENETRATING RADAR TO MAP STRATIGRAPHY OF A DRAINED CAROLINA BAY AND AID ITS WETLAND RESTORATION

by
RYAN PAUL SZUCH

A thesis submitted to the Graduate Faculty of
North Carolina State University
in partial fulfillment of the
requirements for the Degree of
Master of Science

SOIL SCIENCE

Raleigh

2004

APPROVED BY:

_____	_____
Co-Chair of Advisory Committee	Co-Chair of Advisory Committee

BIOGRAPHY

Ryan P. Szuch

Ryan was born in 1978 in Pittsburgh, Pennsylvania and was raised in a rural community 30 miles to the northeast. As a child and young man, he attended Kiski Area School District and was active in the Boy Scouts of America, earning the rank of Eagle. Ryan attended Susquehanna University, located in Selinsgrove, PA, from 1996 to 2000. During his senior year, he completed a thesis entitled "Hydrogeochemical Characterization of the Montandon Marsh, Upper Susquehanna River Valley, Pennsylvania" under the direction of Dr. Benjamin Hayes. Ryan graduated in May 2000 with a self-designed B.S. in Ecosystems Analysis. From May to December 2000, Ryan interned and then worked as head-technician of the Nutrient Laboratory at the Smithsonian Environmental Research Center. During this time, he studied denitrification in wetland soils and hydrogeomorphic wetland assessments. Ryan earned a Fulbright grant to Australia and spent 2001 at the University of New England in Armidale, NSW. While there, Ryan earned a Graduate Diploma in Natural Resources and completed a thesis entitled "Nitrogen Dynamics in a Sand-Slugged Stream of the New England Tablelands, New South Wales" under the direction of Dr. Andrew Boulton. Ryan began his studies at North Carolina State University in the Soil Science Department in January 2002. He expects to earn his M.S. in Soil Science by early 2004. In January 2004, Ryan will begin work as an environmental consultant with Blasland, Bouck, and Lee, Inc. in their Cranbury, NJ office.

ACKNOWLEDGMENTS

I would like to thank my co-chairs, Drs. Jeff White and Mike Vepraskas, who provided continuous guidance and constructive criticism of my work over the past two years. Their time and energy spent on reviewing my thesis chapters was particularly appreciated. Dr. White was also very helpful in aiding me with statistical analysis and mapping with geographic information systems.

The remainder of my advisory committee, Drs. Bill Zanner and Rod Huffman, also made valuable reviews of my thesis and contributed ideas to my research. The entire Juniper Bay Research Group was very helpful in providing periodic reviews of my work during my presentations at our meetings. I thank all members for their support and advice.

Jim Doolittle did an excellent job of leading the GPR survey work, and Wes Tuttle provided valuable assistance. Jim was also helpful in teaching me how to interpret GPR profiles. I thank the NRCS for allowing Jim to work with us on the project.

I would like to thank and acknowledge all individuals who assisted me with my work. During fieldwork at Juniper Bay, I was assisted by Tripp Cox, Alex Baldwin, Pete Caldwell, and Eric Anderson. Much of my laboratory work was performed by Nick Howell and Jason Goodman. Assistance with presentation preparation was provided by Roberta Miller-Haraway. Rob Austin and Eric Anderson often provided instruction and advice on use of geographic information systems. Finally, I would like to thank Alex Adams for his fantastic support of all my field and lab activities.

I appreciate the fine instruction and education that I have received from the faculty of the Soil Science Department and other NC State faculty. Much of what I have learned has aided in my understanding of my research and its importance.

Finally, I would like to thank all the new friends I made in Raleigh for their support and kindness. I thank my parents and brother for their continuous love and support, and I thank Erin for all her love, support, and countless hours spent sharing our frustrations and discussing our work.

I acknowledge the North Carolina Department of Transportation for funding my assistantship and research costs.

TABLE OF CONTENTS

CHAPTER 1 (CONT.)

LIST OF TABLES

CHAPTER 1

CHAPTER 2

CHAPTER 3

CHAPTER 4

LIST OF FIGURES

CHAPTER 1

CHAPTER 2

CHAPTER 3

CHAPTER 3 (CONT.)

CHAPTER 4

CHAPTER 4 (CONT.)

CHAPTER 1
Literature Review: Application of Ground-Penetrating Radar to Investigations of Sediment and Soil Systems

Section 1 - INTRODUCTION

Ground-penetrating radar (GPR) presents numerous advantages over conventional soil and sediment exploration methods such as pits, cores, or trenches. When used properly in appropriate conditions, GPR provides high-resolution and continuous profiles of the subsurface. This yields a much greater amount of information than discrete sampling by coring or digging (Mokma et al., 1990, Poole et al., 1997, Conyers and Goodman, 1997). Even when excavation is necessary in some manner, GPR can aid in the selection of coring sites, maximizing effort in areas of interest or uncertainty (Mellett, 1995, Augustinus and Nichol, 1999). Due to its non-destructive nature, GPR can be valuable in sensitive research settings, such as archaeological sites or protected ecological areas. In general, GPR is an efficient tool that gives researchers the ability to "see" underground.

Use of GPR as a geophysical tool began in the military for identification of buried objects (Asmussen et al., 1986, Conyers and Goodman, 1997) and in environmental applications for considering depths of ice and examining rock formations (Daniels, 1996). Since the late 1970s and 1980s, applications of GPR have expanded to many fields. Brief reviews of these applications can be found for: military and engineering (Mellett, 1995, Daniels, 1996); geology and sedimentology (Daniels, 1996, van Overmeeren, 1998, Cagnolli and Russell, 2000); archaeology (Daniels, 1996, Conyers and Goodman, 1997, Conyers and Cameron, 1998); and soil science (Hubbard et al., 1990, Doolittle and Collins, 1995, and Poole et al., 1997). Recent advances in GPR application include the determination of soil

water content (van Overmeeren et al., 1997, Huisman et al., 2001) and estimation of root biomass (Butnor et al., 2003).

This chapter provides a review of GPR application on soils and sediments. An overview of GPR methodology is provided (Section 2). Then, specific applications of GPR in sediments and soils are reviewed (Section 3). The limitations of GPR in these environments are examined (Section 4). Finally, the financial and efficiency benefits of GPR are considered (Section 5).

Section 2 - GPR METHODOLOGY

General Methodology

Ground-penetrating radar involves the transmission of high-frequency electromagnetic energy into the ground and measurement of the time for this energy to travel to a subsurface discontinuity and reflect back to the surface. A pulse of energy is emitted by an antenna connected to a transceiver, which then receives the reflected energy as well. The travel time from the transceiver to a subsurface discontinuity and back is known as the two-way travel time, usually on the order of nanoseconds (ns). The cycle of emission and reception is repeated over very short time intervals while the antenna and transceiver are moved slowly along the ground surface. In this manner, a virtually continuous record of the received energy is obtained (Conyers and Goodman, 1997, Dagallier et al., 2000). Ground-penetrating radar data is typically presented as a continuous profile or image of this reflected data record. The x-axis of the profile represents distance traveled along the ground surface,

and the y-axis represents the two-way travel time. The intensity of the profile is dependent on the amplitude of reflected energy received at any given x,y coordinate (Fig. 1).

During the typical field application of GPR, the antenna and associated electronics are housed in a small containment unit. The containment unit is connected, at a short distance, to a control unit. This control unit includes the transceiver, a data recorder, power source, and often a display of the GPR profiles. The containment unit would be moved along the ground surface (usually around 2.0 km/hr) by manual towing or by towing with a small vehicle. Most GPR systems currently in use record data digitally. This has much improved the ability to perform post-processing of the data to enhance profile clarity and quality (Conyers and Goodman, 1997).

GPR Propagation and Reflection

As stated in the previous section, the intensity of a GPR profile is controlled by the amplitude of reflected energy received at that point. Even when traveling through relatively homogeneous material, a small amount of radar energy is reflected back towards the surface. Similar in concept to "background noise," this reflected energy is know as clutter (Daniels, 1996). Discontinuities in the subsurface will cause energy to be reflected in excess of the clutter. These high amplitude reflections will be apparent on the resulting profiles (Conyers and Goodman, 1997). Figure 1 shows a prominent GPR reflection typical of those due to subsurface discontinuities.

Discontinuities that produce reflections are caused by changes in the dielectric properties of the medium through which the energy is propagating. Such discontinuities can occur at the interface between stratigraphic units or soil horizons and also at contact with

buried objects, such as mines or pipes. Three characteristics of the medium contribute to its dielectric properties: dielectric permittivity, magnetic permeability, and electrical conductivity (Conyers and Goodman, 1997, Van Dam and Schlager, 2000). Of these, the dielectric permittivity is most important in determining the amplitude of a reflection at a discontinuity or interface. As the difference between the dielectric permittivities across an interface increases, the amplitude of the reflection increases (Conyers and Goodman, 1997, Dagallier et al., 2000, Van Dam and Schlager, 2000). Dielectric permittivity is usually expressed as relative dielectric permittivity (RDP), and its relationship with radar velocity (Conyers and Goodman, 1997) is:

$$(RDP)^{1/2} = C / V \qquad [1]$$

where: RDP = relative dielectric permittivity of medium

C = speed of light (0.2998 m ns^{-1})

V = velocity of radar energy through medium (m ns^{-1})

Typical RDP values for various types of rock, sediment, and soil are given in Table 1.

The RDPs of sediment and soil vary due to their composition, moisture content, bulk density, porosity, physical structure, and temperature (Hubbard et al., 1990, Conyers and Goodman, 1997, Dagallier et al., 2000). Due to the large difference between the RDP of air and water, moisture content is often considered the most important of these factors (Hubbard et al., 1990, Daniels, 1996, Van Dam and Schlager, 2000). In comparing results of GPR profiles with time-domain reflectometry (TDR) and sedimentological analyses, Van Dam and Schlager (2000) found that presence of organic matter, which can increase moisture content of soils, could impact RDP and cause GPR reflections. They also found that when moisture

content was generally high throughout a soil profile, higher porosity caused both moisture content and relative permittivity to increase.

The magnetic permeability and electrical conductivity largely control attenuation of the radar energy (Doolittle and Collins, 1995, Conyers and Goodman, 1997, Dagallier et al., 2000, Van Dam and Schlager, 2000). Attenuation of energy hinders both the transmission of radar waves down through the profile as well as reflection of waves back to the transceiver and thus limits the depth of penetration of the GPR survey (see next subsection). Magnetic permeability of sediment and soils is usually near unity and does not impact radar wave behavior. However, magnetite minerals and certain iron oxides can increase magnetic permeability, which would increase attenuation (Conyers and Goodman, 19997, Van Dam and Schlager, 2000). Electrical conductivity is low for most dry sediments and soils (Van Dam and Schlager, 2000). During saturation, materials with high clay content or soluble salts will have increased electrical conductivity, increasing attenuation. High salinity due to groundwater or seawater will cause heightened conductivity and attenuation as well (Conyers and Goodman, 1997). Amount of attenuation can depend on type of salts and type of clay (Doolittle and Collins, 1995). Ions absorbed on clay particles can exchange with ions in solution to increase conductivity. Because 2:1 clays have a higher cation exchange capacity, they are more likely to influence conductivity in this manner (Doolittle and Collins, 1995). Some specific impacts of these dielectric properties on GPR use are discussed below.

Horizontal and Vertical Resolution

Both the horizontal and vertical resolution of GPR surveys vary based on the frequency of the antenna and the dielectric properties of the medium. Ground-penetrating

radar pulses into the ground do not travel in a tight beam focused directly below the antenna. Instead, they travel through the ground as an elliptical cone whose apex is at the base of the antenna (Conyers and Goodman, 1997). This cone is commonly referred to as the "footprint" of the GPR, and it can be estimated by Eq. 2 as expressed in Fig. 2.

$$A = (\lambda / 4) + (D / [K + 1]^{1/2}) \qquad [2]$$

where: A = approximate long dimension radius of footprint

λ = wavelength of the center frequency of radar energy

D = depth from ground surface to reflection surface

K = average RDP of material from ground surface to depth D

The calculation in Eq. 2 is merely an estimate of the footprint because it is based on the average RDP from the surface to depth D. In reality, the shape of the cone and size of the footprint vary as the radar wave propagates through each soil horizon with a distinct RDP. If the RDP tends to increase with depth, the radar waves will remain focused. Correspondingly, if the RDP decreases with depth, the footprint will rapidly widen and disperse the waves (Conyers and Goodman, 1997). The size of the footprint can be considered the horizontal resolution of the GPR. While this may not be of concern in some sediment and soil investigations (where the subsurface discontinuity of interest has large lateral extent of nearly uniform depth) it may cause significant errors in interpretation in some cases. If the discontinuity changes markedly in slope or depth within the range of the footprint, these changes may be missed by the GPR.

Vertical resolution of GPR is another complex situation that is impacted strongly by both environmental characteristics and the choice of antenna frequency. Antenna frequencies used for GPR vary from about 10-1000 MHz. In choosing a frequency, GPR users

experience a trade-off between vertical resolution and depth of penetration (Conyers and Goodman, 1997). Depth of penetration is the maximum depth from which radar reflections are received by the transceiver. Lower frequency antennas achieve greater depth of penetration but have poorer resolution. Smith and Jol (1995) tested different frequency GPR antennas in quartz-rich gravel sediments to determine their variation in depth of penetration. They found a strong, inverse, linear relationship between depth of penetration and frequency. In practical use on sediments and soils, the range of antennas used seems to be 80-500 MHz. In application, these frequencies will yield depth of penetration ranging from 1 m to tens of meters and infrequently over 100 m. Representing opposite ends of the spectrum, use of a 100 MHz antenna in a limestone rock sequence yielded a depth of penetration of 40 m (Dagallier et al., 2000), while use of a 450 MHz antenna in sandy soil yielded only 2 m (Tomer et al., 1996). At the current stage of GPR technology, it is not possible to change antenna frequency during a GPR survey. Each antenna unit can emit only one central frequency. Thus, the choice of antennas becomes an important decision that must balance desires for depth of penetration and resolution.

Antenna frequency impacts vertical resolution due to the inverse relationship between frequency and wavelength of radar waves. If two reflections are not separated by at least one wavelength, constructive and destructive interference will cause the net wave returned to the transceiver to be unrecognizable (Conyers and Goodman, 1997, Young and Sun, 1999, Nobes et al., 2001). The resolution of GPR has been calculated as one fourth of the wavelength (Langsholt et al., 1998, Dagallier et al., 2000, Bristow et al., 2000). Using a 100 MHz antenna, Bristow et al. (2000) calculated resolution to be 0.43 m in dry sands and 0.30 m in saturated sands. This resolution improved when a 450 MHz antenna was used, but the

higher frequency caused an appreciable decrease in depth of penetration. Tomer et al. (1996) also used a 450 MHz antenna and successfully mapped lamellae that were 3 cm or thinner. Ground-penetrating radar surveys with 200 MHz antennas have calculated resolution to be between 0.1 and 0.2 m when used on glaciofluvial sand/gravel (Langsholt et al., 1998) and floodplain deposits (Nobes et al., 2001). Doolittle et al. (2000) found the resolution of a 200 MHz antenna to be inadequate for mapping depth to a soil horizon. It was felt that this choice of antenna contributed to the poor correlation between GPR interpreted and observed depth to the horizon.

In the study mentioned above, Nobes et al. (2001) achieved the best resolution in saturated sediments where the velocity was slowed. This finding highlights the fact that environmental factors can have drastic impacts on resolution and especially depth of penetration. For example, a 100 MHz antenna achieved a range of depth of penetration from 1.5 to 16.2 m (Mills and Speece, 1997). Variation within this range was strongly influenced by the age of the deposits. Older deposits and residuum had shallower depth of penetration, which was attributed to higher clay content. Use of an 80 MHz antenna yielded varying depths of penetration when used in different environments: clay-rich soils - 1.4 m, unsaturated sand-gravel deposits - 4 m, fill material at a dam - 4 m, and partially consolidated carbonate sand - 4 m (Dominic et al., 1995). As in these two examples, high clay content seems the dominant environmental factor that can increase signal attenuation and decrease depth of penetration (Hubbard et al., 1990, Dominic et al., 1995, Doolittle and Collins, 1995, Cagnolli and Russell, 2000, Van Dam and Schlager, 2000, Nobes et al., 2001). The reason for this is that the presence of clay increases the electrical conductivity of the medium. Wet soils tend to attenuate GPR energy faster than dry soils for this same reason (Doolittle and

Collins, 1995). Any factor that increases electrical conductivity or magnetic permeability will increase attenuation and decrease depth of penetration.

Due to the highly heterogeneous and variable natural of soil systems, dielectric properties often change dramatically along a given GPR survey. Thus, a single antenna (frequency) may not be suitable on adjacent soils (Doolittle and Collins, 1995). Unfortunately, neither GPR methodology or technology has yet to devise a suitable solution to this dilemma.

Calibration / Depth Scaling

The vertical axis on a GPR profile is a measurement of the two-way travel time, being the elapsed time for a wave to travel down to a subsurface discontinuity and back to the surface. In most GPR applications on sediment and soil, the depth to these subsurface features is desired. Two-way travel time can be related to depth through the velocity of wave propagation:

$$D = v * (TWT / 2) \quad [3]$$

where: D = depth (m)

v = velocity (m/ns)

TWT = two-way travel time (ns)

A GPR profile can be "calibrated" or "depth scaled" by ascertaining the wave propagation velocity at one or more locations along the profile and applying it to the GPR interpretation according to Eq. 3. The velocity can be determined by numerous techniques that fall into three categories (Conyers and Goodman, 1997): reflected-wave methods, direct-wave methods, and calculated methods.

Standard Values for Calibration

Environmental factors can so greatly influence dielectric properties, and thus wave propagation, that researchers usually perform calibration at their study site at the time of their GPR survey. Relying on standard values of RDP for a given medium (Table 1) is increasingly uncommon for sediment/soil investigations, but it does still occur in geological (Dagallier et al., 2000) or engineering applications (Mellett, 1995). Dielectric properties are highly spatially and temporally variable; therefore, use of an RDP value from another place or time can cause inaccuracy. Any of the calibration methods discussed below are usually more appropriate than using standard values.

Reflected-Wave Methods

The most straightforward method for measuring wave velocity is to identify a reflection on a GPR profile known to result from an object or interface that occurs at a known depth. The velocity is calculated from the depth of the known object or interface and the TWT of the corresponding reflection.

One approach is to bury an object that is certain to yield an obvious GPR reflection (Mokma et al., 1990, Vogt et al., 1996, Conyers and Goodman, 1997, Conyers and Cameron, 1998, Doolittle et al., 2000). Metal pipes and shovels are often used in this capacity, as the dielectric properties of metal are quite different than those of sediments or soils (Conyers and Goodman, 1997).

Rather than bury an object, calibration by reflected-wave method may utilize a "known and recognizable feature or soil horizon." (Doolittle et al., 2000). The term "reflector-interface matching" will be used in this text to describe such an approach. Coring

or digging is performed to find the depth of an interface between layers likely to have contrasting RDP. The interface is matched to a prominent reflection on the GPR profile. Reflector-interface matching should only be used when there is confidence that the reflection is due to the known interface and not some secondary interface. Various types of interfaces have been used for this technique, including the water table (Birkhead et al., 1996, Bristow et al., 2000), bedrock (Collins et al., 1989, Birkhead et al., 1996), and soil horizons or sediment layers (Collins et al., 1986, Collins and Doolittle, 1987, Dominic et al., 1995, Tomer et al., 1996, Langsholt et al., 1998).

In certain settings, an object may already exist beneath the ground surface prior to the GPR survey. For example, the wall of an ancient town may be a known depth below the ground surface, or a water pipe may have been buried at a known depth. While this would be fortuitous in most sediment/soil investigations, it is often the case during archaeological (Conyers and Goodman, 1997) or engineering (Mellett, 1995) applications of GPR.

Reflected-wave methods are generally accepted as the most accurate way to calibrate GPR profiles (Mellett, 1995, Conyers and Goodman 1997, Doolittle et al., 2000). For this reason, they are sometimes used to confirm the accuracy of other calibration methods (Tomer et al., 1996, Langsholt et al., 1998, Bristow et al., 2000).

Direct-Wave Methods

In direct-wave methods, the transmitting and receiving parts of the GPR system are spatially separated. If this is not possible, two separate GPR units can be utilized (Conyers and Goodman, 1997). The propagation velocity is determined by gradually separating the transmitter and receiver by known distances and observing the resultant changes in the GPR

profile. Such a method can be used to measure the wave velocity through several different mediums. The velocity through air can be determined by the direct air-wave (Fig. 3). The velocity through the very shallow subsurface can be determined by the direct ground-wave. If there is a known interface causing a reflection (as in reflector-interface matching), then the velocity of the material between the ground surface and that interface can be determined. These velocities are calculated by knowing the distance the transmitter and receiver are separated, deducing the travel paths of the GPR waves (as in Fig. 3), and extracting the (one-way) travel time from the GPR profile (Conyers and Goodman, 1997, Van Dam and Schlager, 2000).

The two most common techniques for direct-wave calibration are the common-midpoint method (CMP) and wide-angle reflection and refraction mode (WARR). The principles of both methods are similar, but they differ in how the transmitter and receiver are separated. In CMP, both units are gradually moved incremental and equal distances away from a common midpoint. In WARR, the transmitter is stationary, and the receiver is gradually and incrementally moved away (Conyers and Goodman, 1997). More detail of the setup and calculations of these methods can be found elsewhere: CMP (Boll et al., 1996, Conyers and Goodman, 1997) and WARR (Imai et al., 1987).

Calibration by direct-wave methods is generally considered not as accurate as reflected-wave methods (Conyers and Goodman, 1997); however, several studies have tested direct-wave methods against reflected-wave methods with good success. In glaciomarine and glaciofluvial sediments, calibration by CMP was confirmed by reflector-interface matching (Langsholt et al. 1998). Five attempts at CMP yielded a range in velocity of 0.12 to 0.13 m ns^{-1}, and the reflector-interface matching technique gave a velocity of 0.13 m ns^{-1}.

Bristow et al. (2000) used CMP to estimate velocity between the ground surface and the water table, and subsequent reflector-interface matching again confirmed the CMP results.

In systems with complex stratigraphy, success with CMP calibration can be limited. In a complex wetland system, Lapen et al. (1996) found that CMP was not able to resolve wave velocities for each layer, sometimes incorporating several layers together. An alternative calculated method (described below) was more successful. However, as applicable, CMP and calculated velocities were in good agreement.

Several studies have found that CMP will underestimate wave velocity, which could potentially cause inaccurate GPR interpretation. In their study of floodplain deposits in Australia, Nobes et al. (2001) found that the CMP velocity was often lower than that determined by reflector-interface matching. Theimer et al. (1994) found CMP velocities to be up to 20% too low when using GPR in a peatland. In unconsolidated coastal plain sediments, the velocity assumed by CMP (0.15 m ns^{-1}) was only half the actual velocity (0.3 m ns^{-1}) (Wyatt and Temples, 1996). The conflicting reports of success and inaccuracies with CMP indicate that validation of this and other direct-wave methods should continue.

Calculated Methods

Both reflected-wave and direct-wave methods have the disadvantage that they determine the average velocity between the ground surface and the known interface. Nobes et al. (2001) emphasize that CMP gives a generalized measurement of subsurface velocity, as the velocity is actually changing from bed to bed. The same is true of reflector-interface matching and the use of buried objects. Frustration with this dilemma has induced the use of equations, usually based on volumetric water content, to calculate the dielectric constant and

in turn the velocity of propagation. With appropriate moisture content data, this calculation can be made for each distinct layer or horizon. Success with such calculated methods has been mixed.

Boll et al. (1996) tested two different calibration methods for accuracy in predicting the depth to coarse soil horizons. When moisture content measurements were placed in an equation to determine wave velocity (equation from Topp et al., 1980), error in predicting depth was as great as ± 0.4 m. This large error was attributed to lateral variation in moisture content. With CMP, accuracy was within 7%. The CMP method was greatly preferred as it was more accurate, quicker, and less destructive. Tomer et al. (1996) used GPR to find the depth of narrow lamellae in a sandy soil. Calibration was performed via an equation based on water content (equation from Topp et al., 1980), and results of this calibration method were supported via reflector-interface matching. In a system with highly complex stratigraphy, Lapen et al. (1996) attempted to assign separate wave velocities and depth scales to each layer. CMP was not able to assign velocities for each layer, but calculated methods based on volumetric moisture content were successful. Lapen et al. (1996) used separate equations for mineral soils (equation from Topp et al., 1980) and organic soils (previously unpublished equation).

Overall, use of calculated methods seems promising. As shown by Lapen et al. (1996), such methods offer the advantage of determining velocities for discrete layers. However, the collection of detailed volumetric water content data for each soil/sediment layer is a labor intensive process, involving both field and laboratory work. Such an investment of time and labor acts to negate some of the overwhelming advantages of GPR, time and labor efficiency.

Variation in Wave Velocity

Due to the numerous factors that can impact the dielectric properties of a medium, the true wave propagation velocity is typically changing throughout a given soil/sediment profile and laterally across a study site.

Vertical Variation. Dielectric properties can vary drastically between and even within horizons or layers. For example, moisture content, which is known to strongly influence dielectric properties, is seldom uniform in a field soil (Boll et al., 1996). As discussed in the previous section, calculated calibration methods can facilitate the determination of wave velocity for distinct layers, but this achievement is at the expense of field efficiency.

As a compromise between calculating velocities for each layer and using an average velocity for all layers, some researchers have identified one interface that will have the most dramatic impact on wave velocity. Separate velocities are determined for each side of the interface. This yields a two-velocity model that can be used for calibration of the GPR profile.

The water table is a common interface chosen for segregating layers with generally different velocities. Saturated sediment or soil has a higher RDP, decreasing velocity. Birkhead et al. (1996) used two different dielectric constants during calibration. An unsaturated RDP of 3.0 was used from the ground surface to the water table, and a saturated RDP of 20.0 was used from the water table to the bedrock. These RDPs were determined by reflector-interface matching, using the water table and bedrock surface. These RDP values

corresponded well with accepted values of RDP for dry sand and saturated sand (Table 1). Bristow et al. (2000) performed calibration by CMP and confirmed by reflector-interface matching against the water table. Two velocities were determined, one for dry sand (0.17 m ns^{-1}) and another for saturated sand (0.12 m ns^{-1}). In both studies, the use of a two-velocity model was thought to improve results.

When sediment or soil is saturated in cold climates, a common division is that between frozen and unfrozen. Kettles and Robinson (1997) used CMP to calibrate GPR in peat landforms of Canada and found wave velocity in frozen soil to be two to three times that in unfrozen soil. Thus, two separate depth scales were used for frozen and unfrozen soil. On some occasions, different depth scales will be used based on soil horizonation. Collins and Doolittle (1987) used separate scaling ratios for detecting spodic and argillic horizons, rather than one for the entire soil profile.

Recognition of an interface between mediums of highly contrasting RDP may be possible for many other GPR investigations. Calibrating based on these differing RDPs should improve depth interpretation.

Horizontal Variation. Variability in dielectric properties can be just as great laterally as vertically (Conyers and Goodman, 1997). Lateral variation in moisture content was cited as the primary cause of error in GPR interpretation by Boll et al. (1996). Moisture content of sediment and soil can be impacted by numerous interacting factors that vary across the landscape, such as proximity to a drainage feature, microtopography, porosity, and texture. Lithology or mineralogy are examples of properties besides moisture content that can vary laterally (Conyers and Goodman, 1997). Despite the high potential for lateral variation in

wave velocity, replication and spatial extent of calibration sites are seldom discussed in the literature. Collins and Doolittle (1987) averaged their scaling ratio from coring at four locations. Mills and Speece (1997) used WARR calibration to make 44 subsurface velocity measurements that averaged 0.06 m ns^{-1} with standard deviation of 0.010 m ns^{-1}. They claimed that this amount of variation was small enough to support the standard assumption that wave velocity does not vary greatly along a given GPR transect. While they did not comment on the additional standard assumption that velocity does not vary vertically, it is noteworthy that they acknowledged the potential for lateral variation and collected data to investigate this potential source of error. Future research would benefit from further examination of lateral variation in wave velocity and how it might influence results.

Determining the Ground Surface on GPR Profiles

The top of a GPR profile does not represent the ground surface. The first several returns (bands) on the profile are produced by waves traveling through the air and interacting with the ground surface. Unfortunately, statements in the literature regarding these first several returns and examples of how to adjust depth scales based on these returns are often unclear and sometimes conflicting. In the vast majority of studies, the topic is ignored completely.

Augustinus and Nichol (1999) presented a very clear explanation of this phenomenon and implicitly demonstrated how to adjust one's depth scale accordingly. They recognized the first two returns on a GPR profile as the direct air wave and ground wave (Augustinus and Nichol, 1999). Thus, they concluded that the actual ground surface should be the third

return on the GPR profile. In recognition of this situation, Augustinus and Nichol (1999) set the "zero" of their depth scale below the top of GPR profiles.

Beres et al. (1999) recognized the direct air wave and direct ground wave as the first two positive/negative reflectors on the GPR profile. However, in subsequent figures, they made no adjustment to their depth scale, placing "zero" at the top of the clearly identified air wave. Similarly, Van Dam and Schlager (2000) maintained that the top two horizontal reflections were recognized as the direct air wave and direct ground wave, but on their published GPR profiles they seemed to begin their depth scale above these reflections. If the ground surface is purportedly below air and ground waves, it is unclear how the "zero" depth would not be below them as well. Seemingly, this would have produced an error of approximately 1 m for both studies.

All three of the above studies were performed in sediment deposits. Among soil investigations with GPR, mention of this ground surface phenomenon is sparse. Hubbard et al. (1990) used GPR on coastal plain soils and made mention of the topic.

> "A multiple of two or three bands appears at the top of GPR records [reference to figure]. This represents the signal from the unit rather than reflections of underground features." p.401

The referenced figure contained two GPR records. The ground surface was explicitly labeled on these figures. On one figure the ground surface was the top of the third return, and on the other, it was the top of the fourth return. No explanation was given as to how one might determine whether the ground surface is the third or fourth return. Notably, the depth scales on these figures placed zero below the top of the GPR profile and at the level marked as the ground surface. In another soils investigation, Collins et al. (1989) began their depth scale below the top of the GPR profile, but they offered no explanation as to why this was done. It

seems they must have recognized that the top two lines of the GPR trace were the direct air wave and direct ground wave.

The literature certainly provides no clear resolution of this dilemma regarding the identification of the ground surface on GPR profiles. The problem does not seem trivial. Depths to interfaces could be markedly overestimated without a proper placement of the depth scale below the direct air wave and ground wave. A clear methodology for delineating the ground surface or an explanation as to why such a method is unnecessary is required.

Interpretation of GPR Reflections

General Reflection Appearance

Interpretation of GPR profiles is based upon the identification and delineation of reflections. The reflections correspond to objects or stratigraphic interfaces in the subsurface. The cause of these reflections is related to the dielectric properties, primarily RDP, of the materials above and below the interface. When the contrast in properties across a boundary is less extreme, the reflection will be less bright. Correspondingly, the more contrasting the stratigraphic interface, the brighter and wider the reflection bands will be (Collins and Doolittle, 1987). Additionally, GPR responds best to abrupt boundaries between contrasting layers, rather than gradual transitions in properties (Collins and Doolittle, 1987, Poole et al., 1997, Doolittle et al., 2000). The depth of the objects or interfaces can be estimated based on the calibration of the GPR profile.

In practice, a reflection for a given interface usually occurs in multiples (Hubbard et al., 1990). Typically, a reflection consists of two or three "waveforms" (a positive, negative,

positive sequence), but exceptions to this rule are common (Tomer et al., 1996, Van Dam and Schlager, 2000).

Radar Facies Interpretation

Ground-penetrating radar has been applied extensively to describe the internal composition and stratigraphy of various types of sediment deposits. In such studies, it is common to base interpretation on the identification and delineation of distinct "radar facies." Radar facies are defined by Bristow et al. (2000) as a package of GPR reflectors with a distinct set of attributes, including amplitude, continuity, and shape. An excellent overview of radar facies interpretation was provided by van Overmeeren (1998). Exemplary GPR profiles and associated radar facies diagrams were presented for a variety of depositional environments found in the Netherlands, including glacial, aeolian, fluvial, lacustrine, and marine. Use of radar facies interpretation is very uncommon in soils investigations.

Absence of Reflection

Areas of a GPR profile may lack reflections entirely for one of three reasons: presence of homogeneous medium, signal attenuation, or steeply sloped interfaces. For example, an Ap horizon can display no internal reflections, due to the repeated plowing causing a highly homogeneous zone (Dominic et al., 1995). Once the GPR waves enter a horizon or layer that causes high signal attenuation, distinct reflections are often not apparent beneath this layer. Although a sandy to clayey interface typically causes a sharp reflection, the clayey layer will often attenuate the signal and no reflection will be visible below the clayey layer (Dominic et al., 1995,Van Dam & Schlager, 2000). If an interface dips steeply,

a reflection may not be received because the returning waves are reflected away from the antenna (Nobes et al., 2001).

Discontinuity or Unrecognizable Reflections

Some GPR reflections appear laterally discontinuous or are unrecognizable. This can be attributed to several potential situations. One possible scenario is that the interface is indeed discontinuous, and the discontinuous GPR profile is giving an accurate depiction of the subsurface. However, there are several situations where the interface may in fact be continuous and the GPR would provide a false representation. Apparent discontinuity may occur as reflection depth increases and nears the limit of the depth of penetration (Section 2.3) (Van Dam and Schlager, 2000). The amplitude of reflected waves is so small that over certain sections of the profile, no wave energy arrives at the transceiver. Lateral variation in moisture content, texture, or other properties may also cause a gradation in reflection brightness (Collins and Doolittle, 1987, Dominic et al., 1995, Tomer et al., 1996, Van Dam & Schlager, 2000). Destructive interference can also give the appearance of discontinuity. When two interfaces are closely spaced, their reflections may be superimposed on the radar trace, making interpretation difficult and possibly making either feature unrecognizable (Young and Sun, 1999). When resolution is not high enough for a given layer, the top and bottom of the layer will emit echos of the opposite sign. These returns may cancel each other completely or give the appearance of a weak or discontinuous reflection (Lapen et al., 1996, Nobes et al., 2001).

Near-Field Zone

Interpretation of GPR profiles near the surface can be complicated by the impact of the "near-field" zone (Conyers and Cameron, 1998). The electromagnetic field around the antenna creates a zone near the surface where reflections can often not be seen (Conyers and Goodman, 1997). Theoretically, the size of the near-field zone has been estimated as 1.5 wavelengths, meaning that the near-field zone for antennas of 10, 100, and 1000 MHz would be 30, 3, and 0.3 m, respectively (Conyers and Goodman, 1997).

In field applications, problems with interpretation near the surface have been frequent, but interference is typically not to the depths indicated by this 1.5 wavelength calculation. With a 120 MHz antenna, Hubbard et al. (1990) had difficulty detecting stratigraphic changes in the top 0.3 m. Also with a 120 MHz antenna, Vogt et al. (1996) could distinguish no interfaces within 0.25 to 0.35 m of the surface. According to the above calculation, the near-field zone with these 120 MHz antennas should have been 2.5 m. While using a 100 MHz antenna, Lapen et al. (1996) could not assess reflections from soil horizons within 0.4 m of the surface. Either the near-field zone is much smaller than anticipated when experienced under field conditions, or the interpretation problems of these researchers were due to some other near-surface impact.

Importance of Groundtruthing

Due to these complex issues that surround the interpretation of GPR, results can be highly interpreter dependent (Doolittle and Collins, 1995). For this reason, appropriate groundtruthing measures are very important (Lapen et al., 1996). Even with sufficient

groundtruthing, the identity of some subsurface features may remain ambiguous (Doolittle et al., 2000).

Section 3 - APPLICATION OF GPR

GPR Application for Describing Sediment Deposits

Active Deposition

Ground-penetrating radar facies interpretation has been employed in several instances to examine stratigraphy of deposits within or adjacent to active stream channels. Ground-penetrating radar was used by Bristow et al. (2000) to examine the internal stratigraphy of braided river deposits in Bangladesh. A 100 MHz antenna was used and achieved a depth of penetration of 10 to 14 m. A total of 8 km of GPR traces was performed for this study. Calibration was done via CMP and was confirmed by reflector-interface matching against the water table. The survey allowed the identification of different stratigraphic elements within the deposits, and conclusions were made in regard to accretion and erosion in the braided river.

The structure and bedding of floodplain deposits in New South Wales, Australia were investigated using GPR with 200 and 100 MHz antennae (Nobes et al., 2001). Calibration was performed via CMP. Erosional and depositional features within the deposits were identified with the GPR and confirmed with coring. The signal was attenuated by a sandy clay layer underlying the sediments at around 4 m. Nobes et al. (2001) stressed the

importance of always accompanying GPR studies with a systematic sedimentological investigation.

Rather than using radar facies interpretation and particle size analysis, Birkhead et al. (1996) compared their GPR survey with results of dynamic cone penetration tests. In this manner, they used high frequency (500 MHz) GPR to describe the alluvial stratigraphy of a sand-gravel bar within a South African river. Conclusions were made regarding depositional events on the bar.

Historic Deposition

Ground-penetrating radar has also been used to investigate the historic deposition of sediments. In western Tasmania, Australia, GPR was used to improve knowledge of the stratigraphy and depositional environment of Pleistocene sediments (Augustinus and Nichol, 1999). A 110 MHz antenna was used, yielding a depth of penetration of around 20 m. CMP was used for calibration. Several different sedimentary facies, resulting from different depositional events, were recognized. Their findings were in general agreement with borehole records from the region.

Ground-penetrating radar was used to detect paleochannels, joints, and faults in the unconsolidated coastal plain sediments of South Carolina (Wyatt & Temples 1996). Paleochannels have also been identified with GPR on a Montana floodplain (Poole et al., 1997) and in fluvial sediments of the Netherlands (van Overmeeren,1998).

In North Carolina, GPR was used to explore alluvial fans and some residual soils of the southern Blue Ridge Province (Mills and Speece, 1997). The alluvial sediments were likely debris flows deposited at the foot of slopes. Calibration was performed via WARR. A

100 MHz antenna achieved depths of penetration from 1.5 to 16.2 m. Variation within this range was strongly influenced by the age of the deposits. Older deposits and residuum had shallower depths of penetration, which was attributed to higher clay content. Most of the GPR profiles lacked laterally continuous reflectors. It was hypothesized that not enough soil formation had occurred for there to be distinct horizons that might have differing dielectric properties.

Three-dimensional Surveys

A recent trend in the use of GPR on sediment deposits has been to develop three-dimensional (3D) models of the subsurface. A common application of these models is to gain a better understanding of aquifer properties or make predictions regarding saturated or unsaturated flow.

In Quaternary gravel deltas of Germany, Asprion and Aigner (1999) were able to identify three distinct stratigraphic elements within glaciofluvial deposits. This was achieved with a grid spacing of 1 m and a 300 MHz antenna. No specific depth calibration method was reported, but radar facies apparent in the GPR profiles were compared to outcrops and boring results. Three dimensional block diagrams were created that showed the distribution and extent of the various stratigraphic elements. The authors concluded that GPR surveys could be useful in characterizing these sedimentary aquifers.

A 3D stratigraphic model of unsaturated glaciomarine and glaciofluvial sediments in Norway was developed using a GPR grid (Langsholt et al., 1998). The 200 MHz antenna yielded a depth of penetration of 4.5 m, below which the signal was attenuated by the water table. Calibration by CMP was confirmed with reflector-interface matching. Results

included the creation of 3D fence diagrams and geostatistics. The 3D models will be used to improve understanding of unsaturated flow and transport.

Beres et al. (1999) performed 2D and 3D GPR surveys of glaciofluvial sediments in northeastern Switzerland. A 100 MHz antenna was employed, yielding a depth of penetration of 7 to 10 m. Calibration was performed via CMP. Through comparison with outcrop photographs, it was possible to identify two prominent geomorphic features within the deposits: gravel sheets and scour pools. Distinct radar facies of these features were recognized. The 3D data were found to provide quicker, more complete, and less ambiguous interpretations than the 2D data. These findings revealed the heterogeneities of gravel aquifers and how they might impact groundwater flow.

GPR Application for Mapping or Describing Soils

Soil Mapping

Ground-penetrating radar has been utilized for a variety of applications in soil science. A common application is for the improvement of soil mapping. In such instances, GPR can be used to determine soil texture (Mokma and Doolittle, 1993), determine a horizon's continuity (Mokma et al., 1990), or estimate depth to target horizons (see section below).

Due to the increased attenuation caused by clay, soil investigations with GPR tend to produce more detailed profiles on sandy soils. Hubbard et al. (1990) tested GPR on a variety of Georgia Coastal Plain soils. A range in success was experienced, depending on clay content of the soils. The GPR worked best in sandy soils, moderately well in loamy soils, and poorly in clayey soils. Although less detailed information was obtained from the clayey

soils, GPR could still be utilized to delineate clayey areas of the landscape. Mokma and Doolittle (1993) were able to differentiate between the GPR signature over fine and coarse-loamy textured soils. In Alfisols of Michigan, they used this technique to determine the texture of soils along GPR transects. Coring was performed along the transects, and a determination of the appropriate soil series was made based on both methods. There was 84% agreement between the maps produced by coring and GPR. This was considered satisfactory by the authors.

The continuity of a cemented spodic horizon (an ortstein) was determined via GPR on Michigan Spodosols (Mokma et al., 1990). A 500 MHz antenna was used and calibrated by burying metallic objects. Two soil series were considered: one with nearly continuous ortstein, and one with patchy ortstein. The GPR was able to detect the ortstein at a depth of 0.4 to 0.7 m, and the continuity of the reflection was found to be an accurate indicator of ortstein continuity as confirmed in pits. The authors highlighted the advantage that the continuous GPR record provided in identifying discontinuities in the horizon, stating that augering would have found such discontinuities only by chance.

Due to modern management practices, Histisols in the Everglades region of Florida were expected to have undergone marked subsidence. This process would have reduced the depth of organic soil, and this change needed to be reflected while remapping these soils. GPR transects, totaling tens of kilometers in length, were used to improve mapping by Collins et al. (1986). Using a 120 MHz antenna, the GPR was able to determine the thickness of muck over bedrock. While this effort was successful, leading to significant changes in the soil series mapped in the study area, no information was reported on the accuracy of the depth interpretation.

Describing Soil Systems

Ground-penetrating radar surveys of soil systems are not always meant to improve soil mapping. Many studies use GPR to gain a better general understanding of a system or how a certain soil horizon might impact the system. Kettles and Robinson (1997) used GPR to map peat landforms in the discontinuous permafrost of northern Canada. Using a 50 MHz antenna, a peat to sandy-clay interface was detected at a depth of 3.0 to 4.9 m. This clayey layer was mapped continuously beneath the peat. Specific accuracy of the GPR interpretation was not given, other than to report that interpretations and coring observations corresponded closely.

Illuvial lamellae of clay and iron oxides are important to preferential flow and water storage in sandy Entisols of Minnesota. Tomer et al. (1996) used GPR to map such lamellae. A 450 MHz antenna was utilized to provide the high resolution necessary for the narrow lamellae (3 cm or thinner). Groundtruthing involved coring and trenching with particle size analysis and water content profiles. Calibration was performed via a calculated method and was confirmed with reflector-interface matching. The hydraulically effective lamellae (thickest lamellae, with associated water content increase) were usually detected by the GPR. Although these lamellae were continuous, the corresponding GPR reflection was sometimes not continuous. This was attributed to greater or lesser contrast in properties (such as water content) in some areas. Any secondary lamellae, found below the hydraulically effective lamellae in groundtruthing, were typically not detected by the GPR because the signal had been attenuated. Upward sloping lamellae would often terminate at some point, but the authors could offer no explanation for this occurrence. Water content measurements did show that the sloping lamellae would act to dam water.

Poole et al. (1997) used GPR to examine the subsurface of two riparian systems. The first was a system of beaver ponds and wet meadows in Minnesota, where organic soils of 0.3 to 3.0 m overlaid clays or granite bedrock. The second was a floodplain in Montana, where fluvial silt and clay overlaid gravel, clay, and mudstone. The boundary between the organic soils and clays in the beaver ponds was detected along 60% of the GPR transects. Soils of the wet meadow were higher in clay content, and the signal was attenuated before the soil - parent material boundary was reached. Complexity of the subsurface in the wet meadow made much of the GPR data uninterpretable. Mapping the thickness of peat deposits in the ponds was successful, unless the peat extended below 3.5 m. By this depth, the signal was attenuated. Detection of the water table was not possible at any of the sites due to the capillary fringe in these fine soils. The GPR was able to identify paleochannels in the Montana floodplains.

Ground-penetrating radar was used in fen pools in the Netherlands to identify iron-cemented layers that acted as aquitards (van Overmeeren, 1998). The GPR was able to determine the continuity of the cemented layers because they had contrasting physical characteristics to adjacent sandy layers. In this situation, the radar facies corresponding to the aquitards appeared as "undulating to sub-parallel, high amplitude, highly continuous reflections, bounding reflection-free zones." The presence of the aquitards seemed closely linked to the hydrology of the fens.

Subsurface features of a wetland catena were delineated using GPR in several bogs of Newfoundland (Lapen et al., 1996). A 500 m transect was performed across several bog types with a 100 MHz antenna. Cores were taken along the transect to observe depth of certain features and to obtain volumetric moisture content, porosity, bulk density, and texture

information. Calibration was done via CMP and a calculated method. Comparison of observed versus interpreted depths was done for several interfaces, but only at three points along the transect. Correlation between observed and interpreted was high ($r = 0.99$). Some strong reflections in the top of peat layers were attributed to volumetric water content changes due to variation in the degree of decomposition of the peat. When organic soil was underlain by mineral soil with high volumetric water content, only weak reflections were observed. A cemented horizon, which acted as an aquitard, was found to be discontinuous. The absence of this horizon was associated with the occurrence of heathland (a non-wetland habitat). The authors concluded that GPR was a fast, effective, and non-destructive technique for assessing these systems, but that interpretation can be "dubious" without appropriate groundtruthing.

Ground-penetrating radar was used in a Carolina Bay wetland by Grant et al. (1998). An extensive GPR survey was performed at 4 bays to map subsurface stratigraphy and aid development of new theories on the evolution of Carolina Bays. Ground-penetrating radar traces were conducted along sub-radial or circumferential transects, ranging in length from tens of meters to over 1 km. Either a 500 or 100 MHz antenna was used. Groundtruthing was performed with both coring and pits along the transects, but the specific calibration method was not mentioned. Ground-penetrating radar interpretation showed an absence of reflections in sandy soils adjacent to the bays but complex reflections within a regional underlying fluvial unit. Perched phreatic lenses were identified by the GPR over this fluvial unit. Coring into wedge shaped GPR reflections revealed silty and clayey sediments that were suspected to act as aquitards on portions of the bays' bottoms and sides. Other reflections were observed to slope sharply downward and away from the Bay interior,

suggesting groundwater drainage out of the bays. The information gained via GPR from this survey, combined with hydrologic studies at one of the same bays (Lide et al., 1995), suggest that bay hydrology may be strongly influenced by the local aquitard properties of interior bay sediments. Additionally, the GPR surveys aided in new theoretical constraints on the evolution of Carolina Bays.

These studies represent a wide range of GPR application on soil systems. The type of study site and intent of use varied from study to study, but all were able to gain valuable information through the use of GPR. In general, the studies above determined general characteristics of soil features, such as presence or absence and continuity. In other GPR applications on soils, detailed information on the spacing or depth of horizons is desired.

GPR for Determination of Depth to Stratigraphic Interfaces or Soil Horizons

When calibrated properly, GPR surveys are able to predict the depth of specific subsurface features, such as bedrock, the water table, and soil horizons. Such studies are usually accompanied by detailed groundtruthing, so that the accuracy of depth estimations by GPR can be determined. This ability has been applied extensively to both sediment and soil applications of GPR.

In the glaciated landscape of Maine, Collins et al. (1989) used GPR over a loamy soil to determine depth to bedrock. A combination of grid surveys and transects were performed with a 120 MHz antenna. Ground-penetrating radar interpretation was performed only at 1.5 or 3.0 m intervals along transects, and groundtruthing was done by coring at similar intervals or by digging a trench. Calibration was performed by reflector-interface matching, using the depth of bedrock in the trench. The average depth to bedrock was 1.47m (range 0.28 to 1.73

m), and the average difference between interpreted and observed depth to bedrock was 0.06 m. The correlation coefficient between interpreted and observed was r = 0.98 (alpha = .01). The GPR was considered to be more accurate at detecting the depth to bedrock than coring would have been, due to the fact that an auger can not detect the difference between large rock fragments and bedrock.

On a sand-gravel bar of a South African river, depth to the water table and to underlying bedrock were determined via GPR (Birkhead et al., 1996). A 90 MHz and 500 MHz antennae were used for detecting the bedrock and water table, respectively. Calibration was via reflector-interface matching, using the water table and bedrock surface. Correlation between depths predicted by GPR and observed by coring was very good: $R^2 = 0.97$ for depth to water table, and $R^2 = 0.85$ for depth to bedrock. Average percent error for the depth to water table and bedrock was 7.9% (equivalent to 0.08 m) and 4.4% (0.14 m), respectively. The susceptibility of coring to inaccuracies was cited as the reason for the lower correlation for depth to bedrock. As in the study by Collins et al. (1989), it was noted that boulders can be indistinguishable from bedrock when coring.

Following severe flooding along the Missouri River, GPR was used to map the thickness of floodplain deposits (Vogt et al., 1996). An extensive grid was surveyed with a 120 MHz antenna, covering 13.8 km of linear traces. Ground-penetrating radar was calibrated via reflector-interface matching with a buried metallic object. The depth of sediments was readily delineated on the GPR traces, as there was an abrupt interface between the deposited coarse sand and the underlying medium-textured soils. The sediment thickness ranged from 0 to 2.31 m and averaged 0.63 m. These GPR interpretations were confirmed via coring at 25 locations. Correlation between observed and interpreted thickness of

deposits was high ($R^2 = 0.95$). The average difference between observed and interpreted thickness was 0.06 m. Contour maps of deposit thickness were presented. The authors concluded that GPR was an effective and efficient way to determine the extent and depth of flood deposited material.

In a sandy Spodosol of Florida, GPR was used to map microvariability in depth to spodic and argillic horizons (Collins and Doolittle, 1987). A 90 m^2 grid was surveyed with a 120 MHz antenna. Calibration was performed via reflector-interface matching. The absolute deviation of the interpreted to observed (from coring) values was low: 0 to 6 cm for spodic (average depth of 0.33 m), and 0 to 11 cm for argillic (average depth of 1.05 m). Surface-net diagrams were created to show the microvariability in depth to these horizons.

Doolittle et al. (2000) attempted to use GPR to map the depth to fragipan in a northern Idaho alfisol. A 30.5 m transect was performed with a 200 MHz antenna. Even though GPR provides a continuous record of the subsurface, interpretation of depth were only performed at 1.5 m intervals. The GPR was calibrated with a buried object. The fragipan was expected to cause a bright reflection due to its higher density and moisture content. A trench was dug to groundtruth the GPR interpretation. Maximum depth of penetration was 2.1 m, while the average depth of the fragipan was 1.0 m. The average difference between the observed and interpreted depths was 0.09 m. The correlation between observed and interpreted was low: $r = 0.491$, $p = 0.03$. This low correlation was attributed to several problems: a narrow range in depths, a highly irregular interface, and poor resolution with a 200 MHz antenna. Due to this low correlation, the authors concluded that GPR use at this site would have been unreliable without the trench. Although not commented upon by the authors, 8 of 25 comparisons between observed and interpreted showed that the GPR

overestimated fragipan depth. An adjustment in the placement of the "zero" on the depth axis might have improved the accuracy.

In a sandy soil of Massachusetts, Boll et al. (1996) used GPR to map the coarse and fine layers within the soil in an attempt to predict preferential flow. A 450 MHz antenna was used, and it achieved depths of penetration of 1.5 to 2.0 m. The accuracy in predicting depth to coarse layers was tested for two different depth calibration methods. When moisture content measurements were placed in an equation to determine wave velocity, error was as great as ± 0.4 m. This large error was attributed to lateral variation in moisture content. With CMP, accuracy was within 7%. The CMP method was greatly preferred as it was more accurate, quicker, and less destructive.

In the Coastal Plain soils of Georgia, water that infiltrates below the root zone will recharge groundwater aquifers unless it first encounters a layer of higher density, such as an argillic horizon. When such a horizon is reached, water tends to move laterally and return to streamflow or become evapotranspiration. For this reason, subsurface contours of argillic horizons could potentially impact hydrology. Ground-penetrating radar was used to map depth to argillic horizon in a transect and a grid on the Coastal Plain of Georgia (Asmussen et al., 1986). Antennas used ranged from 80 to 500 MHz. The calibration method was not reported, but depth of penetration was as high as 4 m at one site. Coring was performed to groundtruth GPR interpretations. Correlation between observed depth to argillic and interpreted depth was high: $R^2 = 0.99$ ($p=.0001$) at the grid site, and $R^2 = 0.95$ ($p=.0001$) at the transect site. Average percent error was 7% (equivalent to 0.17 m) and 14% (0.21 m) at the grid and transect sites, respectively. These surveys could be used to prepare subsurface contour maps and evaluate lateral water flow.

These studies show that depth to a variety of interfaces can be measured through a variety of substrates. Although there was a range in accuracy, GPR can generally predict the depth of an interface within 10%. A summary of the accuracy of GPR depth investigations is given in Table 2.

The error observed in these studies is not necessarily due to inherent inaccuracies of the GPR method. Differences between observed and interpreted depths can be explained by a variety of situations: non-vertical alignment of the coring device (Collins et al., 1989, Birkhead et al., 1996); other errors in coring or rounding of observed depths (Collins et al., 1989, Doolittle et al., 2000); rounding of GPR interpretation or interpreter error (Collins et al., 1989, Doolittle et al., 2000); spatial discrepancy between the location of GPR profile and coring (Collins et al., 1989, Doolittle et al., 2000); highly irregular interface or boundary (Birkhead et al., 1996, Doolittle et al., 2000); or highly complex subsurface stratigraphy (Birkhead et al., 1996, Poole et al., 1997, Doolittle et al., 2000).

Section 4 - LIMITATIONS OF GPR APPLICATION

Although GPR use can be successful in numerous settings, there are several external factors that can severely limit the effectiveness of GPR surveys. These limitations can be divided into two categories: site limitations and substrate limitations.

Aboveground characteristics of a site will influence its suitability for GPR surveys. Because GPR surveys typically require an open terrain for dragging the GPR unit along transects or grids, heavy vegetation and high density of woody debris or rocks limit GPR use

(Poole et al., 1997, Conyers and Cameron, 1998). Complex topography or an uneven ground surface can negatively impact GPR results (Conyers and Cameron, 1998). When the ground surface or subsurface interfaces are steeply sloping, GPR reflections can be reflected away from the transceiver, and no return will be generated (Nobes et al., 2001). These site qualities should be examined prior to attempting a GPR survey. Some site limitations can be altered, such as clearing vegetation, but the time and energy spend on such remedies should be considered.

Substrate, or belowground, characteristics of a site must also be considered when planning a GPR survey. Ground-penetrating radar studies have been conducted on a wide range of substrates, including sediments of most potential geomorphic setting and soils from most Soil Taxonomy orders. However, a recurring trend in the literature is that GPR surveys are less successful or obtain less useable data when a clayey substrate or clayey layer is encountered (Hubbard et al., 1990, Dominic et al., 1995, Poole et al., 1997, Conyers and Cameron, 1998, Cagnoli and Russell, 2000, Van Dam & Schlager, 2000, Nobes et al., 2001). Due to its dielectric properties, clay is known to attenuate GPR signal rapidly, and this is the cause of poor results on clayey substrates. Presence of water compounds the attenuation ability of clay, and water is generally responsible for increases in RDP and electrical conductivity. Poole et al. (1997) recognized that both clay layers and the water table would attenuate GPR signal, resulting in no reflections below their depth.

In recognition of these potential substrate limitations, several studies have attempted to use Soil Taxonomy and soil survey information to predict the suitability of a site for GPR use. Doolittle and Collins (1995) found that the family level of Soil Taxonomy provided the best information for assessing the potential for GPR use. From the family classification,

information on both the particle size class and mineralogy can be drawn. They also felt that the prefix "aqu" in any level of taxonomy would negatively impact a soil's potential for GPR use. Following Doolittle and Collins (1995), Williams (1996) used soil survey data to create a rating scheme on the suitability of a location for use of GPR. The main criteria used for the rating scheme were depth to an argillic horizon and drainage class. The rating scheme was linked to a geographic information system (GIS) coverage of Santa Rosa County, Florida. Approaches such as these may be useful in the future when screening sites for GPR suitability.

A final substrate consideration is the overall complexity of the subsurface. Ground-penetrating radar is best suited for relatively simple subsurface structure. With increasing subsurface complexity, additional groundtruthing is needed, detracting from the labor reduction that GPR usually provides (Poole et al., 1997).

Section 5 - EFFICIENCY AND FINANCIAL BENEFITS OF GPR APPLICATION

Numerous literature sources have maintained that GPR is a cost and labor effective alternative to traditional excavation methods, but many provide no explicit evidence to support this claim. Only a limited number of studies have provided a quantitative explanation of these benefits.

Collins and Doolittle (1987) highlighted the time efficiency of GPR surveys. They estimated that the results of their study of soil microvariability would have taken 9 person-hrs to complete by manual coring, when it took only 1 person-hr with the GPR. Mokma and

Doolittle (1993) also estimated the time-savings of using GPR to map soils. The GPR accomplished the mapping more efficiently than coring, with 1.5 person-days for the GPR survey and 3.5 person-days for the coring survey. The only report that included a quantitative estimate of financial benefits was that of Doolittle (1987). When using GPR to aid in soil mapping, he found that GPR decreased cost by 70% and increased productivity by 210%. It seems that further work is warranted to substantiate the claim that GPR offers efficiency and financial benefits.

When considering the benefits of GPR, it is important to consider the resultant product along with efficiency and financial benefits. Is GPR use justified if time and money savings are at the expense of a useable product? When Mokma and Doolittle (1993) reported their time savings with GPR use, they also reported that soil maps produced by coring and GPR were in 84% agreement. They felt this was satisfactory, but such accuracy might not be sufficient in other situations. In detecting depth to bedrock, Collins et al. (1989) found the product from GPR to be superior to that of coring when both were groundtruthed with a trench. In any study when continuity of a subsurface feature is of interest, GPR may indeed provide better results than coring. Mokma et al. (1990) felt this to be the case when they found discontinuities in a spodic horizon via GPR. They felt that these discontinuities might not have been discovered if only coring had been performed. Contrarily, Doolittle et al. (2000) found that a GPR survey of fragipan depth would have been unreliable without the adjacent trench. Groundtruthing with a trench would obviously negate any financial benefit that GPR could offer.

If application of GPR is expected to expand into more mainstream use, then researchers must attempt to make straightforward assessments of its application. Reports on

GPR applications should include evaluation of the product's usefulness and estimates of the efficiency and financial benefits.

Section 6 - SUMMARY

In 1995, the *Journal of Applied Geophysics* (volume 33) devoted a special issue to recent developments in GPR. Cook (1995) authored the preface to this special issue, and he made the following observation: "Ground-penetrating radar seems to have developed in several places, more or less independently. Even today, those working in the art seem to be somewhat isolated, citing mainly publications of their own groups (p. 1)." Nearly ten years later, this situation seems not to have changed. Scientists that use GPR fall broadly into two categories. One group consists of soil scientists, using GPR to improve soil mapping or delineate specific soil horizons. The second group uses GPR to investigate the stratigraphy and internal composition of various sediment deposits and geomorphologic or geologic features. Much could be gained by an increase in the dissemination of knowledge and experience between these two groups.

Despite this separation, the current outlook for GPR application is positive. More attention is being given to the manner in which GPR is calibrated, such as the move by many researchers to two-velocity models and the use of calculated methods. However, the aspect of ground surface identification requires clarification. Skill in the interpretation of GPR seems to be advancing, especially with the popularity of radar facies interpretation.

Investigations in soil systems might gain from the radar facies method, as it seems to have been used exclusively in sediment deposits to this point. The move to digital GPR equipment and emergence of 3D subsurface models should provide more detailed pictures of subsurface stratigraphy, which can enhance knowledge on water flow. Application of GPR for improved soil mapping and description of soil systems continues to grow and usually finds success. The accuracy of depth interpretation by GPR continues to be impressive, but it is recognized that groundtruthing is still vital. Limitations of GPR use have been identified, and screening processes based on these limitations have been established, recently incorporating the use of GIS. While GPR is known to provide valuable products, the presupposed financial and efficiency benefits of GPR should be established more quantitatively in future studies.

REFERENCES

Asmussen, L.E., H.F. Perkins, and H.D. Allison. 1986. Subsurface descriptions by ground-penetrating radar for watershed delineation. Bull. 340. The Georgia Agricultural Experiment Stations, The University of Georgia, Athens.

Asprion, U., and T. Aigner. 1999. Towards realistic aquifer models: three-dimensional georadar surveys of Quaternary gravel deltas (Singen Basin, SW Germany). Sediment. Geol. 129:281-297.

Augustinus, P.C., and S. Nichol. 1999. Ground-penetrating radar imaging of Pleistocene sediments, Boco Plain, western Tasmania. Aust. J. Earth Sci. 46(2):275-282.

Beres, M., P. Huggenberger, A.G. Green, and H. Horstmeyer. 1999. Using two- and three-dimensional georadar methods to characterize glaciofluvial architecture. Sediment. Geol. 129:1-24.

Birkhead, A.L., G.L. Heritage, H. White, and A.W. van Niekerk. 1996. Ground-penetrating radar as a tool for mapping the phreatic surface, bedrock profile, and alluvial stratigraphy in the Sabie River, Kruger National Park. J. Soil Water Conserv. 51(3):234-240.

Boll, J., R.P.G. van Rijn, K.W. Weiler, J.A. Ewen, J. Daliparthy, S.J. Herbert, and T.S. Steenhuis. 1996. Using ground-penetrating radar to detect layers in a sandy field soil. Geoderma 70:117-132.

Bristow, C.S., J.L. Best, and P.J. Ashworth. 2000. The use of GPR in developing a facies model for a large sandy braided river, Brahmaputra River, Bangladesh. p. 95-100. *In* D.A. Noon, G.F. Stickley, and D. Longstaff (ed.) Proc. Int. Conf. Ground Penetrating Radar, 8th. Univ. of Queensland. SPIE Vol. 4084.

Butnor, J.R., J.A. Doolittle, K.H. Johnsen, L. Samuelson, T. Stokes, and L. Kress. 2003. Utility of ground-penetrating radar as a root biomass survey tool in forest systems. Soil Sci. Soc. Am. J. 67:1607-1615.

Cagnolli, B., and J.K. Russell. 2000. Imaging the subsurface stratigraphy in the Ubehebe hydrovolcanic field (Death Valley, California) using ground penetrating radar. J. Volcanol. Geotherm. Res. 96:45-56.

Collins, M.E., and J.A. Doolittle. 1987. Using ground-penetrating radar to study soil microvariability. Soil Sci. Soc. Am. J. 51:491-493.

Collins, M.E., J.A. Doolittle, and R.V. Rourke. 1989. Mapping depth to bedrock on a glaciated landscape with ground-penetrating radar. Soil Sci. Soc. Am. J. 53:1806-1812.

Collins M.E., G.W. Schellentrager, J.A. Doolittle, and S.F. Shih. 1986. Using ground-penetrating radar to study changes in soil map unit composition of selected histosols. Soil Sci. Soc. Am. J. 50:408-412.

Conyers, L.B., and C.M. Cameron. 1998. Ground-penetrating radar techniques and three-dimensional computer mapping in the American Southwest. J. Field Arch. 25:417-430.

Conyers, L.B., and D. Goodman. 1997. Ground-penetrating radar: an introduction for archaeologists. AltaMira Press, Walnut Creek, CA.

Cook, J.C. 1995. Preface. J. Appl. Geophys. 33:1-3.

Dagallier, G., A.I. Laitinen, F. Malartre, I.P.A.M. Van Campenhout, and P.C.H. Veeken. 2000. Ground penetrating radar application in a shallow marine Oxfordian limestone sequence located on the eastern flank of the Paris Basin, NE France. Sediment. Geol. 130:149-165.

Daniels, D.J. 1996. Surface-penetrating radar. Institution of Electrical Engineers, London, UK.

Dominic, D.F., K. Egan, C. Carney, P.J. Wolfe, and M.R. Boardman. 1995. Delineation of shallow stratigraphy using ground penetrating radar. J. Appl. Geophys. 33:167-175.

Doolittle, J.A. 1987. Using ground-penetrating radar to increase the quality and efficiency of soil surveys. p. 11-32. *In* W.U. Reybold, and G.W. Peterson (ed.) Soil Survey Techniques, Soil Sci. Soc. Am. Spec. Publ. No. 20.

Doolittle, J.A., and M.E. Collins. 1995. Use of soil information to determine application of ground penetrating radar. J. Appl. Geophys. 33:101-108.

Doolittle, J.A., G. Hoffmann, P. McDaniel, N. Peterson, B. Gardner, and E. Rowan. 2000. Ground-penetrating radar interpretations of a fragipan in northern Idaho. Soil Surv. Horiz. 41(3):73-82.

Grant, J.A., M.J. Brooks, and B.E. Taylor. 1998. New constraints on the evolution of Carolina Bays from ground-penetrating radar. Geomorphology 22:325-345.

Hubbard, R.K., L.E. Asmussen, and H.F. Perkins. 1990. Use of ground-penetrating radar on upland Coastal Plain soils. J. Soil Water Conserv. 45(3):399-404.

Huisman, J.A., C. Sperl, W. Bouten, and J.M. Verstraten. 2001. Soil water content measurements at different scales: accuracy of time domain reflectmetry and ground-penetrating radar. J. Hydrol. (Amsterdam) 245:48-58.

Imai, T., T. Sakayama, and T. Kanemori. 1987. Use of ground-probing radar and resistivity surveys for archaeological investigations. Geophysics 52(2):137-150.

Kettles, I.M., and S.D. Robinson. 1997. A ground-penetrating radar study of peat landforms in the discontinuous permafrost zone near Fort Simpson, Northwest Territories, Canada. p. 147-160. *In* C.C. Trettin, M.F. Jurgensen, D.F. Grigal, M.R. Gale, and J.K. Jeglum (ed.) Northern forested wetlands: Ecology and management. CRC Lewis Publishers, Boca Raton, FL.

Langsholt, E., N.-O. Kitterød, and L. Gottschalk. 1998. Development of three-dimensional hydrostratigraphical architecture of the unsaturated zone based on soft and hard data. Ground Water 36(1):104-111.

Lapen, D.R., B.J. Moorman, and J.S. Price. 1996. Using ground-penetrating radar to delineate subsurface features along a wetland catena. Soil Sci. Soc. Am. J. 60:923-931.

Lide, R.F., V.G. Meentemeyer, J.E. Pinder, III, and L.M. Beatty. 1995. Hydrology of a Carolina Bay located on the upper Coastal Plain of western South Carolina. Wetlands 15(1):47-57.

Mellett, J.S. 1995. Ground penetrating radar applications in engineering, environmental management, and geology. J. Appl. Geophys. 33:157-166.

Mills, H.H., and M.A. Speece. 1997. Ground-penetrating radar exploration of alluvial fans in the southern Blue Ridge Province, North Carolina. Environ. Eng. Geosci. 3(4):487-499.

Mokma, D.L., and J.A. Doolittle. 1993. Mapping some loamy alfisols in southwestern Michigan using ground-penetrating radar. Soil Surv. Horiz. 34(3):71-77.

Mokma, D.L., R.J. Schaetzl, J.A. Doolittle, and E.P. Johnson. 1990. Ground-penetrating radar study of ortstein continuity in some Michigan haplaquods. Soil Sci. Soc. Am. J. 54:936-938.

Nobes, D.C., R.J. Ferguson, and G.J. Brierley. 2001. Ground-penetrating radar and sedimentological analysis of Holocene floodplains: insight from the Tuross valley, New South Wales. Aust. J. Earth Sci. 48:347-355.

Poole, G.C., R.J. Naiman, J. Pastor, and J.A. Stanford. 1997. Uses and limitations of ground penetrating radar in two riparian systems. p.140-148. *In* J. Gibert, J. Mathieu, and F. Fournier (ed.) Groundwater/surface water ecotones: Biological and hydrological interactions and management options. International Hydrology Series. Cambridge University Press, New York, NY.

Smith, D.G., and H.M. Jol. 1995. Ground penetrating radar: antenna frequencies and maximum probable depths of penetration in Quaternary sediments. J. Appl. Geophys. 33:93-100.

Theimer, B.D., D.C. Nobes, and B.G. Warner. 1994 A study of the geoelectric properties of peatlands and their influence on ground penetrating radar surveying. Geophys. Prospecting 42:179-209.

Tomer, M.D., J. Boll, K.-J.S. Kung, T. Steenhius, and J.L. Anderson. 1996. Detecting illuvial lamellae in fine sand using ground-penetrating radar. Soil Sci. 161(2):121-129.

Topp, G.C., J.L. Davis, and A.P. Annan. 1980. Electromagnetic determination of soil water content: Measurements in coaxial transmission lines. Water Resour. Res. 16:574-582.

Van Dam, R.L, and W. Schlager. 2000. Identifying causes of ground-penetrating radar reflections using time-domain reflectometry and sedimentological analyses. Sedimentology 47:435-449.

van Overmeeren, R.A. 1998. Radar facies of unconsolidated sediments in The Netherlands: a radar stratigraphy interpretation method for hydrogeology. J. Appl. Geophys. 40:1-18.

van Overmeeren, R.A., S.V. Sariowan, and J.C. Gehrels. 1997. Ground penetrating radar for determining volumetric soil water content; results of comparative measurements at two test sites. J. Hydrol. (Amsterdam) 197:316-338.

Vogt, K., J. Doolittle, and R. Fenwick. 1996. Mapping the thickness of flood-plain splay deposits with ground-penetrating radar techniques. Soil Surv. Horiz. 37(3):93-100.

Williams, A. 1996. Linking ground-penetrating radar and geographical information systems in west Florida. Soil Surv. Horiz. 37(4):119-123.

Wyatt, D.E., and T.J. Temples. 1996. Ground-penetrating radar detection of small-scale channels, joints, and faults in the unconsolidated sediments of the Atlantic Coastal Plain. Environ. Geol. 27:219-225.

Young, R.A., and J. Sun. 1999. Revealing stratigraphy in ground-penetrating radar data using domain filtering. Geophysics 64(2):435-442.

Table 1. Typical range of relative dielectric permittivity (RDP) for various natural materials.

Material / Substrate	Relative Dielectric Permittivity (RDP)
Air	1[a,b]
Freshwater	80-81[a,b]
Seawater	81-88[a,b]
Dry Sand	3-6[a,b]
Saturated Sand	10-30[a,b]
Dry Silt	3-30[b]
Saturated Silt	10-40[b]
Dry Clay	2-6[a]
Saturated Clay	15-40[a]
Soil- Dry, Sandy	4-6[a]
Soil- Wet, Sandy	15-30[a]
Soil- Dry, Loamy	4-6[a]
Soil- Wet, Loamy	10-20[a]
Soil- Dry, Clayey	4-6[a]
Soil- Wet, Clayey	10-15[a]
Limestone	4-8[a,b]
Shale	5-15[a,b]
Sandstone	2-10[a]
Granite	5-15[a,b]

[a]Modified from Daniels, 1996.
[b]Modified from Conyers and Goodman, 1997

Table 2. Summary of accuracy in predicting depth to a subsurface interface for various GPR studies. Some studies included data on several interfaces or determined by different methods, and in such cases each result is listed separately. If reported, the distance of GPR survey that included groundtruthing is given. Substrate of the GPR survey site, interface being detected, number of points where predicted and observed depth were compared, correlation/regression results, and average percent error are also given. Percent error is the absolute deviation between observed and predicted divided by the observed depth, on a percent basis. Results are ranked by average percent error.

Source	Surveyed Distance	Substrate	Interface Detected	Number of Observation Points	Relationship Observed vs. Predicted	Average Percent Error
	----km---					---%---
Collins et al., 1989	0.090	loamy soil	bedrock	61	r = 0.98	4.1†
Birkhead et al., 1996	0.090	sand-gravel bar	bedrock	15	R^2 = 0.85	4.4#
Collins and Doolittle, 1987	0.200	sandy spodosol	argillic horizon	4	na	5.2†
Asmussen et al., 1986 - grid	unknown (2.33 ha)	sandy soil	argillic horizon	8	r = 0.99	7.0‡
Birkhead et al., 1996	0.375	sand-gravel bar	water table	70	R^2 = 0.97	7.9#
Collins and Doolittle, 1987	0.200	sandy spodosol	spodic horizon	4	na	9.1†
Doolittle et al., 2000	0.030	Alfisol	fragipan	21	r = 0.49	9.4‡
Lapen et al., 1996	0.500	Bog	various	10	r = 0.99	10.1‡
Vogt et al., 1996	13.800	flood deposits	sediment over soil	25	r^2 = 0.95	10.1†
Asmussen et al., 1986 - transect	1.600	sandy soil	argillic horizon	14	r = 0.95	57.1‡

† = calculated based on average or range of deviation and depth given in source

‡ = calculated based onresults at individual observations points given in source (note: This calculation reveals a more accurate and typically higher percent error than when done based on average deviation and depth.)

= reported as percent error in source

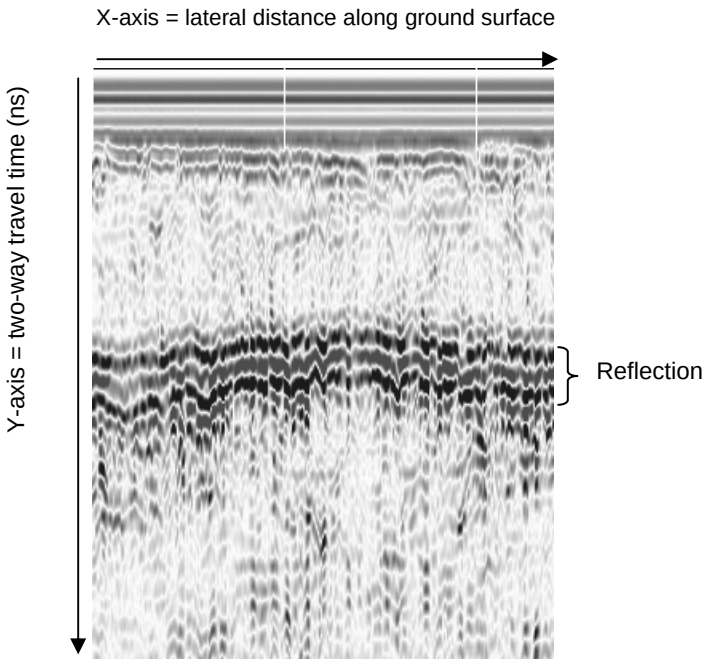

Fig. 1. Example of GPR profile and reflection. Multiple bright lines represent a subsurface discontinuity. X-axis of lateral distance along ground surface and Y-axis of two-way travel time are indicated.

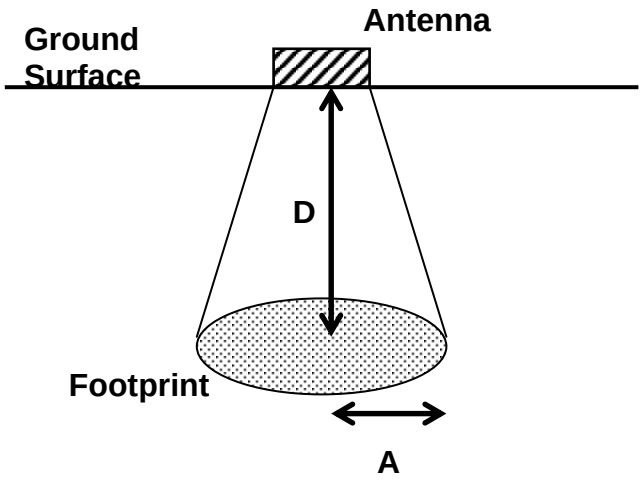

$A = (\lambda / 4) + (D / [K + 1]^{1/2})$ [2]

Where:

A = approximate long dimension radius of footprint

λ = wavelength of the center frequency of radar energy

D = depth from ground surface to reflection surface

K = average RDP of material from ground surface to depth D

Fig. 2. Graphical representation of the GPR "footprint" or horizontal resolution. Eq. 2 defines the approximate geometry of the footprint. (Diagram modified from Conyers and Goodman, 1997.)

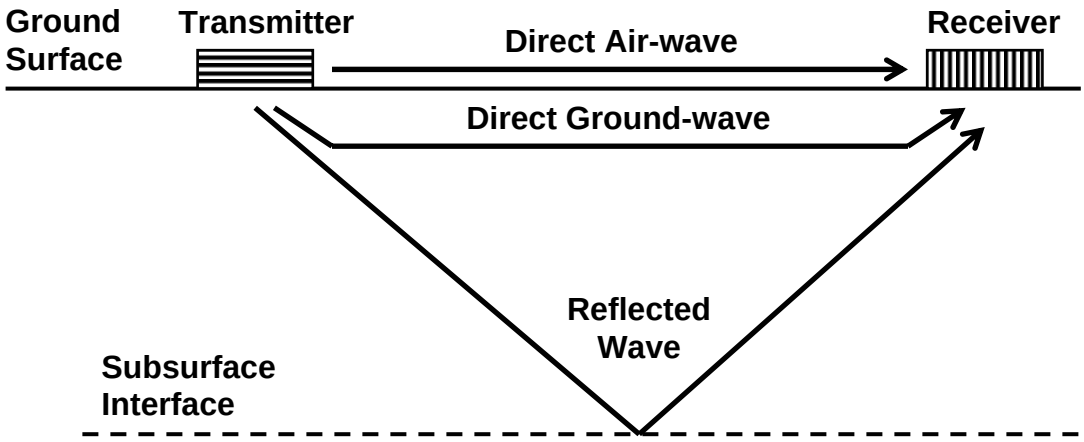

Fig. 3. General arrangement of transmitting and receiving antennas for direct-wave calibration methods such as CMP and WARR. Transmission of direct air-wave, direct ground-wave, and a wave reflected from a subsurface interface are shown. (Diagram modified from Conyers and Goodman, 1997.)

CHAPTER 2

Calibration of a Large-scale Ground-penetrating Radar Survey: implementation of a lift-test and a calibration equation based on multiple points

ABSTRACT

Ground-penetrating radar (GPR) has been applied extensively to determine the depth to subsurface strata; however, a calibration process is required to convert travel time of GPR waves into depth. Two prevalent complications in the calibration process are ambiguity in identifying the ground surface and spatial variation in wave propagation velocity. This study addressed these problems during a GPR survey of clayey soil horizons in a 300 ha drained Carolina Bay in Robeson County, NC. A “lift-test” was developed that clearly delineated the soil surface on GPR transects. A "reflector-interface matching" technique was conducted at multiple locations in the bay to determine wave velocity, and saturation due to the water table was found to markedly decrease wave velocity. Calibration points that involved stratigraphic interfaces of varying depth below the water table were selected and used to obtain a linear calibration equation relating two-way travel time to depth. The average deviation between observed and predicted depth to clayey horizons was 0.25 m (16% error). Error was mainly attributed to the survey's large scale, subsurface complexity, presence of organic soils, and depth of the horizons. The lift-test improved accuracy by 10%. Had calibration been done with data from unsaturated depths, average deviation would have more than doubled. We feel that further studies of GPR's accuracy on large-scale, complex sites are necessary, and our methods should prove valuable for such studies.

INTRODUCTION

Ground-penetrating radar (GPR) presents numerous advantages over conventional soil exploration methods, such as pits, cores, or trenches. When used properly in appropriate conditions, GPR can provide continuous, high-resolution profiles of subsurface stratigraphy. Thus, the technique provides large volumes of data while offering time and effort efficiency. Since the late 1970s and 1980s, applications of GPR have expanded to many fields. Brief reviews of these applications can be found for military and engineering (Mellett, 1995, Daniels, 1996), geology and geomorphology (Daniels, 1996, van Overmeeren, 1998, Cagnolli and Russell, 2000), archaeology (Daniels, 1996, Conyers and Goodman, 1997, Conyers and Cameron, 1998), and soil science (Hubbard et al., 1990, Doolittle and Collins, 1995, Poole et al., 1997). A common application of GPR has been to determine the depth of certain stratigraphic layers or soil horizons. Ground-penetrating radar has been used to map the depth: to bedrock (Collins et al., 1989, Birkhead et al., 1996), to the water table (Birkhead et al., 1996), of floodplain deposits (Vogt et al., 1996), and to soil horizons (Asmussen et al., 1986, Collins and Doolittle, 1987, Boll et al., 1996, Doolittle et al., 2000). Accuracy in predicting depth with GPR has been generally within 10% of the observed depth for these studies.

Ground-penetrating radar operates by sending pulses of high-frequency electromagnetic waves into the subsurface. A GPR unit measures the travel time for waves to propagate down to a stratigraphic interface and reflect back to the surface. This is referred to as the two-way travel time (TWT) (Fig. 1), which can be related to depth via the wave propagation velocity (Eq. 1).

$$D = v * (TWT / 2) \quad [1]$$

where: D = depth (m)

v = velocity (m ns^{-1})

TWT = two-way travel time (ns)

To predict depth to subsurface features with GPR, profiles must be calibrated by ascertaining the wave propagation velocity at one or more locations along the profile and applying it to the GPR interpretation according to Eq.[1]. The velocity can be determined by numerous techniques that fall into three categories (Conyers and Goodman, 1997): reflected-wave methods, direct-wave methods, and calculated methods.

In reflected-wave methods, the velocity is calculated from the depth of a known object/interface and the TWT of the corresponding reflection. One approach is to bury an object, such as a metal pipe or shovel, that is certain to yield an obvious GPR reflection (Mokma et al., 1990, Vogt et al., 1996, Conyers and Goodman, 1997, Conyers and Cameron, 1998, Doolittle et al., 2000). Rather than bury an object, calibration by reflected-wave method may utilize a "known and recognizable feature or soil horizon" (Doolittle et al., 2000, p. 75). The term "reflector-interface matching" will be used in this text to describe such an approach. The depth of an interface is determined by excavation or coring, and it is matched to the TWT of a prominent GPR reflection. Reflector-interface matching has been performed using a variety of interfaces, including the water table (Birkhead et al., 1996, Bristow et al., 2000), bedrock (Collins et al., 1989, Birkhead et al., 1996), and soil or sediment layers (Collins et al., 1986, Collins and Doolittle, 1987, Dominic et al., 1995, Tomer et al., 1996, Langsholt et al., 1998). Reflected-wave methods are generally accepted as the most accurate GPR calibration method (Mellett, 1995, Conyers and Goodman 1997, Doolittle et al., 2000).

In direct-wave methods, propagation velocity is determined by gradually separating the GPR transmitter and receiver by known distances and observing the resultant changes in the GPR profile. Velocities are calculated by knowing the distance between transmitter and receiver, deducing the travel paths of the GPR waves, and extracting the (one-way) travel time from the GPR profile. The two most common techniques for direct-wave calibration are the common-midpoint method (CMP) and wide-angle reflection and refraction mode (WARR). Details of these methods can be found elsewhere: CMP (Boll et al., 1996, Conyers and Goodman, 1997) and WARR (Imai et al., 1987).

Both reflected-wave and direct-wave methods have the disadvantage of determining the average velocity between the ground surface and the known interface. Equations, usually based on volumetric water content (Topp et al., 1980), can be used to determine the propagation velocity for distinct layers or horizons. Success with such calculated methods has been mixed (Boll et al., 1996, Tomer et al., 1996, Lapen et al., 1996), and their disadvantage is the time and effort required to obtain the input data for the equation. Despite the availability of these numerous approaches to calibrate GPR profiles, calibration can still be problematic in certain settings. Two prevalent complications are ambiguity in identifying the ground surface and spatial variation in wave propagation velocity.

Identifying the Ground Surface

The top of a GPR profile does not represent the ground surface. The first several returns (bands) on the profile are produced by waves traveling through the air and the antenna enclosure and interacting with the ground surface. Unfortunately, the literature

offers unclear and sometimes conflicting information regarding these returns and how to adjust depth scales appropriately.

The top two returns have been identified by some authors as the "direct air wave" and "direct ground wave" (Augustinus and Nichol, 1999, Beres et al., 1999, Van Dam and Schlager, 2000). These returns result from the transmission of radar waves from the transmitting to the receiving antenna (usually spatially disjoint if only by a small distance) via the air and via the ground surface, respectively. Concluding that the ground surface would be below the direct waves, Augustinus and Nichol (1999) set the zero of their depth scale at the top of the third return. Other authors, while acknowledging the occurrence of direct waves, made no adjustment and placed the zero depth above the direct waves (Beres et al., 1999, Van Dam and Schlager, 2000). Several studies have made adjustments to the depth scale, placing it variably between the top of the third and fifth return, without sufficient explanation to how this placement was determined (Collins et al., 1989, Hubbard et al., 1990). The vast majority of GPR publications make no mention of direct waves or surface waves, and it is rarely apparent whether any correction to the depth scale was made near the surface. The literature certainly provides no clear resolution of this dilemma regarding the identification of the ground surface on GPR profiles. However, the problem does not seem trivial. Depths to subsurface interfaces could be markedly overestimated without proper placement of the depth scale below the direct air wave and direct ground wave.

Spatial Variation in Wave Velocity

Wave velocity through sediment and soil varies due to differences in texture, composition, moisture content, bulk density, porosity, physical structure, and temperature (Hubbard et al., 1990, Conyers and Goodman, 1997, Dagallier et al., 2000). Due to the large difference between velocity through air and water, moisture content is often considered the most important of these factors (Hubbard et al., 1990, Daniels, 1996, Van Dam and Schlager, 2000). Many of these soil characteristics can vary drastically between and even within horizons or layers; thus, wave velocity typically changes over depth for a given soil-sediment profile and laterally across a study site. When using only one calibration point to calibrate an entire GPR transect or grid, researchers make the often faulty assumption that wave velocity is constant both horizontally and vertically. Calculated calibration methods can facilitate the determination of wave velocity for distinct layers, but this achievement is at the expense of field efficiency.

As a compromise between calculating velocities for each layer and using an average velocity for all layers, some researchers have identified one interface that has the most dramatic impact on wave velocity. Separate velocities are determined for each side of the interface, yielding a two-velocity model for calibration. The most common interface chosen for segregating layers is the water table (Birkhead et al., 1996, Bristow et al., 2000), but other separations include frozen-unfrozen soil (Kettles and Robinson, 1997) and soil horizonation (Collins and Doolittle, 1987).

Variability in wave velocity can be just as great laterally as vertically (Conyers and Goodman, 1997). Lateral variation in moisture content was cited as the primary cause of error in GPR interpretation by Boll et al. (1996). Moisture content of sediment and soil can

be impacted by numerous interacting factors that vary across the landscape, such as proximity to a drainage feature, microtopography, porosity, and texture. Lithology or mineralogy are examples of properties besides moisture content that can vary laterally and impact wave velocity as well (Conyers and Goodman, 1997). Despite the high potential for lateral variation in wave velocity, only a few studies have discussed repetition of GPR calibration or the spatial extent of calibration sites (Collins and Doolittle, 1987, Mills and Speece, 1997, Gish et al., 2002).

For this study, a GPR survey was performed in the Coastal Plain of North Carolina with the intent of delineating clayey soil horizons within a drained Carolina Bay. This paper presents our response to the GPR calibration problems discussed above. The objectives were to 1) develop a clear methodology for identifying the ground surface on GPR traces, and 2) develop a multiple-point calibration equation that allows the investigation of horizontal and vertical variation in wave velocity.

MATERIALS AND METHODS

The study site was Juniper Bay, a 300 ha drained Carolina Bay located near Lumberton, Robeson County, NC (Fig. 2). The bay was drained for agriculture beginning in 1971 by an extensive ditch network. At the time of the GPR calibration, the land was in fallow. Principal soils mapped within Juniper Bay are Leon fine sand, Pantego fine sandy loam, Ponzer muck, and Rutlege loamy sand (McCachren, 1978). The Taxonomic classification of these soils can be found in Table 1.

The area of Juniper Bay can be subdivided into "fieldlets," defined as areas of the bay confined by ditches on all sides (Fig. 3). In 2000, an original investigation of the bay's

stratigraphy was performed via coring with a hydraulic drilling machine. Within the rim of Juniper Bay and in the adjacent area, 29 cores were obtained to depths of 6.1 or 15.2 m. The coring sites were selected by placing an equilateral triangle grid over the bay, and choosing a number of core locations that would yield information representative of each soil type and be economically feasible. This preliminary coring survey revealed that the Coastal Plain sediments underlying the bay consisted of complex, interbedded layers of sandy and clayey material.

The GPR surveys of Juniper Bay were performed in December 2000 and June 2001 to provide additional information on the subsurface. The survey included transects totaling over 23 km. Transects were performed in 15 fieldlets where cores had previously been obtained (Fig. 3). Within each fieldlet, three GPR transects were performed: "center" - longitudinal transect down the center of the fieldlet; "edge" - longitudinal transect along the edge of the fieldlet; "cross" - lateral transect across the fieldlet, intersecting the core location (Fig. 3). Prior to the survey, flags were placed every 30 m along the transects, and their location was marked on the GPR trace by the operator as each flag was passed (Fig. 1). A differential global-positioning system (DGPS) was used to georeference each flag.

The GPR unit used was the Subsurface Interface Radar System-2000 (Geophysical Survey Systems, Inc. [GSSI], North Salem, NH). A 120 MHz antenna was used, with scanning time of 200 nanoseconds (ns). Operation of GPR has been discussed by Doolittle (1987), Daniels (1996), and Conyers and Goodman (1997). The RADAN NT (GSSI, version 2.0) software was used to process the radar profiles. Processing included color transformations, marker editing, distance normalization, and range gain adjustments. All

radar profiles were converted into bitmap images using the Radan to Bitmap Conversion Utility (GSSI, version 1.4).

A "lift-test" procedure was devised to quickly and clearly determine the location of the ground surface on a GPR profile. While stationary on level ground, a GPR scan was initiated. While scanning, the GPR unit was lifted by two people to shoulder height (Fig. 4A). After several seconds, the GPR unit was lowered to the ground, and the GPR scan was ended. Relative to the GPR unit, the ground surface is lower when the unit is lifted, producing a dip on the GPR profile (Fig. 4B). Lines on the GPR profile that do not dip can be considered noise. The uppermost dipping line can be delineated as the ground surface. This procedure was repeated at five locations at the study site.

Use of a buried metallic object to determine wave velocity was unsuccessful in the soils of Juniper Bay; therefore, wave velocity was determined via the reflector-interface matching method. Prominent GPR reflections were matched with abrupt soil horizon boundaries. Depths to horizon boundaries were determined by extracting soil cores and evaluating the texture of each soil layer. Velocity was calculated according to Eq. [1]. Reflector-interface matching was performed at three locations in December 2000, and thirteen more calibrations were done in August 2002.

The velocities determined by reflector-interface matching were examined for horizontal and vertical spatial patterns. Water table records from a concurrent study were used to establish which of the calibration points involved a soil horizon interface below the water table. A subset of the sixteen calibration points was chosen for calibrating the GPR surveys. From this subset of calibration points, a linear equation was obtained that related

TWT to depth of soil horizon interface. The equation was used to convert interpretations of GPR transects from TWT to depth.

Reflectors expected to be clayey soil horizons were interpreted on the GPR transects (Fig. 1). The TWT of the reflectors was recorded at 15 m intervals along all transects and used to predict the depths of the horizons. Depth was calculated using a correction from the lift-test and the calibration equation mentioned above.

A DGPS was used to navigate to a randomly chosen subset of the observation points and coring was done to groundtruth the depth predictions. Groundtruthing was done at 130 points along the center traces and at 44 points along the edge traces. Coring was done by bucket-augering. The occurrence and depth of clayey horizons were recorded in the field and supported by particle size analysis. Samples were collected from layers where interfaces were expected. These were air-dried and ground to pass a 2-mm mesh sieve. Clay percentage was determined by the hydrometer method of Gee and Bauder (1986). Sand fractions in selected samples were determined by sieving. When necessary, organic matter was removed by oxidation with hydrogen peroxide and heat. Accuracy of the GPR surveys was calculated as the absolute deviation between predicted and observed depth to clayey horizons.

$$\text{Absolute Deviation} = |\text{P.D.} - \text{O.D.}| \qquad [2]$$

where: P.D. = predicted depth based on GPR interpretation

O.D. = observed depth based on coring

RESULTS AND DISCUSSION

Lift-test

The findings from the list-test were similar for all five replications. In each of the resulting GPR profiles, the top of the third return was delineated as the ground surface (Fig. 4B). These results supported the approach of Augustinus and Nichol (1999) that a direct air-wave and direct ground-wave occur prior to the first return from the ground surface. It was assumed that the same pattern (ground surface being top of third return) occurred on the GPR profiles for all transects. The TWT represented by the first two returns on any given GPR transect ranged from 8 to10 ns, and this TWT was subtracted from the TWT of the predicted reflectors before converting them to a depth. The lift-test correction decreased the resulting depth by 0.22 to 0.28 m.

Wave Velocity and Calibration Equation

Wave velocity ranged from 0.052 to 0.133 m ns^{-1} (Table 2). No pattern was observed due to location within the bay, but a strong pattern was discovered due to relationship with the water table (Table 2). Wave velocity was slower when purported interfaces were below the water table than when above, with average velocities of 0.063 m ns^{-1} and 0.115 m ns^{-1}, respectively. When interfaces were above the water table, the calibration exercise measured the velocity of GPR waves in unsaturated sediment, or the unsaturated velocity. However, when interfaces were below the water table, the waves entered the ground through unsaturated sediment, encountered saturated sediment, reflected off the interface while in saturated sediment, and reentered unsaturated sediment before returning to the surface. The velocity measured in these instances can be considered an effective saturated velocity (Table

2). Saturation has been the cause of marked decreases in velocity in previous GPR studies (Birkhead et al., 1996, Bristow et al., 2000) and is explained by the much slower velocity of GPR waves through water versus air (Daniels, 1996).

Despite the separation of calibration points due to saturation, a two-velocity model was not chosen for this study. Based on water table depths at the time of the GPR surveys, 99.5% of reflectors delineated during interpretation were below the water table. Thus, calibration was based solely on the eleven saturated calibration points, which had a vertical range of 0.68 to 2.21 m (Fig. 5). For this subset, a linear relationship ($r^2 = 0.87$, $p<0.0001$) was found between TWT and depth to soil interface (Fig. 5). The resulting linear equation (Eq. 3) was used on interpretations of the transects to convert TWT to depth. Equation 3 was chosen over Eq. 1 for making the conversion because Eq. 3 is based upon field data obtained at multiple locations and obtained directly as TWT and depth. Theoretically, there should be no y-intercept term for Eq. 3, and the presence of the intercept term suggests that the relationship between TWT and depth must change slope or become non-linear between 0 and 0.68 m. This was not a concern because less than 1% of the interpreted data were within that range.

$$y = 0.0274x + 0.1631 \quad [3]$$

where: y = predicted depth of reflector

x = predicted TWT of reflector, after lift-test correction

Accuracy

The relationship between depth of clayey horizons determined by coring and predicted by GPR is shown in Fig. 6A. Ideally, the points would fall along a line having

slope of one and y-intercept of zero. A significant linear relationship was found between the predicted and observed depths ($r^2 = 0.62$, $p<0.0001$), but the slope was significantly different than one ($p<0.0001$) and the y-intercept significantly different than zero ($p=0.009$). The points are scattered relatively evenly above and below the 1:1 line, indicating there was not a strong tendency to overestimate or underestimate depth with the GPR interpretation. The calibration points are shown on Fig. 6A to illustrate that few of the interpretations required extrapolation from the calibration equation; extrapolation occurred primarily from 2.2 to 2.8 m.

Absolute deviation (deviation) was calculated for each of the 174 groundtruth points. The deviation ranged from 0 to 0.95 m. This variation is apparent in the relatively low correlation coefficient of the trend-line ($r^2= 0.62$). The average deviation was 0.250 m (SD = 0.189 m). With the range in depth of clayey horizon being 0.60 to 3.20 m, the average percent error (absolute deviation relative to depth) was 16%. These prediction errors are somewhat high compared with other GPR studies that sought the depth of a stratigraphic layer or soil horizon (Table 3). The deviation observed in this and other studies was not necessarily due to inherent inaccuracies of the GPR method. Differences between observed and interpreted depths can be explained by a variety of situations: non-vertical alignment of the coring device (Collins et al., 1989, Birkhead et al. 1996); other errors in coring or rounding of observed depths (Collins et al., 1989, Doolittle et al., 2000); rounding of GPR interpretation or interpreter error (Collins et al., 1989, Doolittle et al., 2000); spatial discrepancy between the location of GPR transect and coring (Collins et al., 1989, Doolittle et al., 2000); highly irregular interface/boundary (Birkhead et al., 1996, Doolittle et al., 2000); or highly complex subsurface stratigraphy (Birkhead et al., 1996, Poole et al., 1997,

Doolittle et al., 2000). The complex stratigraphy and site characteristics at Juniper Bay may have been the primary sources of error in this study. Complex stratigraphy present in much of the bay could have caused destructive interference of GPR waves, making interpretation difficult (Lapen et al., 1996, Young and Sun, 1999, Nobes et al., 2001). The scale of the GPR survey at Juniper Bay was much greater than most surveys listed in Table 3. Thus, some portions of the bay were favorable for the use of GPR, and other areas were quite unfavorable. Clay content and poor drainage conditions have been identified as characteristics that make a site less suitable for GPR surveys (Doolittle and Collins, 1995, Williams, 1996), and parts of Juniper Bay possessed one or both of these negative attributes. Some areas of Juniper Bay were unfavorable for GPR interpretation due to the nature of the interface being detected. Often, the interface from coarse to fine material in Juniper Bay was a gradual boundary, or the change in texture was not extreme. Such conditions produce a less distinct GPR reflection than when the boundary is abrupt and the change in texture great (Collins and Doolittle, 1987). Many of the studies in Table 3 were detecting an interface that was very likley to yield distinct GPR reflections, such as the soil or sediment to bedrock interfaces detected by Collins et al. (1989) and Birkhead et al. (1996).

Given the scale and complexity of Juniper Bay, a more appropriate comparison with the small-scale studies in Table 3 was made by calculating the accuracy of the GPR survey along one transect that had characteristics favorable for GPR use. In fieldlet 12, where predominantly loamy sand horizons overlaid a sandy clay loam to clay horizon, average absolute deviation was 0.180 m or 9.6 %; this is over 6% better than when calculated over the entire site (Table 3). The relationship between observed and predicted ($r^2 = 0.80$) was better when considered for only fieldlet 12. Although the average percent error for fieldlet

12 falls lower in the range presented in Table 3, we believe that our results over the entire bay were more relevant and more valuable. Table 3 shows that most studies of GPR's accuracy involved transects less than 1 km in length, where calibration sites were apt to be very near the groundtruthing sites. Such small-scale studies have reported average percent error between 4 and 10%. The limited number of large-scale studies indicate that accuracy of GPR is 10% or much greater. If GPR is to be used more often in practical applications by industry and consulting firms, then assessments of accuracy must be provided not only for small, favorable field sites, but also for large, variable, and complex sites.

Other factors found to contribute to inaccuracy included differences in soil type and depth of reflection. Based on pit descriptions and remapping by Ewing (unpublished data, 2003), groundtruth points were divided into categories: mineral soil, soil with a histic epipedon (histic), and Histisol. Results of an ANOVA with two orthogonal contrasts showed there to be no significant difference between absolute deviation of histic versus Histisol ($p=0.8475$), but there was a significant difference between mineral and organic (histic and Histisol) ($p=0.0330$). Average deviation was 0.211 m (SD = 0.152) and 0.280 m (SD = 0.206) for mineral and organic soil, respectively. Although some calibration sites were within both mineral and organic soils, organic's larger deviation may be attributed to wave velocity through organic material being dependent on the decomposition state of the material (Lapen et al., 1996). Average deviation was influenced by depth of reflection. In particular, average deviation was much greater when the depth of reflection was above or below the calibration range (average 0.412 m, SD = 0.262) than when within the calibration range (average 0.224 m, SD = 0.162).

A reanalysis of the accuracy results without making the lift-test correction illustrated the impact of this procedure. Fig. 6B shows the relationship between predicted and observed depth to clayey horizons had the lift-test correction not been made. Although the slope and r^2 changed only slightly, the trend-line shifted upward and to the right. This shift was due to the majority of points occurring above the 1:1 line, indicating that depth was overestimated more often without the lift-test correction. Average deviation increased to 0.277 m (SD 0.209) without the lift-test correction.

The decision to use only saturated calibration points for the calibration equation did not have a large impact on the accuracy results. If all sixteen calibration points were used for the equation, rather than only the eleven saturated points, the average deviation increased slightly to 0.253 m (SD 0.191). However, if calibration was only done in unsaturated conditions, accuracy would have been drastically worse. It is not unreasonable to consider this hypothetical situation, as calibration of GPR is often done at only one or two shallow depths. If we had calibrated to only unsaturated depths, the average deviation would have been 0.619 m (SD 0.350), more than double the deviation we actually achieved. Calibration based on the higher velocity in the unsaturated soil (Table 2) would have resulted in gross overestimation of clayey horizon depth in most instances. Figure 6C shows the relationship between predicted and observed depth had only unsaturated calibration points been used. The slope of the trend-line is much less than one, and almost all of the data points fall above the 1:1 line. This comparison highlights the importance of identifying sources of vertical variation in wave velocity.

In Fig. 7, the average deviation of the chosen calibration method (saturated calibration equation with lift-test) is compared to those from the hypothetical scenarios

discussed above. Because the raw interpretation of the GPR profiles was done in TWT, the lift-test correction and calibration equations could be readily altered and recomputed via a spreadsheet. This approach allowed much greater flexibility during calibration than would be possible if interpretation was done via a predetermined depth-scale.

SUMMARY AND CONCLUSION

This study demonstrated two procedures that may aid in the accuracy of depth prediction made with GPR surveys. The lift-test is a simple, quick, and effective method for identifying the ground surface. It is important to leave no ambiguity regarding the location of the ground surface on GPR profiles so that the calibration or depth-scaling can begin at the proper location on the profile. Our results indicated that the lift-test improved accuracy by 0.027m, approximately a 10% improvement. We recommend the practice of using multiple calibration points to create calibration equations that relate TWT to depth. Calibration in this manner permits quick manipulation of data and allows researchers to identify potential sources of spatial variation in wave velocity that could impact accuracy. It is important to cover a vertical range in calibration points so that less extrapolation occurs when calibration is applied to a range of interpreted data. We feel that more studies of GPR's effectiveness are required for large-scale, complex sites, and we believe the use of multiple calibration points will be particularly valuable for such studies.

REFERENCES

Asmussen, L.E., H.F. Perkins, and H.D. Allison. 1986. Subsurface descriptions by ground-penetrating radar for watershed delineation. Bull. 340. The Georgia Agricultural Experiment Stations, The University of Georgia, Athens.

Augustinus, P.C., and S. Nichol. 1999. Ground-penetrating radar imaging of Pleistocene sediments, Boco Plain, western Tasmania. Aust. J. Earth Sci. 46(2):275-282.

Beres, M., P. Huggenberger, A.G. Green, and H. Horstmeyer. 1999. Using two- and three-dimensional georadar methods to characterize glaciofluvial architecture. Sediment. Geol. 129:1-24.

Birkhead, A.L., G.L. Heritage, H. White, and A.W. van Niekerk. 1996. Ground-penetrating radar as a tool for mapping the phreatic surface, bedrock profile, and alluvial stratigraphy in the Sabie River, Kruger National Park. J. Soil Water Conserv. 51(3):234-240.

Boll, J., R.P.G. van Rijn, K.W. Weiler, J.A. Ewen, J. Daliparthy, S.J. Herbert, and T.S. Steenhuis. 1996. Using ground-penetrating radar to detect layers in a sandy field soil. Geoderma 70:117-132.

Bristow, C.S., J.L. Best, and P.J. Ashworth. 2000. The use of GPR in developing a facies model for a large sandy braided river, Brahmaputra River, Bangladesh. p. 95-100. *In* D.A. Noon, G.F. Stickley, and D. Longstaff (ed.) Proc. Int. Conf. Ground Penetrating Radar, 8th. Univ. of Queensland. SPIE Vol. 4084.

Cagnolli, B., and J.K. Russell. 2000. Imaging the subsurface stratigraphy in the Ubehebe hydrovolcanic field (Death Valley, California) using ground penetrating radar. J. Volcanol. Geotherm. Res. 96:45-56.

Collins, M.E., and J.A. Doolittle. 1987. Using ground-penetrating radar to study soil microvariability. Soil Sci. Soc. Am. J. 51:491-493.

Collins, M.E., J.A. Doolittle, and R.V. Rourke. 1989. Mapping depth to bedrock on a glaciated landscape with ground-penetrating radar. Soil Sci. Soc. Am. J. 53:1806-1812.

Collins M.E., G.W. Schellentrager, J.A. Doolittle, and S.F. Shih. 1986. Using ground-penetrating radar to study changes in soil map unit composition of selected histosols. Soil Sci. Soc. Am. J. 50:408-412.

Conyers, L.B., and C.M. Cameron. 1998. Ground-penetrating radar techniques and three-dimensional computer mapping in the American Southwest. J. Field Arch. 25:417-430.

Conyers, L.B., and D. Goodman. 1997. Ground-penetrating radar: an introduction for archaeologists. AltaMira Press, Walnut Creek, CA.

Dagallier, G., A.I. Laitinen, F. Malartre, I.P.A.M. Van Campenhout, and P.C.H. Veeken. 2000. Ground penetrating radar application in a shallow marine Oxfordian limestone sequence located on the eastern flank of the Paris Basin, NE France. Sediment. Geol. 130:149-165.

Daniels, D.J. 1996. Surface-penetrating radar. Institution of Electrical Engineers, London, UK.

Dominic, D.F., K. Egan, C. Carney, P.J. Wolfe, and M.R. Boardman. 1995. Delineation of shallow stratigraphy using ground penetrating radar. J. Appl. Geophys. 33:167-175.

Doolittle, J.A. 1987. Using ground-penetrating radar to increase the quality and efficiency of soil surveys. p. 11-32. *In* W.U. Reybold, and G.W. Peterson (ed.) Soil Survey Techniques, Soil Sci. Soc. Am. Spec. Publ. No. 20.

Doolittle, J.A., and M.E. Collins. 1995. Use of soil information to determine application of ground penetrating radar. J. Appl. Geophys. 33:101-108.

Doolittle, J.A., G. Hoffmann, P. McDaniel, N. Peterson, B. Gardner, and E. Rowan. 2000. Ground-penetrating radar interpretations of a fragipan in northern Idaho. Soil Surv. Horiz. 41(3):73-82.

Gee, G.W., and J.W. Bauder. 1986. Particle-size analysis. p. 383. In Klute et al. (ed.) Methods of soil analysis. Part 1 Physical and mineralogical methods. ASA, CSSA, and SSSA, Madison, WI.

Gish, T.J., W.P. Dulaney, K.-J.S. Kung, C.S.T. Daughtry, J.A. Doolittle, and P.T. Miller. 2002. Evaluating use of ground-penetrating radar for identifying subsurface flow pathways. Soil Sci. Soc. Am. J. 66:1620-1629.

Hubbard, R.K., L.E. Asmussen, and H.F. Perkins. 1990. Use of ground-penetrating radar on upland Coastal Plain soils. J. Soil Water Conserv. 45(3):399-404.

Imai, T., T. Sakayama, and T. Kanemori. 1987. Use of ground-probing radar and resistivity surveys for archaeological investigations. Geophysics 52(2):137-150.

Kettles, I.M., and S.D. Robinson. 1997. A ground-penetrating radar study of peat landforms in the discontinuous permafrost zone near Fort Simpson, Northwest Territories, Canada. p. 147-160. *In* C.C. Trettin, M.F. Jurgensen, D.F. Grigal, M.R. Gale, and J.K. Jeglum (ed.) Northern forested wetlands: Ecology and management. CRC Lewis Publishers, Boca Raton, FL.

Langsholt, E., N.-O. Kitterød, and L. Gottschalk. 1998. Development of three-dimensional hydrostratigraphical architecture of the unsaturated zone based on soft and hard data. Ground Water 36(1):104-111.

Lapen, D.R., B.J. Moorman, and J.S. Price. 1996. Using ground-penetrating radar to delineate subsurface features along a wetland catena. Soil Sci. Soc. Am. J. 60:923-931.

McCachren, C.M. 1978. Soil survey of Robeson County, North Carolina. USDA-SCS, North Carolina Agricultural Experiment Station and Robeson County Board of Commissioners, U.S. Gov. Print. Office, Washington, D.C.

Mellett, J.S. 1995. Ground penetrating radar applications in engineering, environmental management, and geology. J. Appl. Geophys. 33:157-166.

Mills, H.H., and M.A. Speece. 1997. Ground-penetrating radar exploration of alluvial fans in the southern Blue Ridge Province, North Carolina. Environ. Eng. Geosci. 3(4):487-499.

Mokma, D.L., R.J. Schaetzl, J.A. Doolittle, and E.P. Johnson. 1990. Ground-penetrating radar study of ortstein continuity in some Michigan haplaquods. Soil Sci. Soc. Am. J. 54:936-938.

Nobes, D.C., R.J. Ferguson, and G.J. Brierley. 2001. Ground-penetrating radar and sedimentological analysis of Holocene floodplains: insight from the Tuross valley, New South Wales. Aust. J. Earth Sci. 48:347-355.

Poole, G.C., R.J. Naiman, J. Pastor, and J.A. Stanford. 1997. Uses and limitations of ground penetrating radar in two riparian systems. p.140-148. *In* J. Gibert, J. Mathieu, and F. Fournier (ed.) Groundwater/surface water ecotones: Biological and hydrological interactions and management options. International Hydrology Series. Cambridge University Press, New York, NY.

Tomer, M.D., J. Boll, K.-J.S. Kung, T. Steenhius, and J.L. Anderson. 1996. Detecting illuvial lamellae in fine sand using ground-penetrating radar. Soil Sci. 161(2):121-129.

Topp, G.C., J.L. Davis, and A.P. Annan. 1980. Electromagnetic determination of soil water content: Measurements in coaxial transmission lines. Water Resour. Res. 16:574-582.

Van Dam, R.L, and W. Schlager. 2000. Identifying causes of ground-penetrating radar reflections using time-domain reflectometry and sedimentological analyses. Sedimentology 47:435-449.

van Overmeeren, R.A. 1998. Radar facies of unconsolidated sediments in The Netherlands: a radar stratigraphy interpretation method for hydrogeology. J. Appl. Geophys. 40:1-18.

Vogt, K., J. Doolittle, and R. Fenwick. 1996. Mapping the thickness of flood-plain splay deposits with ground-penetrating radar techniques. Soil Surv. Horiz. 37(3):93-100.

Williams, A. 1996. Linking ground-penetrating radar and geographical information systems in west Florida. Soil Surv. Horiz. 37(4):119-123.

Young, R.A., and J. Sun. 1999. Revealing stratigraphy in ground-penetrating radar data using domain filtering. Geophysics 64(2):435-442.

Table 1. Classification of soils mapped at Juniper Bay.

Soil Series	Family Taxonomy
Leon	sandy, siliceous, thermic Aeric Alaquods
Rutlege	sandy, siliceous, thermic Typic Humaquepts
Pantego	fine-loamy, siliceous, semiactive, thermic Umbric Paleaquults
Ponzer	loamy, mixed, dysic, thermic Terric Haplosaprists

McCachren, 1978

Table 2. Comparison of GPR wave propagation velocity data above and below water table.

Moisture Condition	Number of Points	Average Velocity	S.E.	Maximum	Minimum
		----------m ns^{-1}----------			
Effective Saturated	11	0.063	0.002	0.079	0.052
Unsaturated	5	0.115	0.006	0.133	0.099

Table 3. Summary of accuracy in predicting depth to a subsurface interface for various GPR studies. Some studies included data on several interfaces or determined by different methods, and in such cases each result is listed separately. If reported, the distance of GPR survey that included groundtruthing is given. Substrate of the GPR survey site, interface being detected, number of points where predicted and observed depth were compared, correlation/regression results, and average percent error are also given. Percent error is the absolute deviation between observed and predicted divided by the observed depth, on a percent basis. Results are ranked by average percent error. Current study is shown in bold. The row labeled "entire" represents all groundtruthing at Juniper Bay, and the row marked "transect" represents groundtruthing only within fieldlet 12.

Source	Surveyed Distance	Substrate	Interface Detected	Number of Observation Points	Relationship Observed vs. Predicted	Average Percent Error
	----km---					---%---
Collins et al., 1989	0.090	loamy soil	bedrock	61	r = 0.98	4.1†
Birkhead et al., 1996	0.090	sand-gravel bar	bedrock	15	R^2 = 0.85	4.4#
Collins and Doolittle, 1987	0.200	sandy spodosol	argillic horizon	4	na	5.2†
Asmussen et al., 1986 - grid	unknown (2.33 ha)	sandy soil	argillic horizon	8	r = 0.99	7.0‡
Birkhead et al., 1996	0.375	sand-gravel bar	water table	70	R^2 = 0.97	7.9#
Collins and Doolittle, 1987	0.200	sandy spodosol	spodic horizon	4	na	9.1†
Doolittle et al., 2000	0.030	Alfisol	fragipan	21	r = 0.49	9.4‡
Szuch 2004 - transect	0.630	sandy soil	clayey horizon	9	r^2 = 0.80	9.6‡
Lapen et al., 1996	0.500	Bog	various	10	r = 0.99	10.1‡
Vogt et al., 1996	13.800	flood deposits	sediment over soil	25	r^2 = 0.95	10.1†
Szuch 2004 - entire	23.200	various soils	clayey horizon	174	r^2 = 0.62	16.0‡
Asmussen et al., 1986 - transect	1.600	sandy soil	argillic horizon	14	r = 0.95	57.1‡

† = calculated based on average or range of deviation and depth given in source

‡ = calculated based on results at individual observations points given in source (note: This calculation reveals a more accurate and typically higher percent error than when done based on average deviation and depth.)

= reported as percent error in source

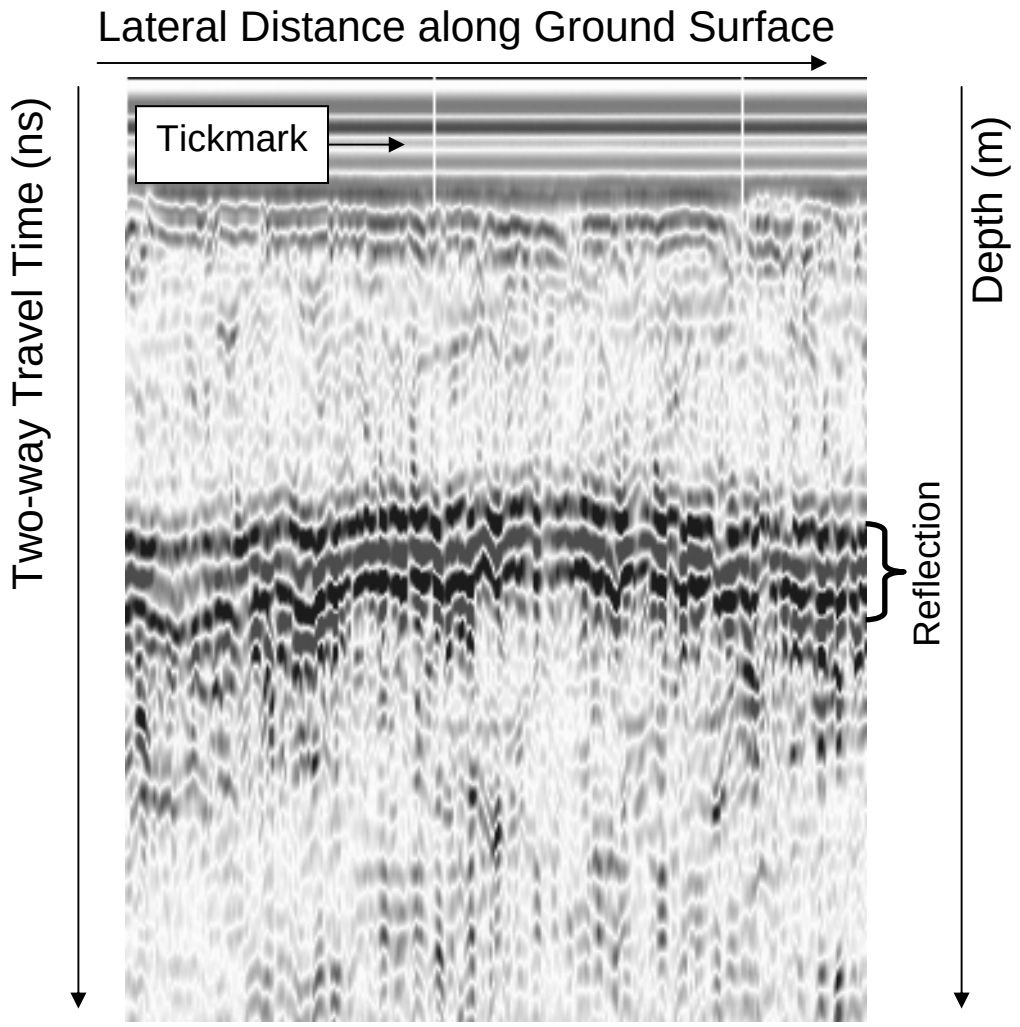

Fig. 1. Example of GPR profile from survey at Juniper Bay. Horizontal axis depicts lateral distance along ground surface. Tickmarks were placed by GPR operator in the field and correspond to the location of survey flags every 30 m. Vertical axis originally depicts two-way travel time (left side) and after calibration with wave propogation velocity depicts depth (right side). Multiple bright lines indicate a GPR reflection and are expected to represent a sandy to clayey soil horizon interface.

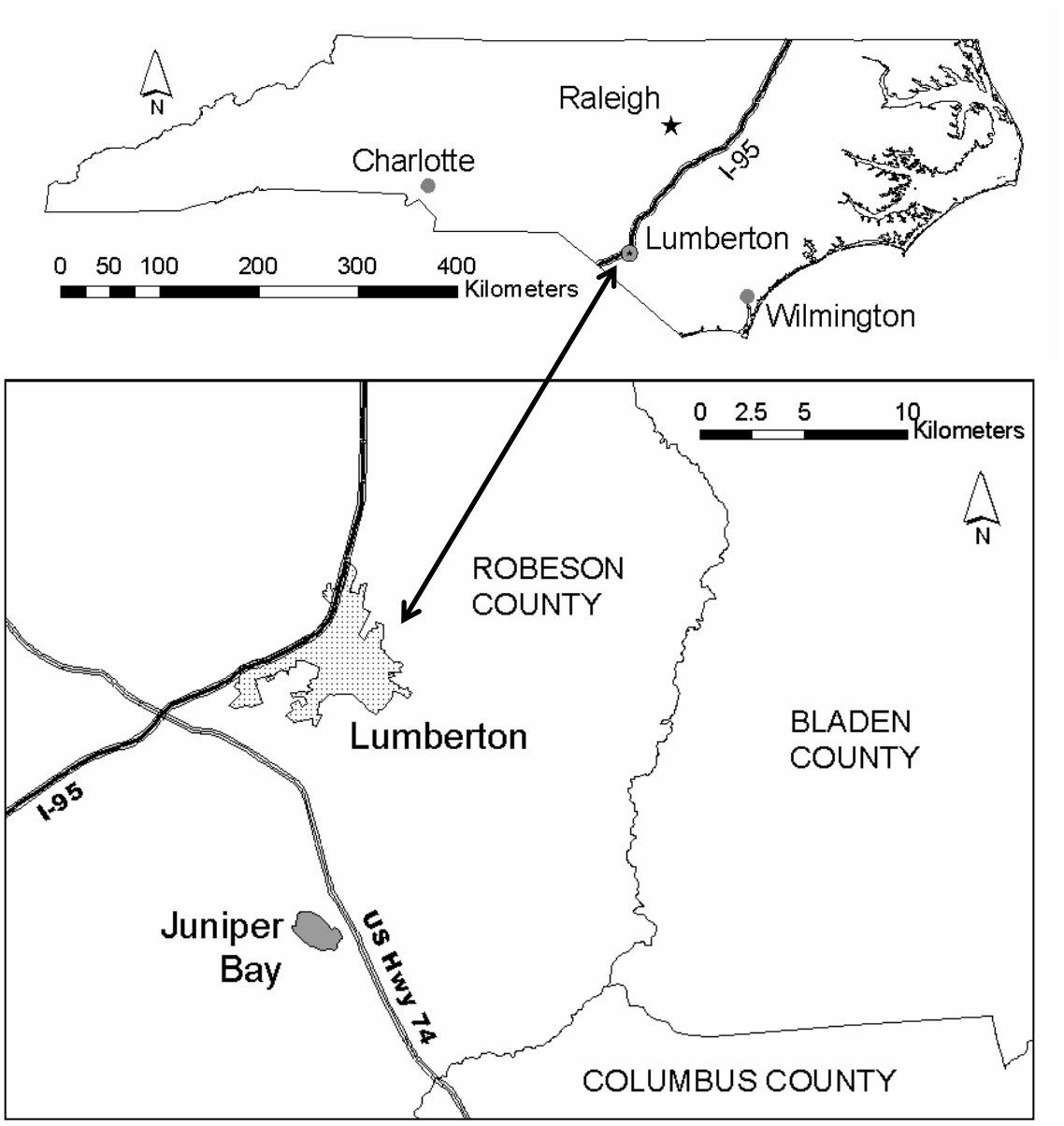

Fig. 2. Map of North Carolina and Lumberton area showing location of the Juniper Bay study site. Arrow shows the location of Lumberton on both large and small scale maps.

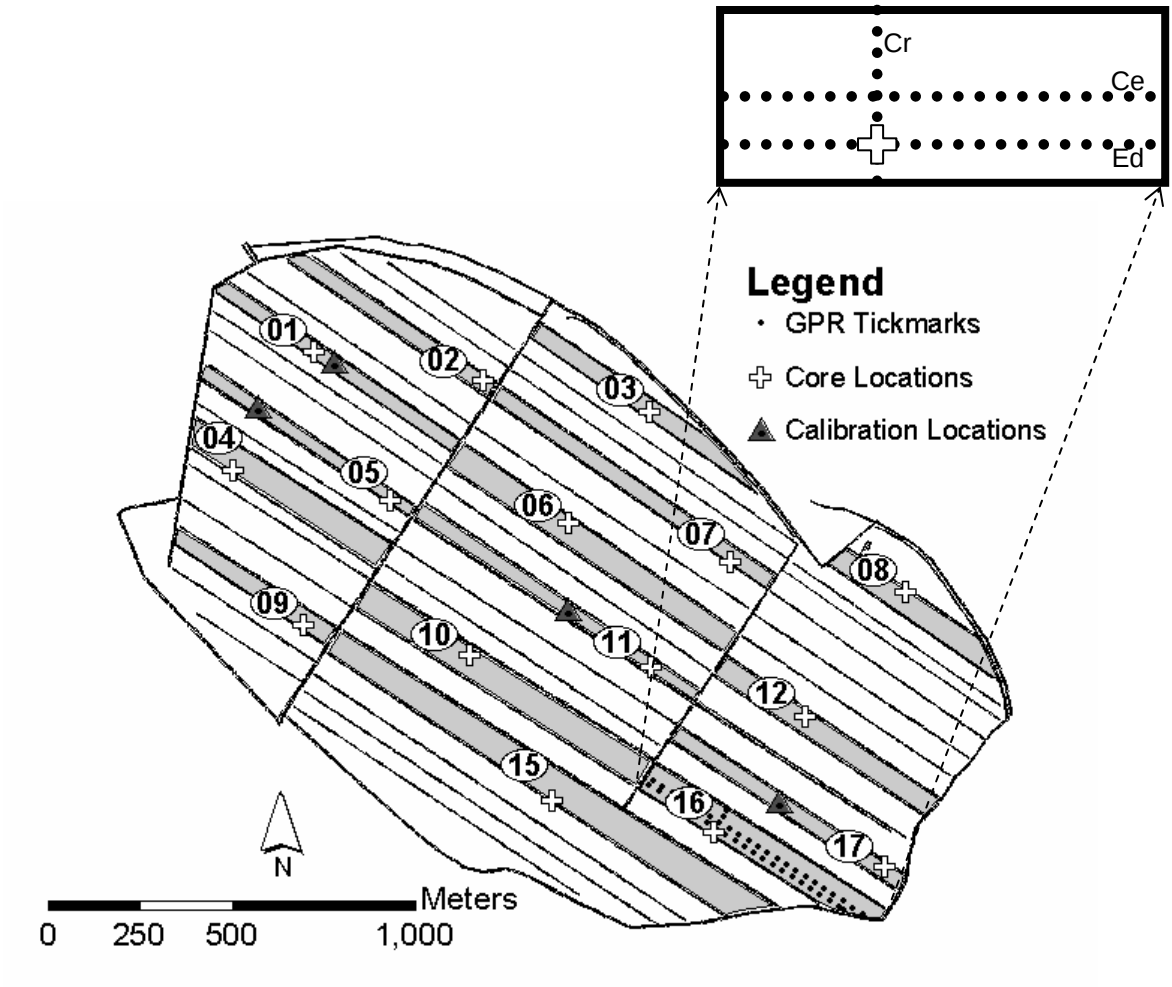

Fig. 3. Map of Juniper Bay showing fieldlets where GPR surveys were conducted highlighted in gray and numbered for identification. Location of cores for preliminary survey are shown with bold crosses. In fieldlet 16 and in the blowup diagram, an example of the orientation of the center (Ce), edge (Ed), and cross (Cr) GPR transects is shown along with the location of the core. Each dot represents a tickmark from the GPR transect, located every 30 m. The known locations of calibration points are shown with triangles.

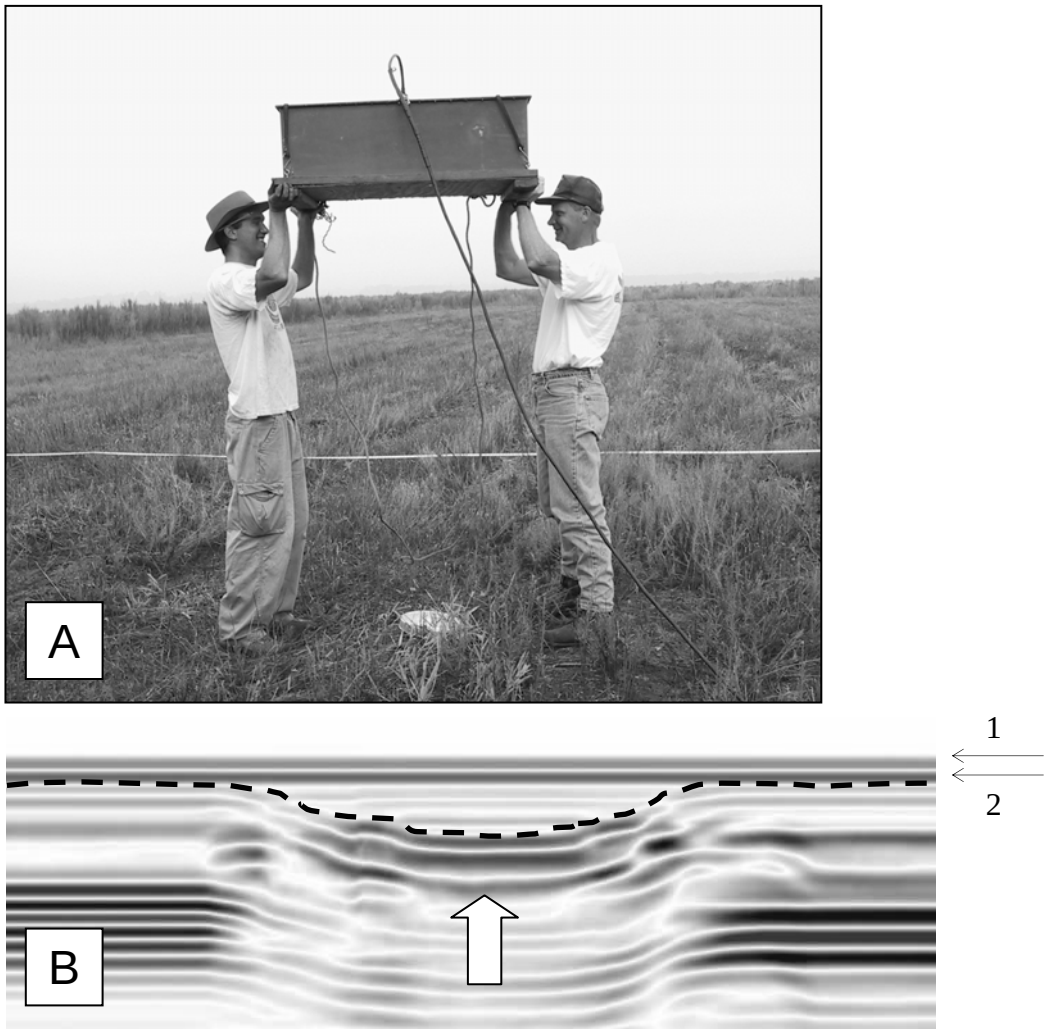

Fig. 4. (A) Photograph of lift-test being implemented in the field, during step when GPR unit is raised to shoulder height while scanning. (B) Bitmap image resulting from lift-test and used to locate the soil surface on GPR profiles. Soil surface is the upper most dipping line, which is indicated by dotted black line. Stick arrows labeled 1 and 2 correspond to the direct air-wave and direct ground-wave, respectively. The white block arrow points to the spot on the bitmap that corresponds to the timing of the photograph.

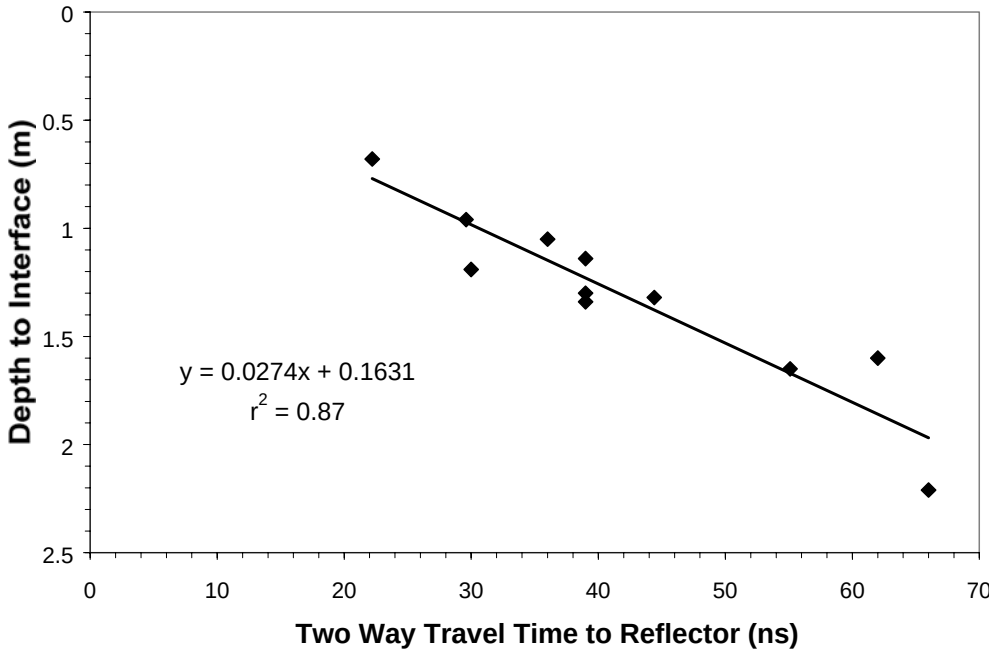

Fig. 5. Plot of calibration dataset for interfaces in saturated soil and resultant regression equation used to convert TWT to depth.

Fig. 6. Comparisons between observed and predicted depth to clayey horizons in Juniper Bay. Observed depths determined via coring. Predicted depths interpreted from GPR surveys. Predicted depths calculated using **(A)** the chosen calibration method of lift-test correction and saturated calibration equation, **(B)** a hypothetical calibration method of no lift-test correction and saturated calibration equation, **(C)** a hypothetical calibration method of lift-test correction and unsaturated calibration equation. The best-fit line, linear equation, and r^2 are shown for each scenario, and the best-fit line of scenario A is maintained on the subsequent plots.

Fig. 6. (continued)

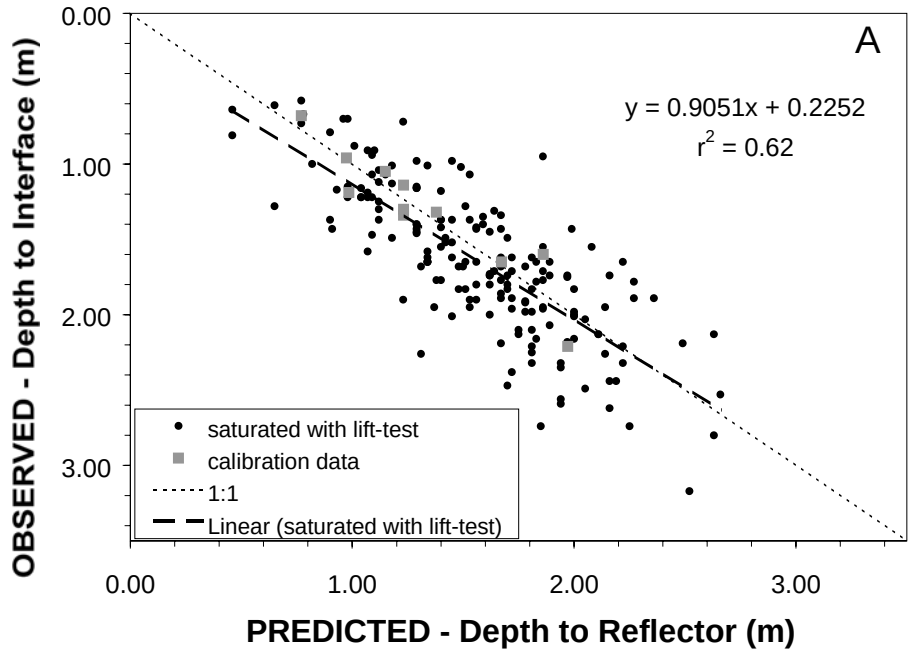

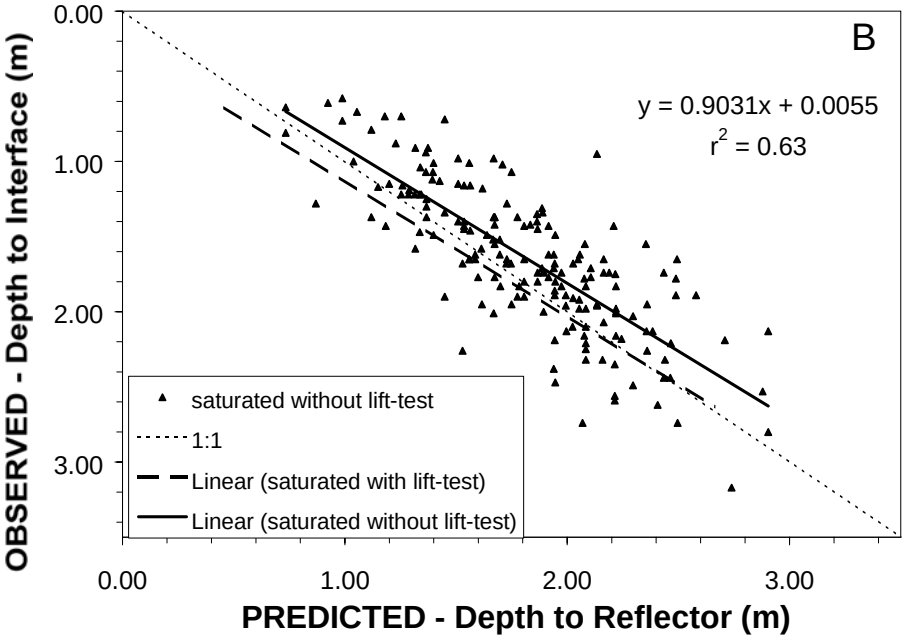

Fig. 6. (continued)

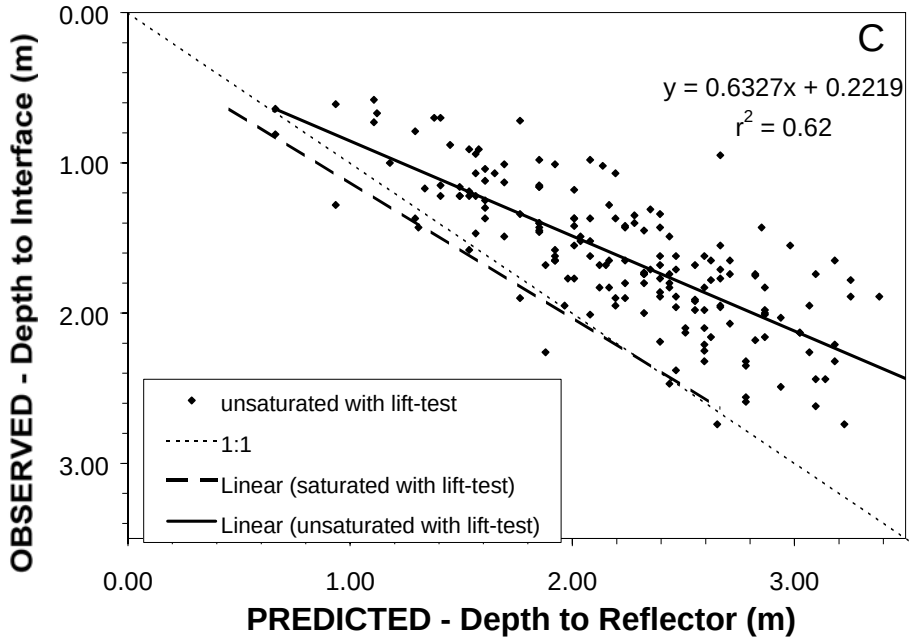

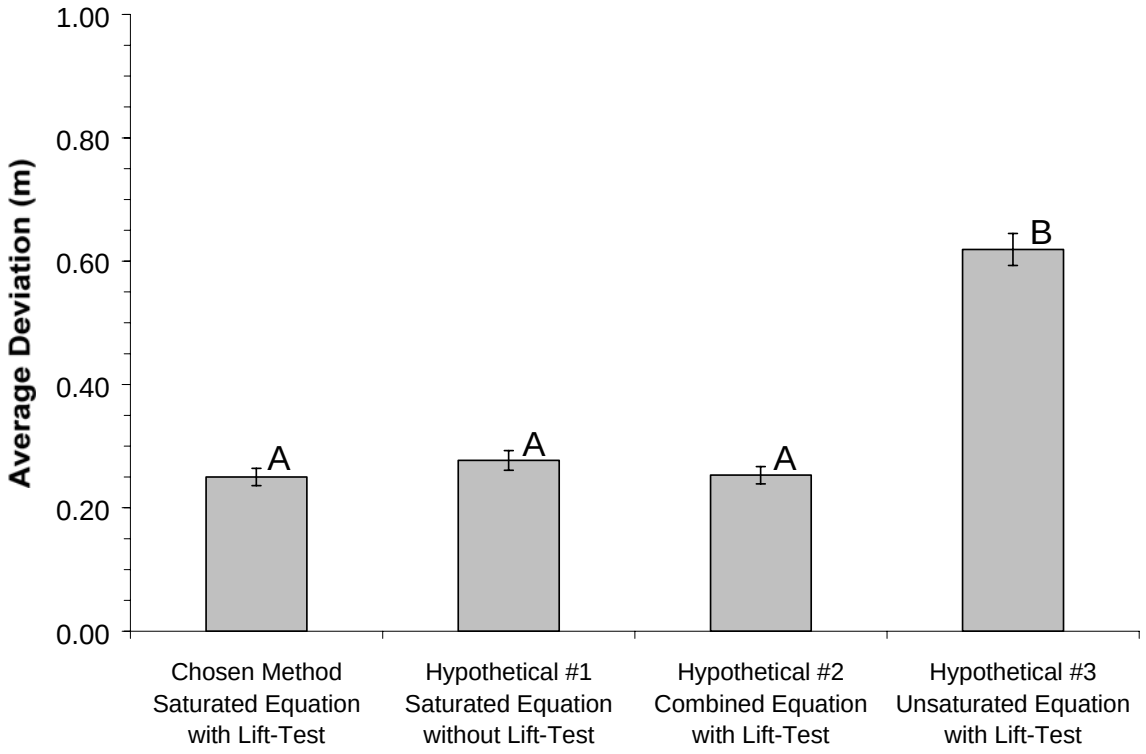

Fig. 7. Average deviation between observed and predicted depth to clayey horizons for the chosen calibration method compared with other hypothetical calibration scenarios. Error bars are standard error of the average deviation. Letters indicate groupings that are not significantly different according to protected LSD procedure ($p<0.0001$).

CHAPTER 3
Description of Subsurface Stratigraphy of a Carolina Bay via Ground-Penetrating Radar and a Conceptual Model for Bay Formation

INTRODUCTION

Carolina Bays (bays) are a wetland type found along the Atlantic Coastal Plain. Bays occur as shallow, oval-shaped, depressions. The geographical extent of bays ranges from New Jersey to northern Florida (Melton and Schriever, 1933, Frey, 1950, Prouty, 1952, Bliley and Pettry, 1979), but they are most prevalent within the Carolinas. An estimated 500,000 bays exist along the Coastal Plain, with about 80% of these occurring within the Carolinas (Prouty, 1952). Bays occur in sizes between one and thousands of hectares (Prouty, 1952, Thom, 1970). The unique characteristics and values of bays were recently reviewed by Sharitz (2003).

The origin of bays has been debated for many years. Current knowledge suggests that the typical expression of these features is due to wind-driven waves acting upon shallow ponds or water-filled depressions (Thom, 1970, Kaczorowski, 1977, Grant et al., 1998). The cause of the original depression remains uncertain, but processes such as spring activity, solution, deflation, or abandonment of channel segments have been offered as possibilities (Grant et al., 1998).

Soils of Carolina Bays can be quite variable (Frey, 1950, Saunders, 1990, Reese and Moorehead, 1996). Many bays contain continuous or nearly continuous clayey horizons in the subsurface (Sharitz and Gibbons, 1982). These clayey horizons often have a strong impact on the hydrology of bays (Johnson, 1942, Lide et al., 1995, Sharitz, 2003). Studies of near-surface soil horizons have reported predominantly sandy (Gamble et al., 1977,

Saunders, 1990) or organic soils (Saunders, 1990, May and Warne, 1999). Knowledge of soils and stratigraphy of Carolina bays may aid our understanding of their hydrologic setting and geomorphic origin.

Ground-penetrating radar (GPR) is a geophysical technique often used to study shallow stratigraphy of soils and sediments. Because it obtains continuous data along survey paths, GPR provides a much greater amount of information than discrete sampling by coring or digging (Mokma et al., 1990, Poole et al., 1997, Conyers and Goodman, 1997). Ground-penetrating radar has been used to describe the stratigraphy of glaciofluvial sediments (Langsholt et al., 1998, Beres et al., 1999), deltaic sediments (Asprion and Aigner, 1999), fluvial sediments (Birkhead et al., 1996, Mills and Speece, 1997, Bristow et al., 2000, Nobes et al., 2001), soils (Mokma et al., 1990, Tomer et al., 1996), and wetlands (Lapen et al., 1996, Poole et al., 1997, van Overmeeren, 1998). When calibrated properly (Conyers and Goodman, 1997, Szuch et al., 2004a), GPR surveys are able to estimate the depth of specific subsurface features, including soil horizons (Asmussen et al., 1986, Collins and Doolittle, 1987, Boll et al., 1996, Doolittle et al., 2000).

An extensive GPR survey was performed at four bays in South Carolina to map subsurface stratigraphy (Grant et al., 1998). The results of the GPR survey, combined with geological, archaeological, and ecological data, fostered modification of theories on the evolution of Carolina Bays and supported hydrological research (Lide et al., 1995) at one of the bays. The GPR study identified clayey interior bay sediments that were expected to influence hydrology and provided information on the formation and erosion of the bays' sandy rims.

The objective of this study was to investigate the stratigraphy of Juniper Bay, a drained bay in southeastern North Carolina, using GPR surveys. Juniper Bay is being restored for wetland mitigation credit, and results of the GPR study may aid in the restoration plan (Szuch et al., 2004b). The results also may be used to support research on the geomorphic setting and formation of Juniper Bay (Zanner, 2003) and the hydrology of Juniper Bay (Kreiser, unpublished data, 2003).

MATERIALS AND METHODS

The study site was Juniper Bay, a 300 ha drained Carolina Bay located near Lumberton, Robeson County, NC (Fig. 1). The bay was drained for agriculture beginning in 1971 by an extensive ditch network. In 2000, the North Carolina Department of Transportation (NCDOT) purchased the property and intends to restore Juniper Bay to receive wetland mitigation credit. Restoration efforts were initiated in June 2003. Principal soils mapped within Juniper Bay are Leon fine sand, Pantego fine sandy loam, Ponzer muck, and Rutlege loamy sand (McCachren, 1978) (Table 1).

The area of Juniper Bay can be subdivided into "fieldlets," defined as areas of the bay confined by ditches on all sides (Fig. 2). In 2000, an original investigation of the bay's stratigraphy was performed via coring with a hydraulic drilling machine. Within the rim of Juniper Bay and in the surrounding area, 29 cores were obtained to depths of 6.1 or 15.2 m. The coring sites were selected by placing an equilateral triangle grid over the bay, and choosing a number of core locations that would yield information representative of each soil type and be economically feasible. This preliminary coring survey revealed that the Coastal

Plain sediments underlying the bay consisted of complex, interbedded layers of sandy and clayey material.

The GPR surveys of Juniper Bay were performed in December 2000 and June 2001 to provide additional information on the subsurface. At the time of the GPR survey, the land was in fallow. The survey included transects totaling over 23 km. Transects were performed in 15 fieldlets where cores had previously been obtained (Fig. 2). Within each fieldlet, three GPR transects were performed: "center" - longitudinal transect down the center of the fieldlet; "edge" - longitudinal transect along the edge of the fieldlet; "cross" - lateral transect across the fieldlet, intersecting the core location (Fig. 2). Flags were placed every 30 m along the transects, which were marked on the GPR trace by the operator as each flag was passed (Fig. 3). A differential global-positioning system (DGPS) was used to georeference each flag.

The GPR unit used was the Subsurface Interface Radar System-2000 (Geophysical Survey Systems, Inc. [GSSI], North Salem, NH). A 120 MHz antenna was used, with scanning time of 200 nanoseconds (ns). Operation of GPR has been discussed by Doolittle (1987), Daniels (1996), and Conyers and Goodman (1997). The RADAN NT (GSSI, version 2.0) software was used to process the radar profiles. Processing included color transformations, marker editing, distance normalization, and range gain adjustments. All radar profiles were converted into bitmap images using the Radan to Bitmap Conversion Utility (GSSI, version 1.4). The GPR was calibrated using a lift-test to define the soil surface and a calibration equation based on reflector-interface matching at multiple points (Szuch et al., 2004a).

Reflectors expected to be clayey soil horizons were interpreted on the GPR transects (Fig. 3). The two-way travel time of the reflectors was recorded at 15 m intervals along all transects and used to predict the depths of the horizons. Depth was calculated using a correction from the lift test and the calibration equation mentioned above.

A DGPS was used to navigate to a randomly chosen subset of the observation points and coring was done to groundtruth the depth predictions. Groundtruthing was done at 130 points along the center traces and at 44 points along the edge traces. Coring was done by bucket-augering. The occurrence and depth of clayey horizons were recorded in the field and supported by particle size analysis. Samples were collected from layers where interfaces were expected. These were air-dried and ground to pass a 2-mm mesh sieve. Clay percentage was determined by the hydrometer method of Gee and Bauder (1986). Sand fractions in selected samples were determined by sieving. When necessary, organic matter was removed by oxidation with hydrogen peroxide and heat. Accuracy of the GPR surveys was calculated as the absolute deviation between predicted and observed depth to clayey horizons:

$$\text{Absolute Deviation} = |\text{P.D.} - \text{O.D.}| \qquad [1]$$

where: P.D. = predicted depth based on GPR interpretation

O.D. = observed depth based on coring

In GPR surveys of sediment deposits, it is common to base interpretations on the identification and delineation of distinct "radar facies." Radar facies are defined by Bristow et al. (2000) as a package of GPR reflectors with a distinct set of attributes, including amplitude, continuity, and shape. An excellent overview of radar facies interpretation was

provided by van Overmeeren (1998). Exemplary GPR profiles and associated radar facies diagrams are presented for a variety of depositional environments found in the Netherlands, including glacial, aeolian, fluvial, lacustrine, and marine. Use of radar facies interpretation is very uncommon in soils investigations, but the GPR profiles from Juniper Bay were compared with those presented by van Overmeeren (1998) in an attempt to determine the depositional environment of Juniper Bay.

RESULT AND DISCUSSION

Delineating Clayey Horizon Stratigraphy with GPR

The GPR interpretation of depth to a clayey horizon was accurate within 16% of actual depth on average. As calculated via Eq. [1], the average absolute deviation between predicted and observed depth to clayey horizons was 0.25 m (SD = 0.19). Further discussion of GPR accuracy in this study can be found in Szuch et al. (2004a).

Ground-penetrating radar interpretation was able to delineate clayey horizons occurring at depths between 0.47 and 5.26 m. According to the GPR, the average depth to a clayey horizon was 1.64 m. At 72% of GPR observation points, the depth to a clayey horizon was between 1.0 and 2.0 m (Fig. 4).

Although the water table was within the depth of penetration of the GPR, no reflections on the GPR profiles are thought to represent the water table. Ground-penetrating radar has been used to identify the water table (Birkhead et al., 1996, van Overmeeren, 1998), but this is typically only successful in very homogeneous and coarse-textured

material. The presence of finer texture materials, with large capillary fringes, and complex stratigraphy likely masks the water table on GPR profiles of Juniper Bay.

Along 35% of the GPR transects, a second or third reflection was detected below the shallowest clayey horizon. In some but not all instances, coring confirmed that these reflections were underlying clayey layers. On several occasions, the high water table and sandy material induced sloughing of soil into the augerhole and prevented confirmation of the identity of secondary or tertiary GPR reflections. Accuracy of depth prediction via GPR decreased with depth. Average deviation between predicted and observed depth to clayey horizon was 0.22 and 0.36 m for horizons above and below 2 m, respectively. Typically, these underlying reflections were more irregular in their topography than the shallowest clay horizon (Fig. 5). These irregular surfaces likely indicate cycles of erosion and burial have occurred in Juniper Bay (Zanner, 2003).

According to particle size analysis, the range of texture for layers identified as clayey horizons by GPR interpretation was sandy loam to clay. The overlying and interbedded coarse material was sand to sandy loam. More detailed information on the textures above and below detected interfaces can be found in Appendix B. The fact that these ranges overlap in the sandy loam textural class may be explained as follows. Soils in the sandy loam textural class can range in clay content from 0 to 20%, and sandy loam textures in Juniper Bay ranged from 6.5 to 19.2% clay. Situations where sandy loam overlaid sandy clay loam or finer material produced GPR reflections, and situations where sandy loam was overlaid by loamy sand or coarser material also produced reflections. In some areas of the bay, surface horizons were organic soil or mucky mineral soil.

Interpreting Geomorphic Environments with GPR

Based on analysis of coring records and a review of the geomorphic history of the North Carolina coastal plain, Zanner (2003) suggested that considerable variation in deposition or erosion patterns have occurred across Juniper Bay. The results of the GPR survey supported this conclusion. As can be seen in Fig. 6, the general pattern of GPR reflections showed great variation across the bay.

Radar facies interpretation of the GPR transects at Juniper Bay revealed two starkly contrasting patterns. The majority of the bay exhibited radar facies typical of a lacustrine environment. As shown in Fig. 7, the reflectors were undulating and subparallel. High intensity and highly continuous reflectors bounded reflection-free zones (van Overmeeren, 1998). In the southeast corner of the bay, an area of approximately 4 to 8 ha had radar facies consisting of high intensity and chaotic reflections (Fig. 8). This radar facies was interpreted to represent fluvial deposition, where grain size can change abruptly either vertically or horizontally (van Overmeeren 1998). Particle size analysis of a deep core within this area showed sandy textures for the upper 5.2 m followed by 0.6 m of silt loam and then clay until 7.3 m. The sand distribution through the upper horizons was 50-60% medium sand and 12-40% fine sand with smaller percentages of other sand classes. The high proportion of fine sand indicates that the deposit may have been partially due to aeolian processes. As would be expected for a fluvial environment, the grain size distribution changed vertically without a fining or coarsening trend, as is shown in Fig. 9. The hypothesis that this part of the bay had a fluvial influence is supported by the presence of an active stream channel, Big Indian Swamp, approximately 30 m to the southeast of the bay. The fluvial feature depicted by the

GPR may represent a previous location of this meandering stream, and areas adjacent to the fluvial feature may represent floodplain deposits.

Within the western third of Juniper Bay, several GPR reflections were sharply dipping or trough-shaped (Fig. 10). These reflections may represent paleochannels as compared with findings of Wyatt and Temples (1996), Poole et al. (1997), and van Overmeeren (1998). Coring in the vicinity of the GPR transect in Fig. 10 showed that a clayey horizon is associated with this reflection. We hypothesize that a period of incision by the channel was followed by a depositional event that left fine material over the entire bay. Other features identified in the GPR transects indicated that multiple events have deposited fine material in the bay. Figure 11 shows three high intensity reflections that correspond to multiple clayey layers encountered during coring.

CONCLUSION: Toward A Conceptual Model of Bay Formation

These findings from the GPR surveys, and groundtruthing, indicate that multiple geomorphic events have shaped the stratigraphy apparent at Juniper Bay. Zanner (2003) showed that cycles of exposure and burial have occurred at Juniper Bay since the Cretaceous period (142 to 66 million years ago) due to the regression and transgression of the sea level along the Coastal Plain. These cycles are responsible for the interbedded layers of fine and coarse material beneath Juniper Bay. The last regression of the sea level, during the Plio-Pleistocene epoch (around 3 million years ago) deposited the uppermost layer of sandy material and left two slightly elevated ridges to the northeast and southwest of Juniper Bay's current location. Some Cretaceous period deposits were encountered in coring, but probably

only the deepest of GPR reflections (3 to 5 m) represent Cretaceous period clay deposits. The northeast corner of Juniper Bay may be the exception to this, as thick clayey deposits of the Cretaceous are within 1 m of the surface in this area. We hypothesize that the Cretaceous clayey deposits and Plio-Pleistocene ridges were initially responsible for the ponding of water in the Juniper Bay area. Saunders (1990) similarly concluded that a fine-textured layer that extended into adjacent areas was responsible for the initial ponding of water.

Besides those in the northeast corner, shallow GPR reflections represent clayey layers deposited as part of bay formation, probably during the Quaternary period (2 million years ago to present). In the central part of Juniper Bay, reflections show basin-shaped topography (Fig. 6). Toward the eastern edge of this basin, the single reflection diverges into multiple reflections, indicating multiple depositional events due to a fluctuating water table (Fig. 11). We hypothesize that the bay formed over several cycles of ponding and drying. This would explain the multiple clayey layers seen in Fig. 11 and the multiple reflections apparent in several central traces on Fig. 6. The deepest clay layer, or reflection, would be due to fine sediment settling in the initial basin. When the water table dropped, sandy material accreted on top of the clayey base. Once the water table rose again, a new basin was formed and another deposition of fine material occurred. This assessment is in agreement with that of Grant et al. (1998), who concluded that the present-day stratigraphy of bays in South Carolina was the result of multiple periods of accretion and erosion during the Holocene epoch (10,000 years ago to present). Our hypothesis also explains the presence of a clayey horizon along the base of paleochannels in Fig. 10. Streams caused incision during a period of low water table, and the clayey horizon was deposited in the incised channels during the next period of high water table.

As described by Grant et al. (1998), it is during the periods of high water table that wind driven waves caused the oval shape of the bay. During periods of low water table, winds moved the eroded sand toward the basin edges, forming the typical sandy rim. We hypothesize that erosion caused by this wind and wave action resulted in expansion of the original bay. At the present-day site of Juniper Bay, we suggest that three landforms were once apparent: a large bay centered toward the west, a small bay found to the northeast, and a large incised channel to the southeast. Because the depth to the Cretaceous aquitard was greatest in the large western bay, this bay held the most water and was more active in eroding its oval geometry. The eastern side of this large bay migrated further east and captured the smaller bay and the channel. The anomalous GPR reflection apparent in Fig. 8 depicts the incised channel, possibly filled by a combination of fluvial processes from the stream and aeolian and wave processes from the expanding bay.

Based on the current state of research at Juniper Bay, a conceptual model of Juniper Bay's evolution is depicted in Fig. 12. Further work with GPR surveys may aid our assessment of bay stratigraphy and evolution. Ground-penetrating radar transects to be interpreted in the future include transects adjacent to Juniper Bay, transects within undrained reference bays, and three-dimensional grid surveys of certain parts of Juniper Bay, such as the fluvial deposit. Ground-penetrating radar has proven a useful tool in investigating the stratigraphy of Juniper Bay, especially when coordinated with extensive groundtruthing and studies of bay hydrology and geology.

REFERENCES

Asmussen, L.E., H.F. Perkins, and H.D. Allison. 1986. Subsurface descriptions by ground-penetrating radar for watershed delineation. Bull. 340. The Georgia Agricultural Experiment Stations, The University of Georgia, Athens.

Asprion, U., and T. Aigner. 1999. Towards realistic aquifer models: three-dimensional georadar surveys of Quaternary gravel deltas (Singen Basin, SW Germany). Sediment. Geol. 129:281-297.

Beres, M., P. Huggenberger, A.G. Green, and H. Horstmeyer. 1999. Using two- and three-dimensional georadar methods to characterize glaciofluvial architecture. Sediment. Geol. 129:1-24.

Birkhead, A.L., G.L. Heritage, H. White, and A.W. van Niekerk. 1996. Ground-penetrating radar as a tool for mapping the phreatic surface, bedrock profile, and alluvial stratigraphy in the Sabie River, Kruger National Park. J. Soil Water Conserv. 51(3):234-240.

Bliley, D.J., and D.E. Pettry. 1979. Carolina bays on the eastern shore of Virginia. Soil Sci. Soc. Am. J. 43:558-564.

Boll, J., R.P.G. van Rijn, K.W. Weiler, J.A. Ewen, J. Daliparthy, S.J. Herbert, and T.S. Steenhuis. 1996. Using ground-penetrating radar to detect layers in a sandy field soil. Geoderma 70:117-132.

Bristow, C.S., J.L. Best, and P.J. Ashworth. 2000. The use of GPR in developing a facies model for a large sandy braided river, Brahmaputra River, Bangladesh. p. 95-100. *In* D.A. Noon, G.F. Stickley, and D. Longstaff (ed.) Proc. Int. Conf. Ground Penetrating Radar, 8th. Univ. of Queensland. SPIE Vol. 4084.

Collins, M.E., and J.A. Doolittle. 1987. Using ground-penetrating radar to study soil microvariability. Soil Sci. Soc. Am. J. 51:491-493.

Conyers, L.B., and D. Goodman. 1997. Ground-penetrating radar: an introduction for archaeologists. AltaMira Press, Walnut Creek, CA.

Daniels, D.J. 1996. Surface-penetrating radar. Institution of Electrical Engineers, London, UK.

Doolittle, J.A. 1987. Using ground-penetrating radar to increase the quality and efficiency of soil surveys. p. 11-32. *In* W.U. Reybold, and G.W. Peterson (ed.) Soil Survey Techniques, Soil Sci. Soc. Am. Spec. Publ. No. 20.

Doolittle, J.A., G. Hoffmann, P. McDaniel, N. Peterson, B. Gardner, and E. Rowan. 2000. Ground-penetrating radar interpretations of a fragipan in northern Idaho. Soil Surv. Horiz. 41(3):73-82.

Frey, D.G. 1950. Carolina Bays in relation to the North Carolina Coastal Plain. J. Elisha Mitchell Sci. Soc. 66:44-52.

Gamble, E.E., R.B. Daniels, and W.H. Wheeler. 1977. Primary and secondary rims of Carolina Bays. Southeast Geol. 18:199-211.

Grant, J.A., M.J. Brooks, and B.E. Taylor. 1998. New constraints on the evolution of Carolina Bays from ground-penetrating radar. Geomorphology 22:325-345.

Gee, G.W., and J.W. Bauder. 1986. Particle-size analysis. p. 383. In Klute et al. (ed.) Methods of soil analysis. Part 1 Physical and mineralogical methods. ASA, CSSA, and SSSA, Madison, WI.

Johnson, D.W. 1942. Nature of the bays. *In* The origin of the Carolina Bays. Columbia University Press, New York, NY.

Kaczorowski, R.T. 1977. The Carolina Bays: a comparison with modern oriented lakes. Technical Report 13-CRD, Coastal Research Division Dept. Geo. Univ. South Carolina, Columbia.

Langsholt, E., N.-O. Kitterød, and L. Gottschalk. 1998. Development of three-dimensional hydrostratigraphical architecture of the unsaturated zone based on soft and hard data. Ground Water 36(1):104-111.

Lapen, D.R., B.J. Moorman, and J.S. Price. 1996. Using ground-penetrating radar to delineate subsurface features along a wetland catena. Soil Sci. Soc. Am. J. 60:923-931.

Lide, R.F., V.G. Meentemeyer, J.E. Pinder, III, and L.M. Beatty. 1995. Hydrology of a Carolina Bay located on the upper Coastal Plain of western South Carolina. Wetlands 15(1):47-57.

May, J.H., and A.G. Warne. 1999. Hydrogeologic and geochemical factors required for the development of Carolina Bays along the Atlantic Gulf of Mexico Coastal Plain, USA. Environ. Eng. Geosci. 5(3):261-270.

McCachren, C.M. 1978. Soil survey of Robeson County, North Carolina. USDA-SCS, North Carolina Agricultural Experiment Station and Robeson County Board of Commissioners, U.S. Gov. Print. Office, Washington, D.C.

Melton, F.A., and W. Schriever. 1933. The Carolina Bays: are they meteorite scars? J. Geol. 41:52-66.

Mills, H.H., and M.A. Speece. 1997. Ground-penetrating radar exploration of alluvial fans in the southern Blue Ridge Province, North Carolina. Environ. Eng. Geosci. 3(4):487-499.

Mokma, D.L., R.J. Schaetzl, J.A. Doolittle, and E.P. Johnson. 1990. Ground-penetrating radar study of ortstein continuity in some Michigan haplaquods. Soil Sci. Soc. Am. J. 54:936-938.

Nobes, D.C., R.J. Ferguson, and G.J. Brierley. 2001. Ground-penetrating radar and sedimentological analysis of Holocene floodplains: insight from the Tuross valley, New South Wales. Aust. J. Earth Sci. 48:347-355.

Poole, G.C., R.J. Naiman, J. Pastor, and J.A. Stanford. 1997. Uses and limitations of ground penetrating radar in two riparian systems. p.140-148. *In* J. Gibert, J. Mathieu, and F. Fournier (ed.) Groundwater/surface water ecotones: Biological and hydrological interactions and management options. International Hydrology Series. Cambridge University Press, New York, NY.

Prouty, W.F. 1952. Carolina Bays and their origin. Geol. Soc. Am. Bull. 63:167-224.

Reese, R.E., and K.K. Moorhead. 1996. Spatial characteristics of soil properties along an elevation gradient in a Carolina Bay wetland. Soil Sci. Soc. Am. J. 60:1273-1277.

Saunders, C.L., III. 1990. Substrate variability and internal sediments of three Carolina Bays, south-central Coastal Plain, North Carolina. M.S. thesis. East Carolina Univ. Greenville, NC.

Sharitz, R.R. 2003. Carolina Bay wetlands: unique habitats of the southeastern United States. Wetlands 23(3):550-562.

Sharitz, R.R., and Gibbons, J.W. 1982. The ecology of southeastern shrub bogs (Pocosins) and Carolina Bays: a community profile. FWS/OBS-82/04. US Fish and Wildlife Service Biological Services Program, Slidell, LA.

Szuch, R.P., J.G. White, M.J. Vepraskas, and J.A. Doolittle. 2004a. Calibration of a large-scale ground-penetrating radar survey: implementation of a lift-test and a calibration equation based on multiple points. Soil Sci. Soc. Am. J. *In review*.

Szuch, R.P., J.G. White, M.J. Vepraskas, and J.A. Doolittle. 2004b. Application of ground-penetrating radar to aid restoration plans for a drained Carolina Bay. Wetlands *In review*.

Thom, B.G. 1970. Carolina Bays in Horry and Marion counties, South Carolina. Geol. Soc. Am. Bull. 81:783-814.

Tomer, M.D., J. Boll, K.-J.S. Kung, T. Steenhius, and J.L. Anderson. 1996. Detecting illuvial lamellae in fine sand using ground-penetrating radar. Soil Sci. 161(2):121-129.

van Overmeeren, R.A. 1998. Radar facies of unconsolidated sediments in The Netherlands: a radar stratigraphy interpretation method for hydrogeology. J. Appl. Geophys. 40:1-18.

Wyatt, D.E., and T.J. Temples. 1996. Ground-penetrating radar detection of small-scale channels, joints, and faults in the unconsolidated sediments of the Atlantic Coastal Plain. Environ. Geol. 27:219-225.

Zanner, C.W. 2003. Surficial geology of southern North Carolina and Juniper Bay. p. 13-37. *In* M.J. Vepraskas et al., Methodology to assess soil, hydrologic, and site parameters that affect wetland restoration. Final Report No. FWHA/NC/2003-06. North Carolina Dept. Transportation, Raleigh, NC.

Table 1. Classification of soils mapped at Juniper Bay.

Soil Series	Family Taxonomy
Leon	sandy, siliceous, thermic Aeric Alaquods
Rutlege	sandy, siliceous, thermic Typic Humaquepts
Pantego	fine-loamy, siliceous, semiactive, thermic Umbric Paleaquults
Ponzer	loamy, mixed, dysic, thermic Terric Haplosaprists

McCachren, 1978

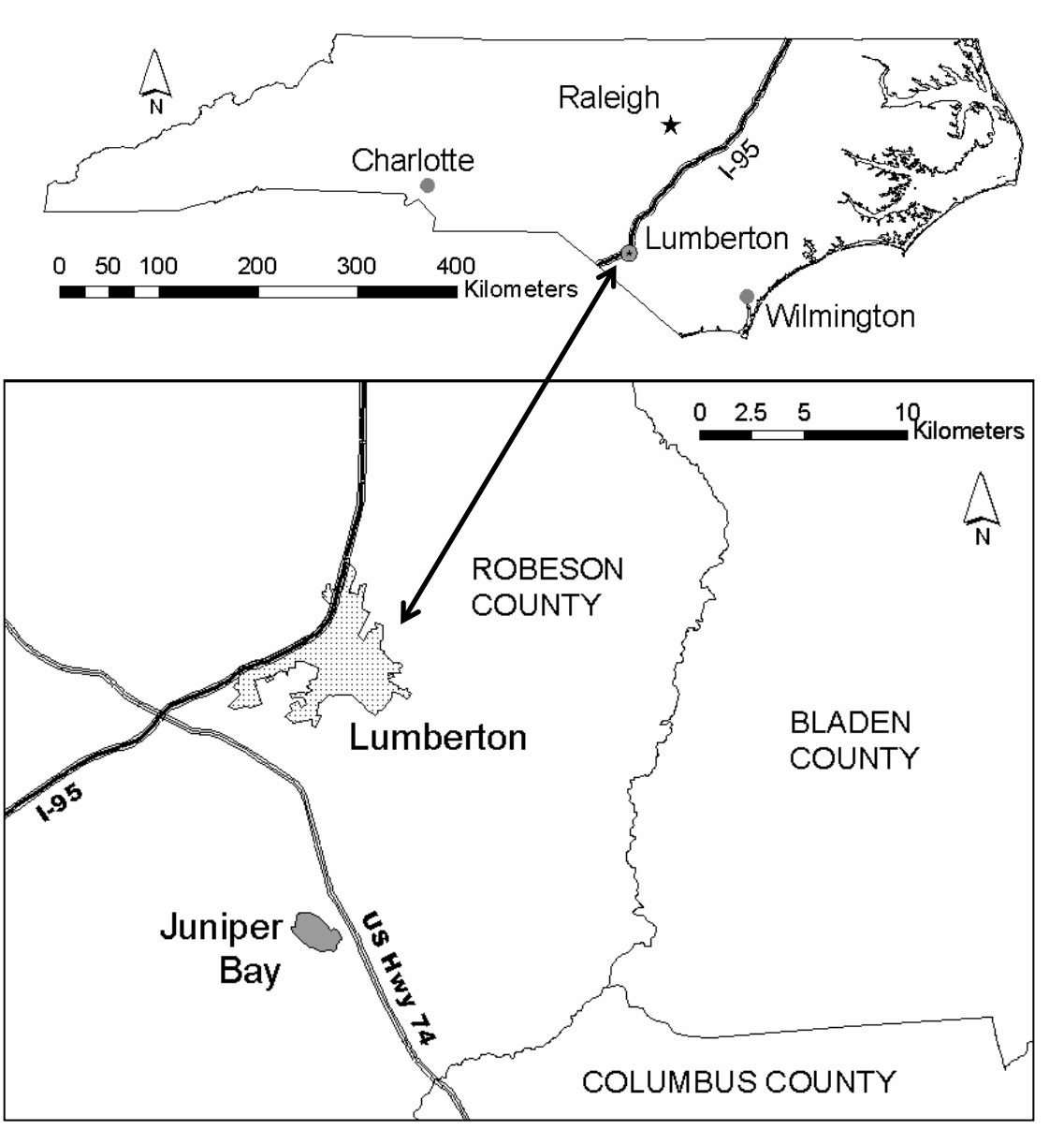

Fig. 1. Map of North Carolina and Lumberton area showing location of the Juniper Bay study site. Arrow shows the location of Lumberton on both large and small scale maps.

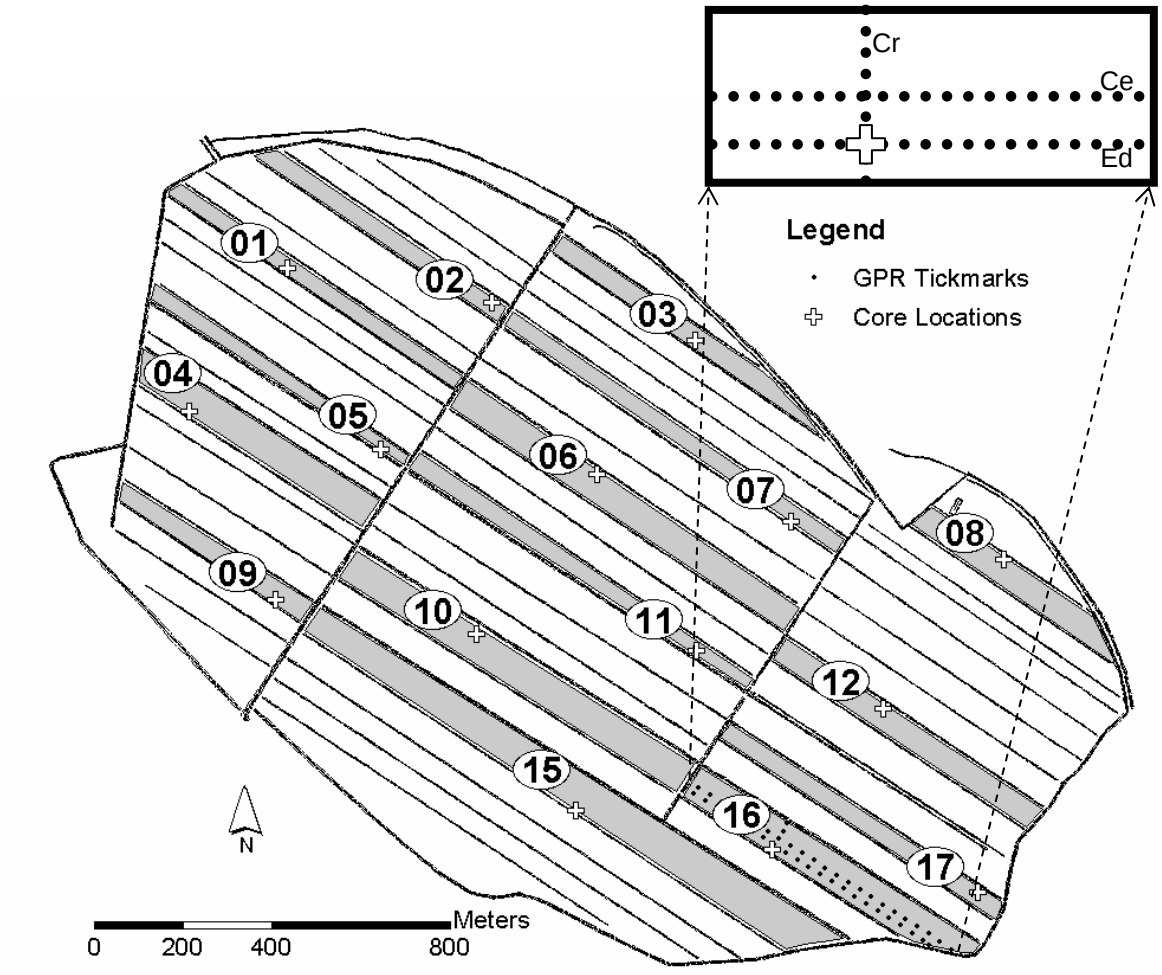

Fig. 2. Map of Juniper Bay showing fieldlets where GPR surveys were conducted highlighted in gray and numbered for identification. Location of cores for preliminary survey are shown with bold crosses. In fieldlet 16 and in the blowup diagram, an example of the orientation of the center (Ce), edge (Ed), and cross (Cr) GPR transects is shown along with the location of the core. Each dot represents a tickmark from the GPR transect, located every 30 m.

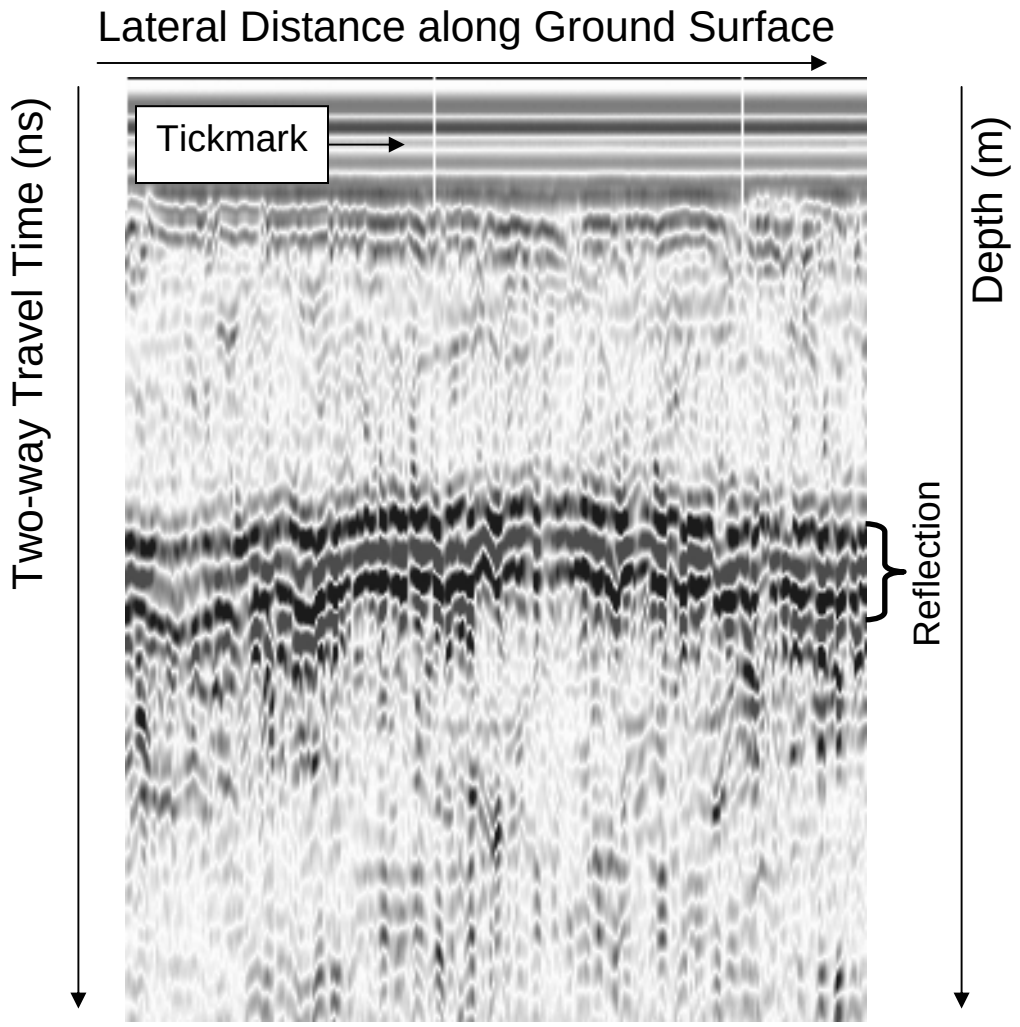

Fig. 3. Example of GPR profile from survey at Juniper Bay. Horizontal axis depicts lateral distance along ground surface. Tickmarks were placed by GPR operator in the field and correspond to the location of survey flags every 30 m. Vertical axis originally depicts two-way travel time (left side) and after calibration depicts depth (right side). Multiple bright lines indicate a GPR reflection and are expected to represent a sandy to clayey soil horizon interface.

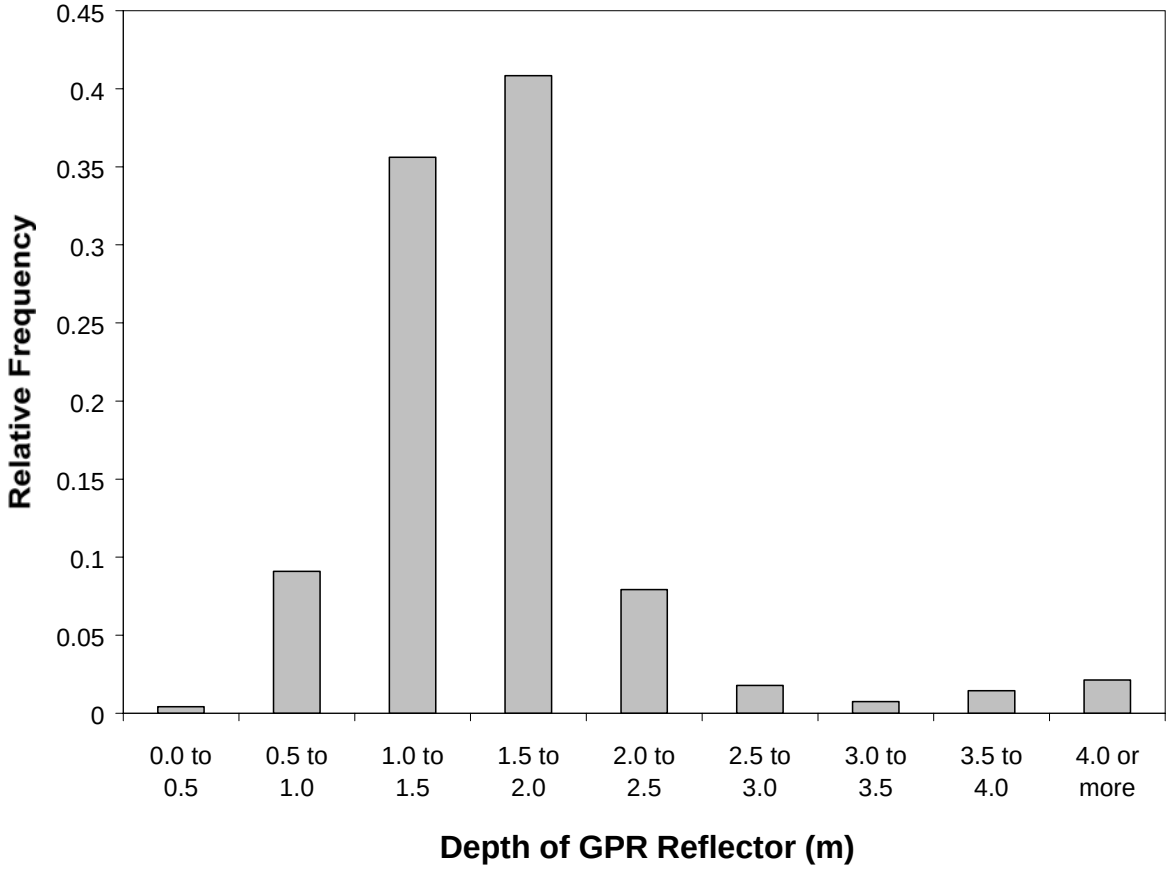

Fig. 4. Relative distribution of depth to GPR reflectors expected to represent clayey soil horizons in Juniper Bay.

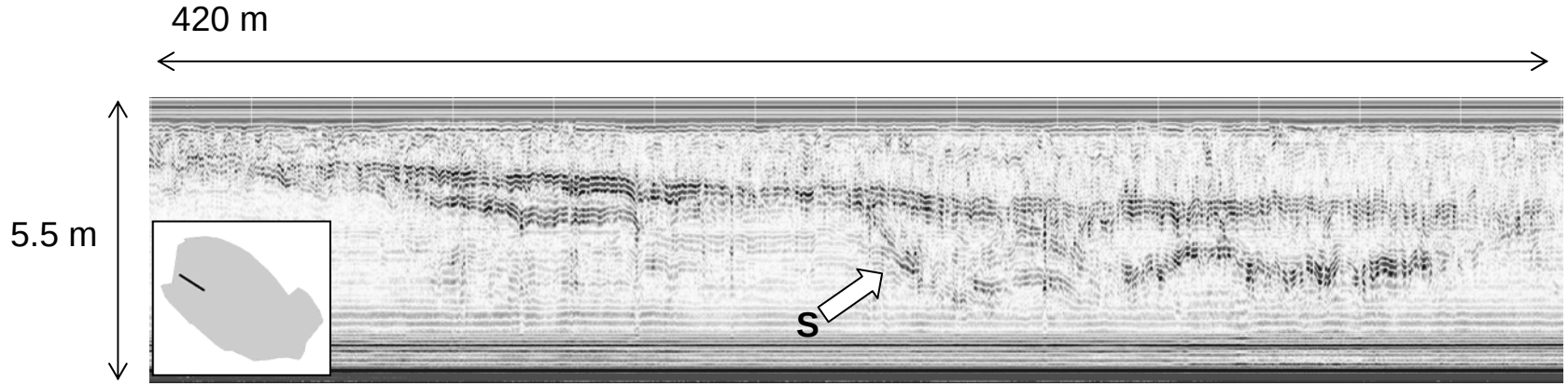

Fig. 5. Partial GPR profile from fieldlet 4, showing the irregular topography of a secondary reflection (S). Horizontal and vertical distance displayed by this GPR profile are indicated. The location of this profile within Juniper Bay is indicated by the black line on the diagram in the bottom left corner.

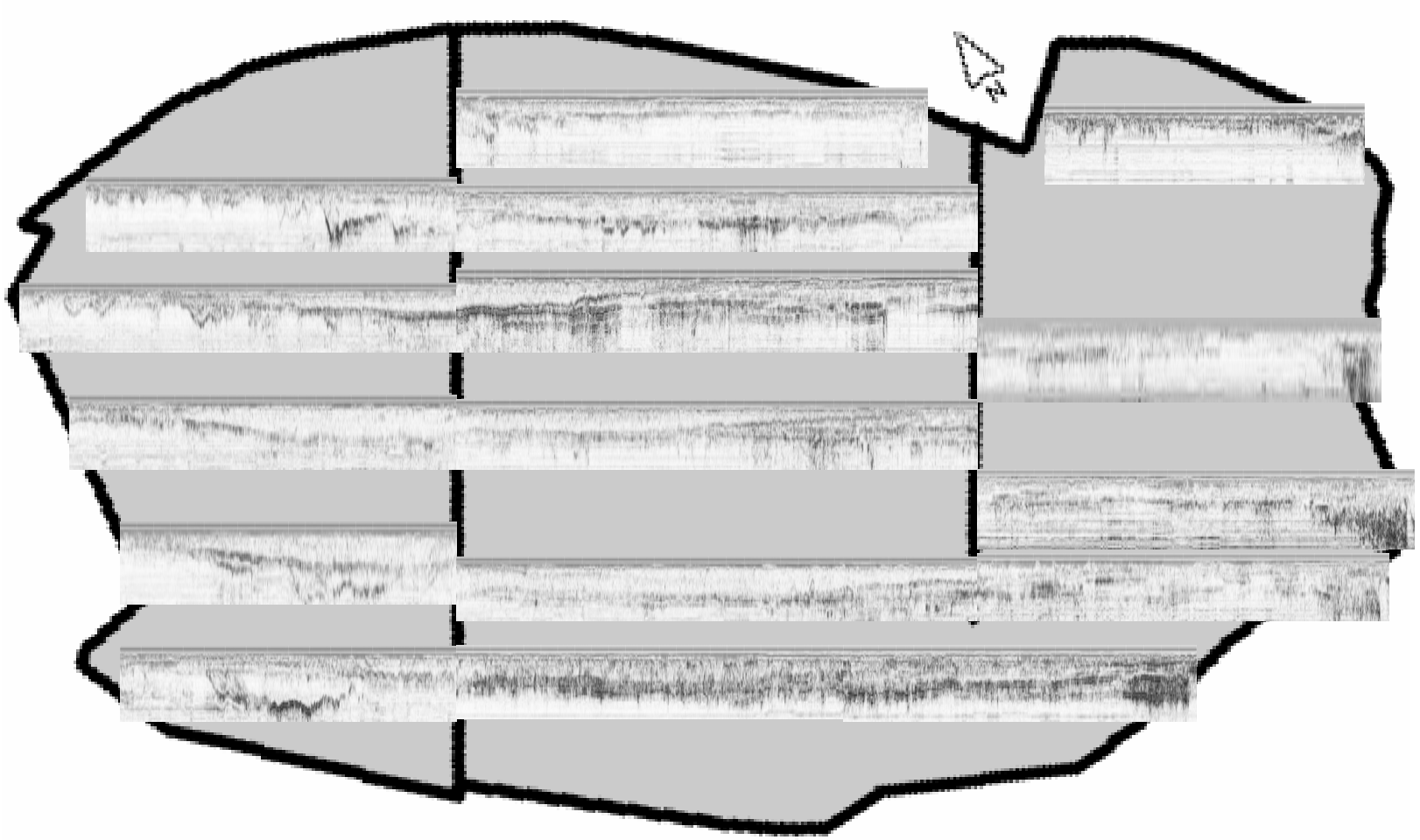

Fig. 6. Composite of center GPR transects for all of Juniper Bay. North arrow, perimeter ditch, and two main internal ditches are shown for reference (see Fig. 2). GPR profiles are somewhat vertically exaggerated for easier viewing. Various GPR reflections can be seen throughout the site, which is indicative of the complex subsurface stratigraphy.

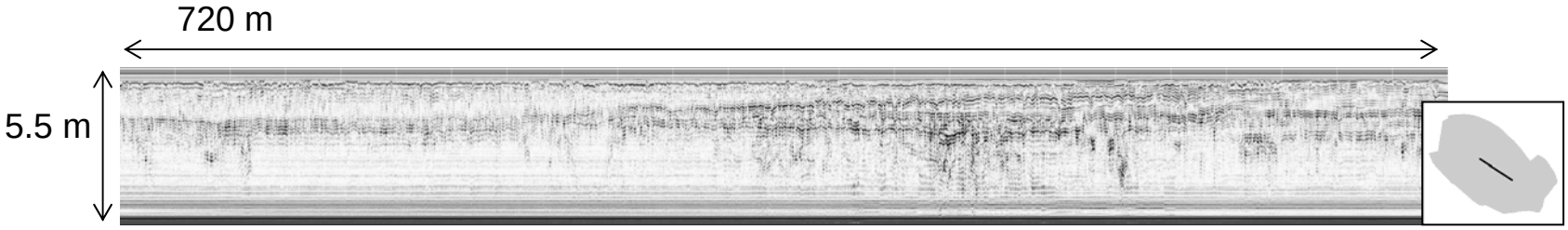

Fig. 7. Partial GPR profile from fieldlet 11, showing radar facies that indicate lacustrine deposition. Horizontal and vertical distance displayed by this GPR profile are indicated. The location of this profile within Juniper Bay is indicated by the black line on the diagram to the right.

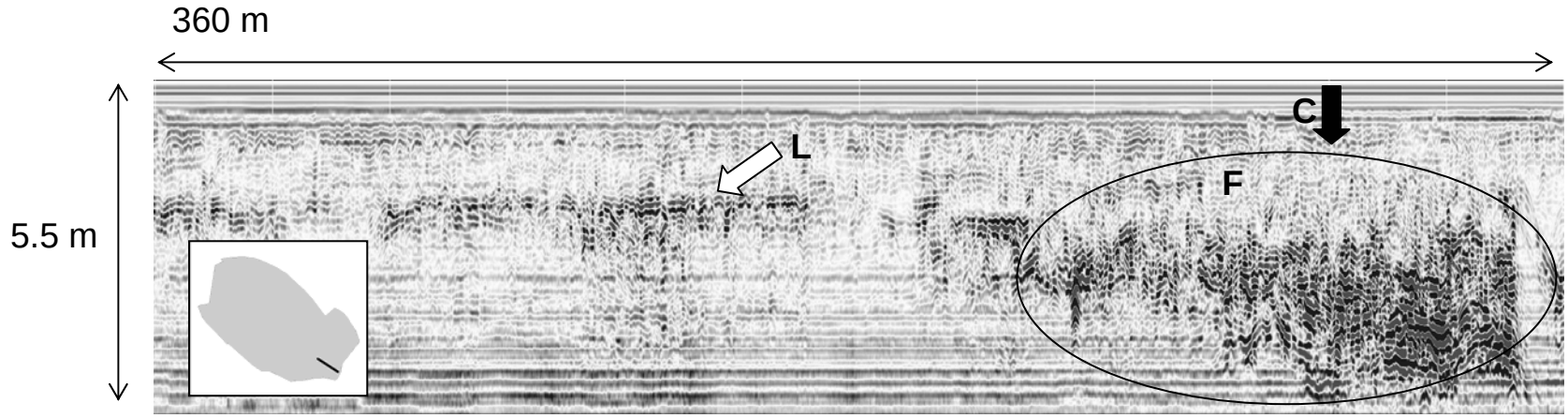

Fig. 8. Partial GPR profile from fieldlet 17, showing radar facies that indicate lacustrine (L) and fluvial (F) deposition. Location of core (C) that provided data for Fig. 9 is shown. Horizontal and vertical distance displayed by this GPR profile are indicated. The location of this profile within Juniper Bay is indicated by the black line on the diagram in the bottom left corner.

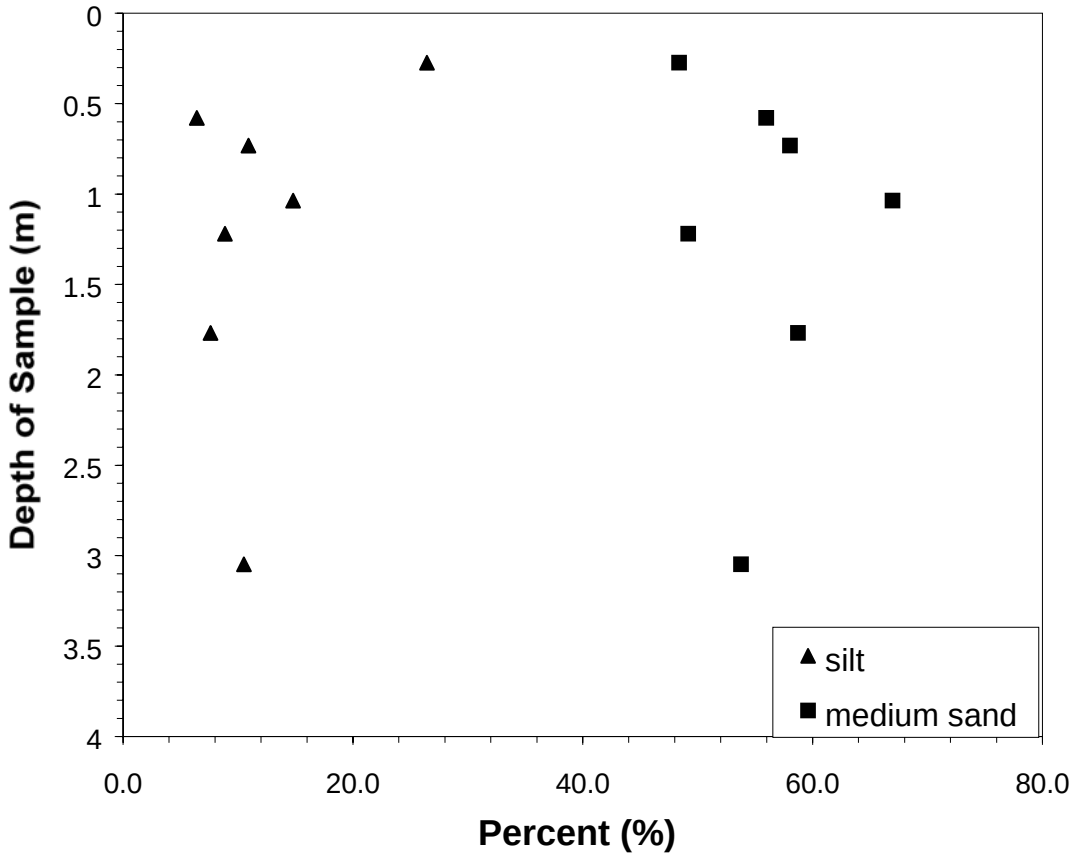

Fig. 9. Distribution of particle size within sand layers of a suspected fluvial deposit in Juniper Bay. Core was taken from fieldlet 17 where indicated by the black arrow in Fig. 8. Incremental core samples were analyzed for particle size, including sand subclasses. Data is shown only for silt and medium sand fractions but shows a chaotic pattern in the percent fraction with depth.

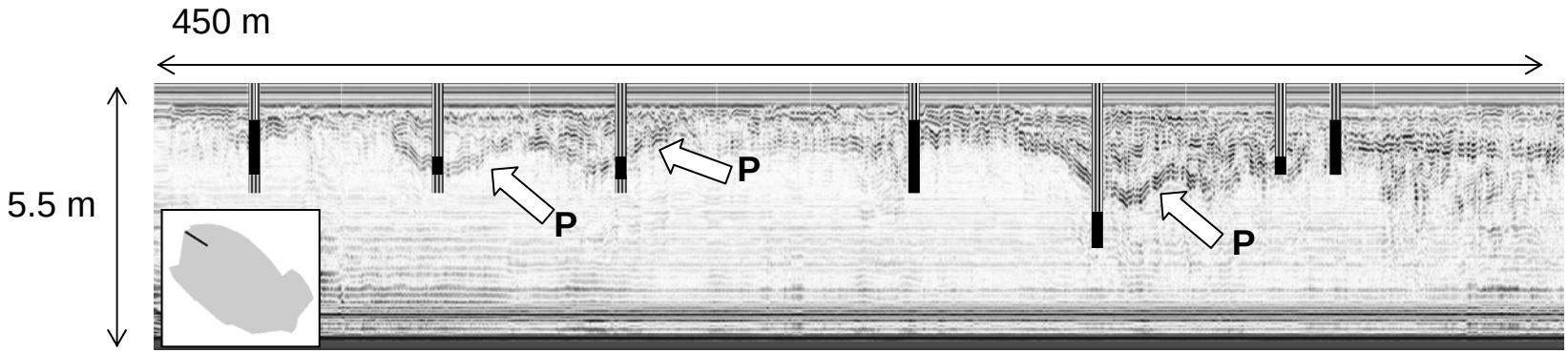

Fig. 10. Partial GPR profile from fieldlet 1, showing reflections that may represent paleochannels (P). Vertical bars along profile represent core locations. Black areas of bars indicate C, SC, or SCL texture, and vertically cross-hatched areas of bars indicate SL, LS, or S texture. Horizontal and vertical distance displayed by this GPR profile are indicated. The location of this profile within Juniper Bay is indicated by the black line on the diagram in the bottom left corner.

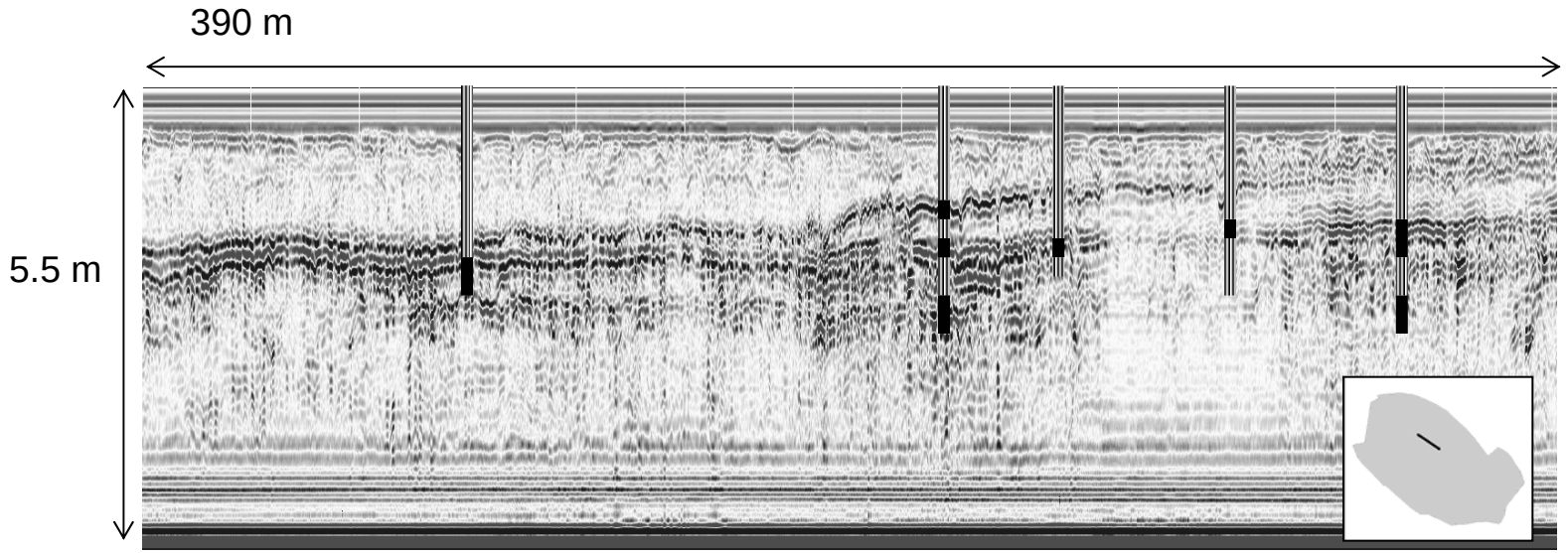

Fig. 11. Partial GPR profile from fieldlet 6, showing multiple reflections that represent overlying clayey horizons. Vertical bars along profile represent core locations. Black areas of bars indicate C, SC, or SCL texture, and vertically cross-hatched areas of bars indicate SL, LS, or S texture. Horizontal and vertical distance displayed by this GPR profile are indicated. The location of this profile within Juniper Bay is indicated by the black line on the diagram in the bottom right corner.

Fig. 12. Diagrammatic representation of conceptual model for Juniper Bay's formation. Conceptual model includes five stages, A through E. Each stage is depicted by a plan view and cross-sectional view and is accompanied by an explanatory caption. The key for the diagrams is found below.

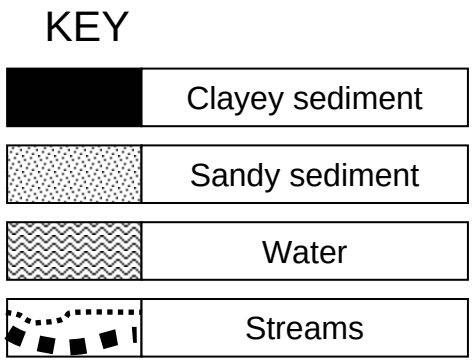

Fig. 12 (continued)

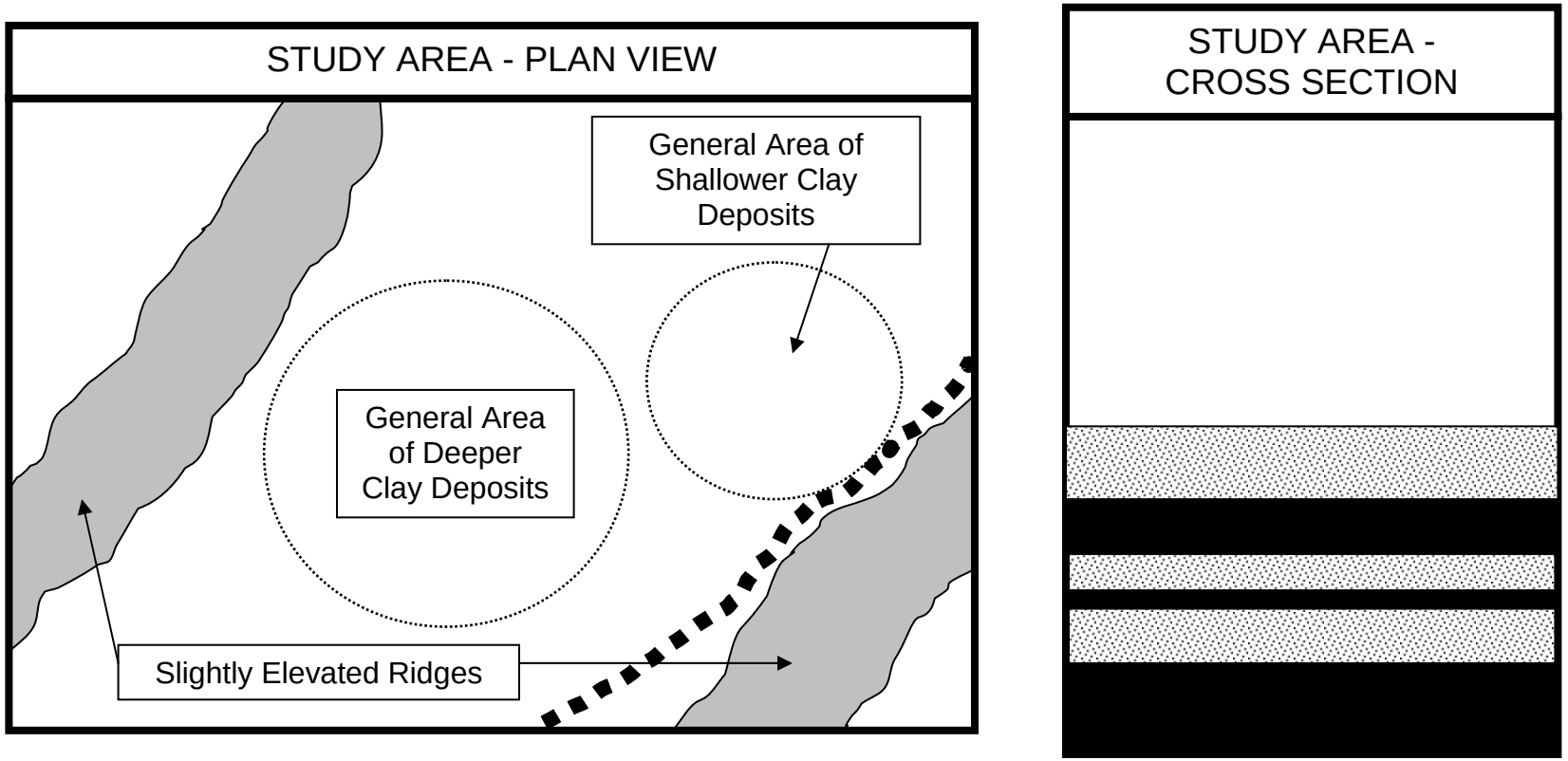

Fig. 12A - Stage A. Since the Cretaceous period, the sea level goes through cycles of regression and transgression, leaving overlying deposits of fine and coarse material. The final regression, during the Plio-Pleistocene epoch, leaves two small ridges to the northwest and southeast of the current study area. Clayey Cretaceous deposits are shallower in the northeast corner of the study area. The uppermost clayey deposit is overlaid by sandy material. A sizeable stream flows along the base of the southeast ridge.

Fig. 12 (continued)

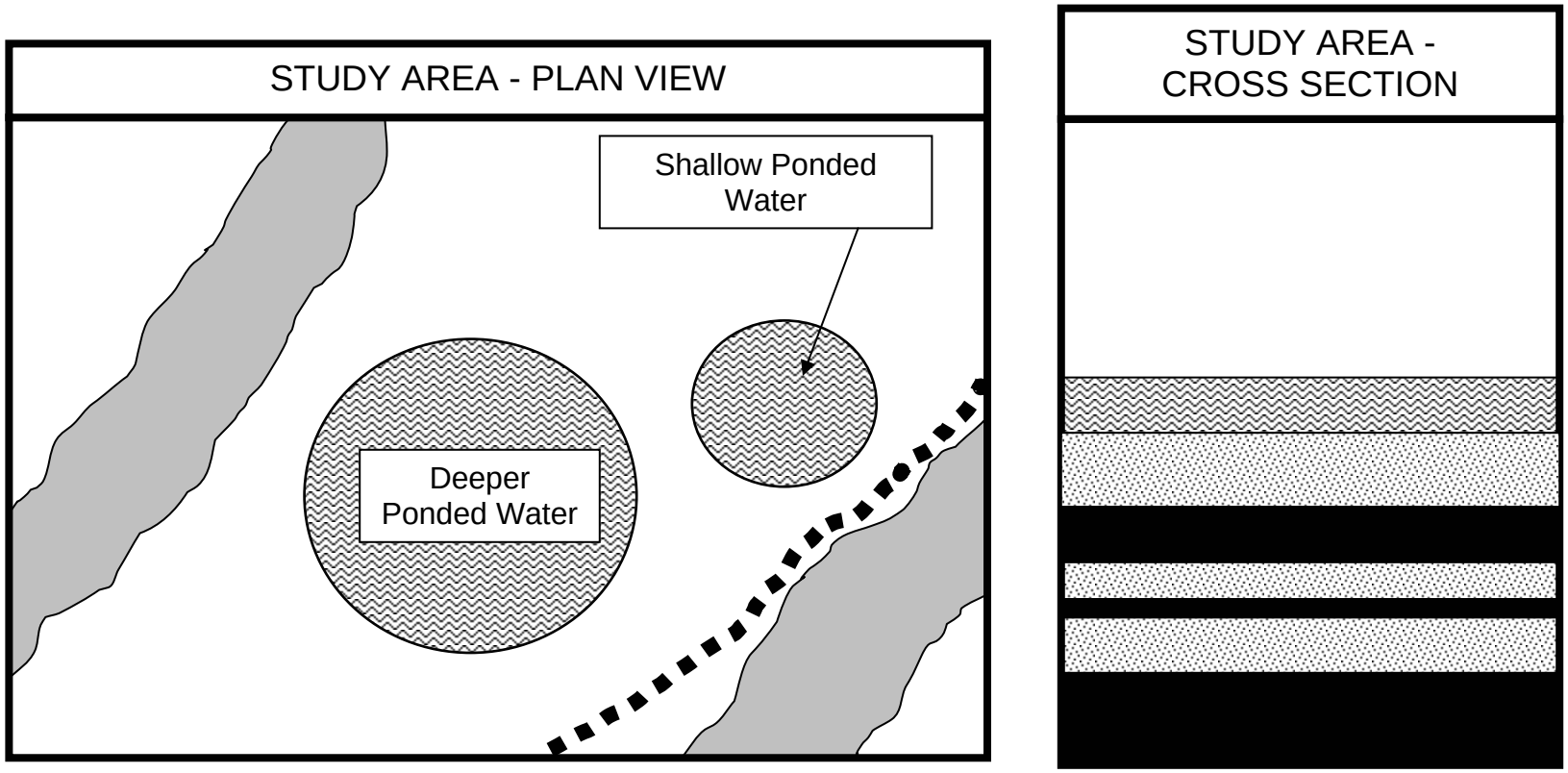

Fig. 12B - Stage B. At some point during the Quaternary period, sea levels are such that water is ponded over the Cretaceous clay layers and saturates the sandy surface material. This scenario is a precursor to formation of Carolina bays.

Fig. 12 (continued)

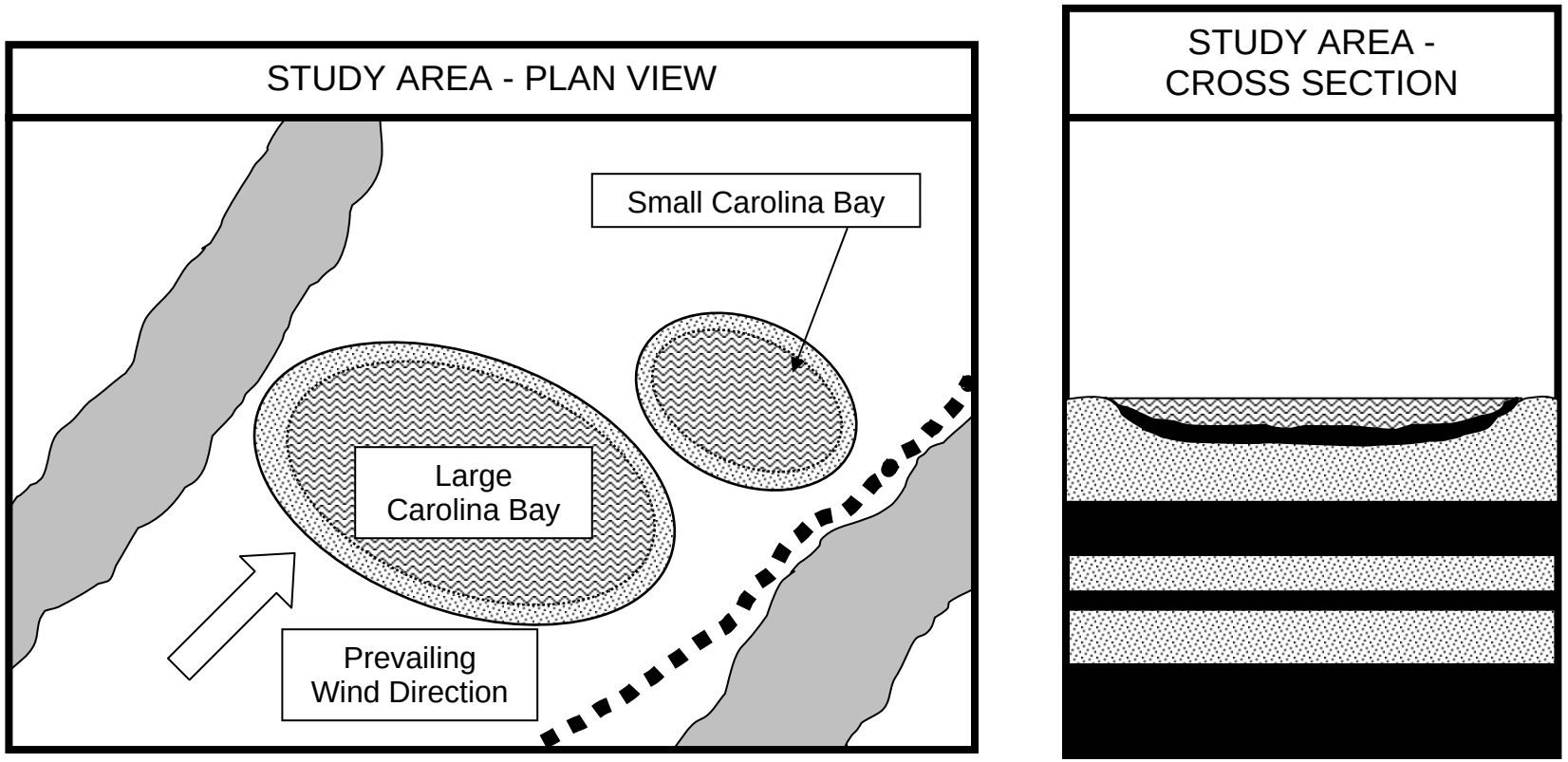

Fig. 12C - Stage C. Both ponds of water begin forming the characteristic geometry of Carolina Bays. Prevailing winds from the southwest move water towards the northeast corner of the ponds. The water is diverted along the edge of the pond, causing erosion along the edge, and creating the typical oval shape. At this point, two Carolina Bays exist in the study area. Fine material is deposited at the base of the Carolina Bay basins. These clayey layers are much younger than those deposited during the Cretaceous. The stream channel is still present.

Fig. 12 (continued)

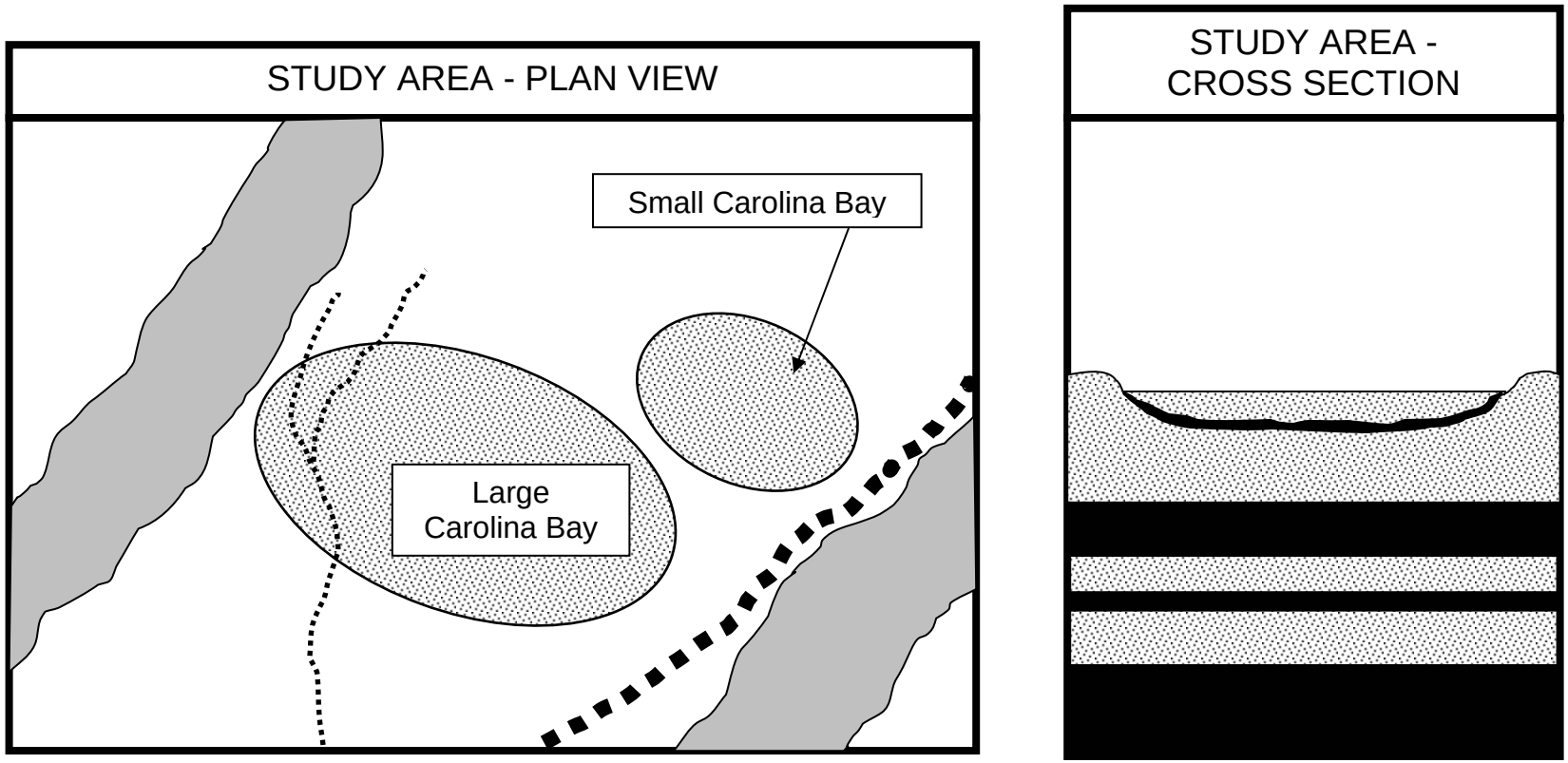

Fig. 12D - Stage D. During the Quaternary period and during this period of bay formation, the water table rises and falls periodically. During a time of low water table, several streams cross the western side of the large bay. They cause incision into the sediments. The large stream along the southeastern ridge is probably incising during this time as well. Sandy material from the bay edges erodes and fills the bay, covering the recent clayey deposit. Winds blow some of the eroded sandy material to the edges of the bay, creating the typical sandy rim.

Fig. 12 (continued)

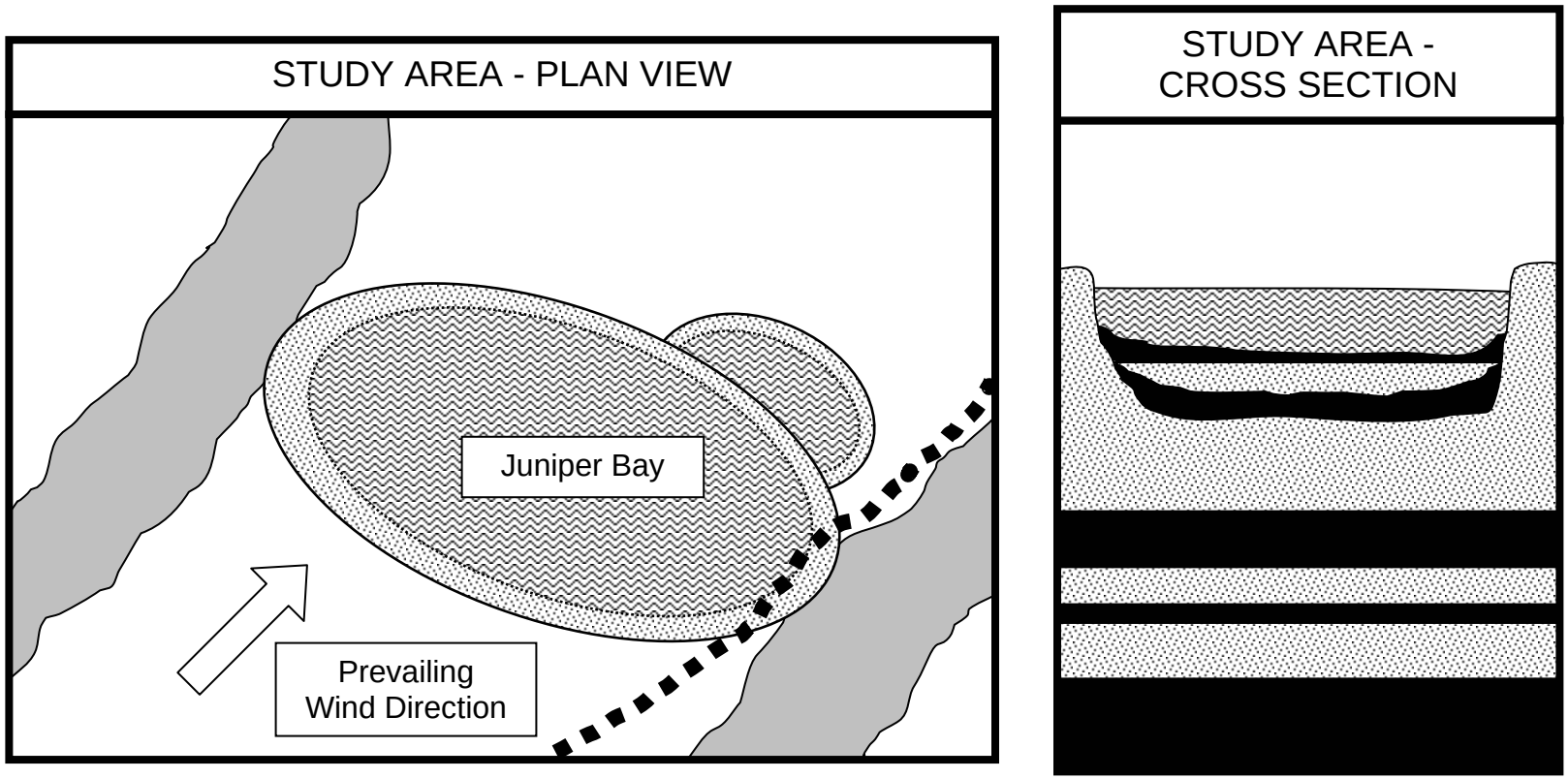

Fig. 12E - Stage E. During another period of high water table, bay formation continues. Prevailing winds continue to cause the erosion of the shoreline. Due to its deeper water levels, the large bay allows more wave action. It begins to expand, and it overtakes both the smaller bay and the channel of the large stream. The stream channel already contained some fluvial sediments and is now completely filled by the progressing bay rim. Thus, Juniper Bay is a composite of a large bay, small bay in the northeast corner, and fluvial feature in the southeast corner. Given slight changes in water level and impacts from human activity, this scenario seems quite similar to the geomorphology apparent at the site at present time.

CHAPTER 4
Application of Ground-penetrating Radar to Aid Restoration Plans for a Drained Carolina Bay

ABSTRACT

Carolina Bays (bays) are a wetland type found along the Atlantic Coastal Plain that occur as shallow, oval-shaped, depressions. Clayey subsurface strata are typical in most bays and act as an aquitard to influence their hydrology. Bays have frequently been drained for conversion to agriculture, but modification to the drainage system might often lead to restoration of wetland conditions. A ground-penetrating radar (GPR) survey was conducted at Juniper Bay, a 300 ha drained bay in NC that will be restored by the North Carolina Department of Transportation (NCDOT). The GPR interpretations found that clayey aquitards underlay most of the bay at an average depth of 1.64 m. According to groundtruthing, GPR predicted the depth to aquitards within 16% of the actual depth on average. An anomalous GPR reflection in the southeast corner of the bay was interpreted as a fluvial deposit that does not contain aquitards until a depth of 3 to 5 m. NCDOT may need to consider alternative restoration plans for this area. By comparing the depths of aquitards and drainage ditches, several areas were identified as likely locations of ditch-induced aquitard discontinuity. NCDOT may choose to fill or line suspect ditches to prevent potential water losses. A hypothetical proposal by two professional firms indicated that GPR can provide large volumes of data with cost and time efficiency. Ground-penetrating radar surveys are suggested as a useful tool for determining suitability of potential wetland restoration sites.

INTRODUCTION

Carolina Bays (bays) are a wetland type found along the Atlantic Coastal Plain that occur as shallow, oval-shaped, depressions. Bays are found from New Jersey to northern Florida (Melton and Schriever 1933, Frey 1950, Prouty 1952, Bliley and Pettry 1979), but they are most prevalent within the Carolinas. An estimated 500,000 bays exist along the Coastal Plain, with about 80% of these occurring within the Carolinas (Prouty 1952). Bays occur in sizes between one and thousands of hectares. The unique characteristics and values of bays were recently reviewed by Sharitz (2003).

Because bays are relatively flat and often contain productive soils, they frequently have been drained and converted to agriculture (Sharitz and Gresham 1998). In a study of bays of South Carolina, Bennett and Nelson (1991) found that 97% of bays have been disturbed, mainly by agriculture (71%) or logging (34%). Modifications of the drainage systems of converted bays could often lead to the restoration of wetland hydrology. For this reason, the numerous drained Carolina Bays present an excellent opportunity for wetland mitigation.

Although soils of Carolina Bays can be quite variable (Frey 1950, Saunders 1990, Reese and Moorehead 1996), many bays contain continuous or nearly continuous clayey horizons in the subsurface (Sharitz and Gibbons 1982). These clays may act to perch water tables during certain times of the year. Even if perching of water does not occur, these clayey horizons would be very important in controlling lateral flow and hydraulic gradients within the bays (R.L. Huffman, personal communication, 2003). Johnson (1942) and Lide et al. (1995) suggest that hydraulic gradients into bays are controlled by subsurface flow over

fine-textured soil horizons. A ground-penetrating radar (GPR) survey of several bays in South Carolina, including that studied by Lide et al. (1995), identified clayey interior bay sediments that were suspected to have a strong influence on bay hydrology (Grant et al. 1998).

Ground-penetrating radar has been used in various settings to map clayey soils and sediments (Collins and Doolittle 1987, Hubbard et al. 1990, Dominic et al. 1995, Kettles & Robinson 1997, Doolittle et al. 2000, Van Dam and Schlager 2000, Nobes et al. 2001). In environments other than wetlands, GPR surveys have delineated clayey soil horizons that were shown to strongly impact local hydrology (Asmussen et al. 1986, Tomer et al. 1996,). Soil horizons with aquitard properties that were important to sustaining wetland hydrology have been mapped by GPR as well (Lapen et al. 1996, van Overmeeren 1998). Lapen et al. (1996) mapped the continuity of a placic horizon (strongly cemented, iron-rich, mineral horizon) along a wetland catena in Newfoundland. The GPR survey revealed that the placic horizon was present beneath wetland bogs but absent beneath upland heath communities. The authors found that the placic horizon was perching water and was thus hydrologically and ecologically important in sustaining the bogs. Similarly, van Overmeeren (1998) found that GPR was useful for mapping cemented layers that acted to perch water tables in fens of the Netherlands.

The aim of this study was to demonstrate the usefulness of GPR for aiding wetland restoration of a Juniper Bay, a 300 ha drained Carolina Bay in North Carolina. Specific objectives were 1) to determine the depth, extent, and continuity of clayey aquitards throughout Juniper Bay, and 2) to determine where drainage ditches may have pierced aquitards, potentially allowing water to exit the site. Proposed surveys via GPR and

conventional methods (i.e., coring) were compared to determine if GPR can provide a cost and effort efficient alternative for screening restoration sites and supplementing restoration plans.

MATERIALS AND METHODS

Study Area

The study site was Juniper Bay, a 300 ha drained Carolina Bay located near Lumberton, Robeson County, NC (Figure 1). The bay was drained for agriculture beginning in 1971 by an extensive ditch network. At the time of the GPR surveys, the bay was in fallow. Principal soils mapped within Juniper Bay are Leon fine sand, Pantego fine sandy loam, Ponzer muck, and Rutlege loamy sand (McCachren, 1978). The Taxonomic classification of these soils can be found in Table 1. In 2000, the North Carolina Department of Transportation (NCDOT) purchased the property and intends to restore Juniper Bay to receive wetland mitigation credit. Restoration efforts were initiated in June of 2003.

The area of Juniper Bay can be subdivided into "fieldlets," defined as areas of the bay confined by ditches on all sides (Figure 2). In 2000, an original investigation of the bay's stratigraphy was performed via coring with a hydraulic drilling machine. Within the rim of Juniper Bay and in the adjacent area, 29 cores were obtained to depths of 6.1 or 15.2 m. The coring sites were selected by placing an equilateral triangle grid over the bay, and choosing a number of core locations that would yield information representative of each soil type and be economically feasible. This preliminary coring survey revealed that the Coastal Plain sediments underlying the bay consisted of complex, interbedded layers of sandy and clayey material.

GPR Survey

The GPR surveys of Juniper Bay were performed in December 2000 and June 2001 to provide additional information on the subsurface. The survey included transects totaling over 23 km. Transects were performed in 15 fieldlets where cores had previously been obtained (Figure 2). Within each fieldlet, three GPR transects were performed: "center" - longitudinal transect down the center of the fieldlet; "edge" - longitudinal transect along the edge of the fieldlet; "cross" - lateral transect across the fieldlet, intersecting the core location (Figure 2). Prior to the survey, flags were placed every 30 m along the transects, and their location was marked on the GPR trace by the operator as each flag was passed (Figure 3). A differential global-positioning system (DGPS) was used to georeference each flag.

The GPR unit used was the Subsurface Interface Radar System-2000 (Geophysical Survey Systems, Inc. [GSSI], North Salem, NH). A 120 MHz antenna was used, with scanning time of 200 nanoseconds (ns). The RADAN NT (GSSI, version 2.0) software was used to process the radar profiles. Processing included color transformations, marker editing, distance normalization, and range gain adjustments. All radar profiles were converted into bitmap images using the Radan to Bitmap Conversion Utility (GSSI, version 1.4).

The GPR was calibrated using a lift-test to define the soil surface and a calibration equation based on reflector-interface matching at 11 locations throughout the bay (Szuch et al. 2004). Operation of GPR has been discussed by Doolittle (1987), Daniels (1996), and Conyers and Goodman (1997). Reflectors expected to be clayey soil horizons were interpreted on the GPR profiles from these transects (Figure 3). Based on the GPR profiles, the depths of these clayey horizons were predicted at 15 m intervals along all transects.

The depth to the shallowest clayey horizon was interpolated over the entire area of Juniper Bay. GS+ (Gamma Design, Plainwell, MI) was used to model the semivariogram for the interpolation data. This model was used to set the krigging parameters in ArcGIS - Geostatistical Analyst (ESRI, Redlands, CA).

Groundtruthing Survey

Coring at a subset of these observation points was done to groundtruth the depth predictions. A DGPS was used to navigate to the observation points. Coring was mainly by bucket-augering, but several deep cores were taken by hydraulic drill rig. The occurrence and depth of clayey horizons was recorded in the field and supported by particle size analysis. Samples were collected from layers where interfaces were expected. These were air-dried and ground to pass a 2-mm mesh sieve. Clay percentage was determined by the hydrometer method of Gee and Bauder (1986). Sand fractions in selected samples were determined by sieving. When necessary, organic matter was removed by oxidation with hydrogen peroxide and heat.

Groundtruthing was done at 130 observation points selected randomly along the center traces and at 44 points selected randomly along the edge traces. Accuracy of the GPR surveys was calculated as the absolute deviation between predicted and observed depths to clayey horizons:

$$\text{Absolute Deviation} = |\text{P.D.} - \text{O.D.}| \quad [1]$$

where: P.D. = predicted depth based on GPR interpretation

O.D. = observed depth based on coring

Determining Depth of Ditches

The main source for determining the depth of drainage ditches was a detailed topographic map created by aerial photogrammetry. This was performed by the NCDOT and imported from MicroStation CAD into ArcGIS geographic information system (GIS). The accuracy of the GIS map was tested by measuring ditch depths manually in the field at 38 locations.

Comparison of Cost and Time Requirements of GPR and Conventional Methods

For the comparison of GPR and conventional methods, a hypothetical request for proposal (RFP) was created and submitted to two consulting firms (that shall remain anonymous). One firm would address the RFP via a GPR survey, and the other would employ a coring survey. The RFP asked that the depth of clayey aquitards be determined along the entire 43.6 km length of ditches at Juniper Bay. The proposals included the time and cost of fieldwork, associated analysis or interpretation, and report preparation. The GPR proposal included six cores that would be necessary for calibration and groundtruthing. Three variations of the coring survey were considered, involving spacings of 15, 60, and 300 m between coring sites along the ditches.

RESULTS AND DISCUSSION

Accuracy

The GPR interpretations were accurate within 16% of actual depth on average. As calculated via Equation 1, the average absolute deviation between predicted and observed depth to clayey aquitards was 25 cm (SD = 18.9). This measure of accuracy is somewhat

higher than, but comparable to, other GPR studies that have predicted depth to a specific horizon or layer, as shown in Table 2. The GPR survey at Juniper Bay was of much greater scale than that of most studies in Table 2; therefore, spatial variation in soil properties that would impact GPR interpretation was greater as well. This spatial variation is likely the main cause of the elevated percent error at Juniper Bay. Further discussion of GPR use and accuracy for this study can be found in Szuch et al. (2004).

The GIS map of Juniper Bay's topography was found to be accurate within an average of 23 cm for determining ditch depth. There was no apparent trend for the GIS map to either overestimate or underestimate ditch depth.

Mapping Clayey Aquitards with GPR

Clayey soil horizons were successfully mapped throughout Juniper Bay using GPR survey and interpretation. These clayey horizons are expected to have lower hydraulic conductivity than adjacent sandy horizons and should act as aquitards within the bay. The textural class of horizons detected by the GPR ranged from sandy loam to clay. The sandy loam horizons were detected by the GPR when they were overlaid by sand or loamy sand horizons. Aquitards were found over most of the survey transects, and in many instances there were two to several clayey horizons overlying each other (Figure 3). Depths to aquitards ranged from 0.47 to 5.26 m, with an average depth of 1.64 m. The interpolation map (Figure 4) shows variation in aquitard depth across Juniper Bay. Aquitards are shallow enough that they should impact vertical soil moisture gradients near the surface and should affect lateral hydraulic gradients within the bay. As shown in Figure 4, the aquitards are shallowest in the northeast corner of the bay, near fieldlet eight. Field observations have

consistently shown that this region of the bay remains wet throughout the year; thus, the aquitards may play a significant role in maintaining wet conditions. During restoration planning, the NCDOT might use Figure 4 to determine the amount of excavation or grading required to bring the soil surface nearer to the existing aquitards.

Based on our survey, a small portion of Juniper Bay is thought to have no aquitard present. In the southeast corner of Juniper Bay, an anomalous GPR signature was recorded. This signature was unlike that throughout the rest of Juniper Bay (Figure 5). A guide to interpreting geomorphology using "radar facies" was presented by van Overmeeren (1998). Based on diagrams in that report, most of Juniper Bay appears to be of a lacustrine nature. However, this anomalous GPR signature appears fluvial in nature. Coring by bucket-auger within the area of the anomalous signature revealed no clayey horizon to a depth of at least 3 m. Coring by hydraulic drilling machine at six locations within the area encountered no clayey horizon until 5.8 m. The coring and GPR data suggest that the depositional environment in this region was different than that in the remainder of the bay and did not allow for the formation of an aquitard. According to GPR transects from this region of the bay, the anomalous zone has a total area of 4.4 to 8.3 ha (Figure 4). Without the continuous subsurface profiles provided by the GPR survey, this anomalous area may not have been identified or accurately mapped by NCDOT. Although the depositional nature of this area is not yet fully understood, it seems likely that NCDOT should consider alternative restoration plans there. Specific hydraulic controls may be necessary, or an assemblage of wetland vegetation suited to somewhat drier conditions might be planted.

Ongoing hydrologic studies at Juniper Bay should help define the potential impact of clayey aquitards on bay hydrology and restoration. This, along with information provided by

the GPR survey on aquitard continuity, extent, and depth, should be useful to restoration planning. Given the large number of converted bays present throughout the Coastal Plain, there are many opportunities for the use of GPR to characterize sites for possible wetland restoration projects. Especially in the Carolinas, where bays account for 50% of the ground surface in some areas (May and Warne 1999), GPR could provide an assessment of a site's suitability for restoration. GPR might be an effective tool for assessing wetland restoration sites other than Carolina Bays as well. Much of the Coastal Plain contains soils with argillic or kandic horizons (subsurface zones of clay accumulation). These horizons have low hydraulic conductivity and could be exploited to great advantage during wetland restoration projects if their extent and depth were known. Argillic or kandic horizons have been successfully mapped in several instances using GPR (Asmussen et al. 1986, Collins and Doolittle 1987, Hubbard et al. 1990, Mokma and Doolittle 1993, Doolittle et al. 2000).

Ditch Induced Aquitard Discontinuities

The depths of aquitards interpreted from GPR were compared to the depths of adjacent ditches determined from the GIS map. This comparison could be made at the ends of the "center" and "cross" traces and along the entire "edge" traces, as the edge traces were proximal to the lateral ditches (Figure 2). Depths of horizons along the edge traces and at the ends of the cross traces were compared to the depths of the lateral (approximately east-west) ditches. Depths of horizons at the ends of the edge and center traces were compared to either the main (approximate north-south) ditches or the perimeter ditch. In these comparisons, it is important to recognize that GPR interpretation cannot indicate the thickness of clayey

horizons. The GPR interpretation can determine only the depth of the horizons and thus be used only to predict where the top of clayey aquitards may be pierced by ditches.

If the GPR interpretations and the ditch topopgraphy map were absolutely accurate, then a ditch could be known to pierce the aquitard top if the ditch depth were greater than the aquitard depth. However, the GPR and GIS data were inaccurate on average 25 and 23 cm, respectively. To account for this uncertainty, a classification scheme was created that ranked the likelihood of a ditch having pierced the aquitard top. The classification scheme ranged from a very high to very low risk that a ditch pierced the aquitard top (Table 3).

The risk of ditches piercing the aquitard top is low or very low throughout most of Juniper Bay (Figure 6). The main areas where lateral ditches pose a higher risk include fieldlet 8; the western side of fieldlets 1, 2, 4, and 5; the western side of fieldlets 10 and 15, and the eastern side of fieldlet 10. Along the perimeter ditch, there is a higher risk of piercing along both the eastern and western sides of the bay. The secondary main ditch seems to pose little threat of piercing aquitard tops; however, the primary main ditch shows a moderate to very high risk in numerous locations along its extent.

Coring data can be used to supplement the risk assessment and determine whether a ditch has not only pierced an aquitard top but also pierced through the entire aquitard. The depths of aquitards as confirmed by coring were compared to ditch depths within the areas of high risk. This investigation revealed that in most instances, the aquitards were thick enough that it is unlikely that they have been entirely pierced by ditches. Exceptions to this were: 1) along the western side of the perimeter ditch, 2) the western sections of fieldlets 10 and 15, 3) the eastern section of fieldlet 10, and 4) the southern portion of the primary main ditch. In first three exceptions, the shallowest aquitard (around 1 to 1.5 m) has probably been pierced

by ditching, but underlying aquitards (around 2 to 3 m) have not been. It is likely that the primary main ditch has pierced all detected aquitards along its southern extent, especially around fieldlets 9, 10 and 15. Further GPR surveys and groundtruthing are planned for late 2003 and 2004 and should clarify the potential for ditch-induced aquitard discontinuity. Where aquitard piercing does occur, hydraulic gradients and drainage of the bay are likely to be impacted. NCDOT may choose to install impervious liners in the affected ditches or plug them with fill material having low hydraulic conductivity.

As discussed above, confirmation with coring records revealed that some high risk areas were indeed potential sites of ditch-induced aquitard discontinuity, but many labels of high risk were misleading. This was due to the inaccuracies of the GPR interpretation and topographic map. However, the GPR survey and risk assessment served as a valuable screening tool, focusing attention on high risk areas that warranted more detailed investigation. The linear, continuous nature of GPR profiles makes them ideal for comparison with drainage ditches. Because drainage via ditching has been a common impact on wetlands throughout the country, the application of GPR in this manner has potential for widespread utilization

Comparison of Cost and Time Requirements between GPR and Conventional Methods

The comparison of proposals submitted for GPR and conventional methodologies revealed a marked advantage for GPR in time and monetary investment (Table 4). The proposal for the GPR survey would cost $20,488 and could be provided in 15 days. Depending on the spacing between coring sites, the proposal for the coring survey ranged in

cost from $24,555 to $391,512 and in days from 16 to 257. The data in Table 4 includes a calculation of the time and monetary savings provided by the GPR survey.

These benefits of GPR have been revealed in several previous studies as well. Collins and Doolittle (1987) used GPR to study soil microvariability and estimated that productivity was increased by 800% compared to manual coring. Mokma and Doolittle (1993) made a direct comparison of soil maps achieved by GPR and by coring, and they found GPR increased productivity by 133%. The only known report that included a quantitative estimate of financial benefits of GPR was that of Doolittle (1987). While using GPR to aid in soil mapping, he found that GPR decreased cost by 70% and increased productivity by 210%. When considering the efficiency and financial benefits of GPR, it is important to consider the resultant product along with benefits. Is GPR use justified if time and money savings are at the expense of a useable product? When Mokma and Doolittle (1993) reported their time savings with GPR use, they additionally reported that soil maps produced by coring and GPR were in 84% agreement. Although some studies have found GPR to yield an unreliable result without expansive (and expensive) groundtruthing (Doolittle et al. 2000), in most situations where continuity of a subsurface feature is of interest, GPR may indeed provide better results than coring (Collins et al. 1989, Mokma et al. 1990).

For the Juniper Bay comparison, the different core spacing scenarios were chosen intentionally to create a meaningful contrast between the resulting products. The 15 m core spacing matches the spacing of observation points during the actual GPR survey at Juniper Bay. Thus, this variation in the coring proposal would provide the same density of depth information. The coring survey would provide more reliable data, as it does not involve

potential interpretation error, but this reliability requires an extreme time and cost commitment. Even the coring scenario with 60 m spacing would probably be cost and time prohibitive. The coring variation with 300 m spacing was chosen because it could be achieved in approximately the same time as the GPR survey. However, the product of the 300 m coring survey provides a very low density of information compared to the other coring surveys or the GPR survey. Even though the time investment is comparable between the 300 m coring survey and the GPR survey, the cost of the coring survey is nearly 20% greater. Although this comparison of GPR and coring surveys was based on professional proposals and not actual work performed, it does indicate that GPR can provide a large volume of reliable data with a fraction of the time and money required by conventional methods.

SUMMARY AND CONCLUSIONS

The GPR survey at Juniper Bay was successful in revealing the depth and extent of clayey aquitards and in comparing the depth of aquitards with that of drainage ditches. Based on the GPR results, several recommendations could be made for the wetland restoration plans at Juniper Bay. Revised restoration plans may be needed for the southeast corner of the bay that does not seem to posses a shallow aquitard. Certain ditches may need plugged or lined to prevent negative impacts on drainage or hydraulic gradients. A similar GPR assessment could be performed on other drained Carolina Bays and in other areas of the Coastal Plain to determine site suitability for wetland restoration. Based on proposals by professional firms, GPR was shown to provide a large volume of data in a time and cost effective manner. Given the positive results obtained in this study and the efficient

characteristics of GPR surveys, it is suggested that our approach could be valuable in future wetland restoration projects.

REFERENCES

Asmussen, L. E., H. F. Perkins and H. D. Allison. 1986. Subsurface descriptions by ground-penetrating radar for watershed delineation. Bull. 340. The Georgia Agricultural Experiment Stations, The University of Georgia, Athens.

Bennett, S. H. and J. B. Nelson. 1991. Distribution and status of Carolina Bays in South Carolina. Nongame and Heritage Trust Pulication No. 1. SC Wildlife and Marine Resources Dept. Columbia, SC.

Birkhead, A.L., G.L. Heritage, H. White, and A.W. van Niekerk. 1996. Ground-penetrating radar as a tool for mapping the phreatic surface, bedrock profile, and alluvial stratigraphy in the Sabie River, Kruger National Park. J. Soil Water Conserv. 51(3):234-240.

Bliley, D. J. and D. E. Pettry. 1979. Carolina bays on the eastern shore of Virginia. Soil Sci. Soc. Am. J. 43:558-564.

Collins, M. E. and J. A. Doolittle. 1987. Using ground-penetrating radar to study soil microvariability. Soil Sci. Soc. Am. J. 51:491-493.

Collins, M. E., J. A. Doolittle and R. V. Rourke. 1989. Mapping depth to bedrock on a glaciated landscape with ground-penetrating radar. Soil Sci. Soc. Am. J. 53:1806-1812.

Conyers, L. B. and D. Goodman. 1997. Ground-penetrating radar: an introduction for archaeologists. AltaMira Press, Walnut Creek, CA.

Daniels, D. J. 1996. Surface-penetrating radar. Institution of Electrical Engineers, London, UK.

Dominic, D. F., K. Egan, C. Carney, P. J. Wolfe and M. R. Boardman. 1995. Delineation of shallow stratigraphy using ground penetrating radar. J. Appl. Geophys. 33:167-175.

Doolittle, J. A. 1987. Using ground-penetrating radar to increase the quality and efficiency of soil surveys. p. 11-32. *In* W.U. Reybold, and G.W. Peterson (ed.) Soil Survey Techniques, Soil Sci. Soc. Am. Spec. Publ. No. 20.

Doolittle, J. A., G. Hoffmann, P. McDaniel, N. Peterson, B. Gardner and E. Rowan. 2000. Ground-penetrating radar interpretations of a fragipan in northern Idaho. Soil Surv. Horiz. 41(3):73-82.

Frey, D. G. 1950. Carolina Bays in relation to the North Carolina Coastal Plain. J. Elisha Mitchell Sci. Soc. 66:44-52.

Grant, J. A., M. J. Brooks and B. E. Taylor. 1998. New constraints on the evolution of Carolina Bays from ground-penetrating radar. Geomorphology 22:325-345.

Gee, G.W., and J.W. Bauder. 1986. Particle-size analysis. p. 383. In Klute et al. (ed.) Methods of soil analysis. Part 1 Physical and mineralogical methods. ASA, CSSA, and SSSA, Madison, WI.

Hubbard, R. K., L. E. Asmussen and H. F. Perkins. 1990. Use of ground-penetrating radar on upland Coastal Plain soils. J. Soil Water Conserv. 45(3):399-404.

Johnson, D. W. 1942. Nature of the bays. *In* The origin of the Carolina Bays. Columbia University Press, New York, NY.

Kettles, I. M. and S. D. Robinson. 1997. A ground-penetrating radar study of peat landforms in the discontinuous permafrost zone near Fort Simpson, Northwest Territories, Canada. p. 147-160. *In* C.C. Trettin, M.F. Jurgensen, D.F. Grigal, M.R. Gale, and J.K. Jeglum (ed.) Northern forested wetlands: Ecology and management. CRC Lewis Publishers, Boca Raton, FL.

Lapen, D. R., B. J. Moorman and J. S. Price. 1996. Using ground-penetrating radar to delineate subsurface features along a wetland catena. Soil Sci. Soc. Am. J. 60:923-931.

Lide, R. F., V. G. Meentemeyer, J. E. Pinder, III and L. M. Beatty. 1995. Hydrology of a Carolina Bay located on the upper Coastal Plain of western South Carolina. Wetlands 15(1):47-57.

May, J. H. and A. G. Warne. 1999. Hydrogeologic and geochemical factors required for the development of Carolina Bays along the Atlantic Gulf of Mexico Coastal Plain, USA. Environ. Eng. Geosci. 5(3):261-270.

McCachren, C. M. 1978. Soil survey of Robeson County, North Carolina. USDA-SCS, North Carolina Agricultural Experiment Station and Robeson County Board of Commissioners, U.S. Gov. Print. Office, Washington, D.C.

Melton, F.A., and W. Schriever. 1933. The Carolina Bays: are they meteorite scars? J. Geol. 41:52-66.

Mokma, D. L. and J. A. Doolittle. 1993. Mapping some loamy alfisols in southwestern Michigan using ground-penetrating radar. Soil Surv. Horiz. 34(3):71-77.

Mokma, D. L., R. J. Schaetzl, J. A. Doolittle and E. P. Johnson. 1990. Ground-penetrating radar study of ortstein continuity in some Michigan haplaquods. Soil Sci. Soc. Am. J. 54:936-938.

Nobes, D. C., R. J. Ferguson and G. J. Brierley. 2001. Ground-penetrating radar and sedimentological analysis of Holocene floodplains: insight from the Tuross valley, New South Wales. Aust. J. Earth Sci. 48:347-355.

Prouty, W. F. 1952. Carolina Bays and their origin. Geol. Soc. Am. Bull. 63:167-224.

Reese, R. E. and K. K. Moorhead. 1996. Spatial characteristics of soil properties along an elevation gradient in a Carolina Bay wetland. Soil Sci. Soc. Am. J. 60:1273-1277.

Saunders, C. L., III. 1990. Substrate variability and internal sediments of three Carolina Bays, south-central Coastal Plain, North Carolina. M.S. thesis. East Carolina Univ. Greenville, NC.

Sharitz, R. R. 2003. Carolina Bay wetlands: unique habitats of the southeastern United States. Wetlands 23(3):550-562.

Sharitz, R. R. and J.W. Gibbons. 1982. The ecology of southeastern shrub bogs (Pocosins) and Carolina Bays: a community profile. FWS/OBS-82/04. US Fish and Wildlife Service Biological Services Program, Slidell, LA.

Sharitz, R. R. and C.A. Gresham. 1998. Pocosins and Carolina Bays. p. 343-377. *In* M.M. Messina, and W.H. Conner (ed.) Southern forested wetlands, ecology and management. Lewis CRC Press, Boca Raton, FL.

Szuch, R. P., J. G. White, M. J. Vepraskas and J. A. Doolittle. 2004a. Calibration of a large-scale ground-penetrating radar survey: implementation of a lift-test and a calibration equation based on multiple points. Soil Sci. Soc. Am. J. *In review*.

Tomer, M. D., J. Boll, K. -J. S. Kung, T. Steenhius and J. L. Anderson. 1996. Detecting illuvial lamellae in fine sand using ground-penetrating radar. Soil Sci. 161(2):121-129.

Van Dam, R. L and W. Schlager. 2000. Identifying causes of ground-penetrating radar reflections using time-domain reflectometry and sedimentological analyses. Sedimentology 47:435-449.

van Overmeeren, R. A. 1998. Radar facies of unconsolidated sediments in The Netherlands: a radar stratigraphy interpretation method for hydrogeology. J. Appl. Geophys. 40:1-18.

Vogt, K., J. Doolittle, and R. Fenwick. 1996. Mapping the thickness of flood-plain splay deposits with ground-penetrating radar techniques. Soil Surv. Horiz. 37(3):93-100.

Table 1. Classification of soils mapped at Juniper Bay.

Soil Series	Family Taxonomy
Leon	sandy, siliceous, thermic Aeric Alaquods
Rutlege	sandy, siliceous, thermic Typic Humaquepts
Pantego	fine-loamy, siliceous, semiactive, thermic Umbric Paleaquults
Ponzer	loamy, mixed, dysic, thermic Terric Haplosaprists

McCachren, 1978

Table 2. Summary of accuracy in predicting depth to a subsurface interface for various GPR studies. Some studies included data on several interfaces or determined by different methods, and in such cases each result is listed separately. If reported, the distance of GPR survey that included groundtruthing is given. Substrate of the GPR survey site, interface being detected, number of points where predicted and observed depth were compared, correlation/regression results, and average percent error are also given. Percent error is the absolute deviation between observed and predicted divided by the observed depth, on a percent basis. Results are ranked by average percent error. Current study is shown in bold. The row labeled "entire" represents all groundtruthing at Juniper Bay, and the row marked "transect" represents groundtruthing only within fieldlet 12.

Source	Surveyed Distance	Substrate	Interface Detected	Number of Observation Points	Relationship Observed vs. Predicted	Average Percent Error
	----km---					---%---
Collins et al., 1989	0.090	loamy soil	bedrock	61	r = 0.98	4.1†
Birkhead et al., 1996	0.090	sand-gravel bar	bedrock	15	R^2 = 0.85	4.4#
Collins and Doolittle, 1987	0.200	sandy spodosol	argillic horizon	4	na	5.2†
Asmussen et al., 1986 - grid	unknown (2.33 ha)	sandy soil	argillic horizon	8	r = 0.99	7.0‡
Birkhead et al., 1996	0.375	sand-gravel bar	water table	70	R^2 = 0.97	7.9#
Collins and Doolittle, 1987	0.200	sandy spodosol	spodic horizon	4	na	9.1†
Doolittle et al., 2000	0.030	Alfisol	fragipan	21	r = 0.49	9.4‡
Szuch et al. 2004 - transect	0.630	sandy soil	clayey horizon	9	r^2 = 0.80	9.6‡
Lapen et al., 1996	0.500	Bog	various	10	r = 0.99	10.1‡
Vogt et al., 1996	13.800	flood deposits	sediment over soil	25	r^2 = 0.95	10.1†
Szuch et al. 2004 - entire	23.200	various soils	clayey horizon	174	r^2 = 0.62	16.0‡
Asmussen et al., 1986 - transect	1.600	sandy soil	argillic horizon	14	r = 0.95	57.1‡

† = calculated based on average or range of deviation and depth included in source

‡ = calculated based on results at individual observations points included in source (note: This calculation reveals a more accurate and typically higher percent error than when done based on average deviation and depth.)

= reported as percent error in source

Table 3. Classification scheme used to determine the risk that the top of an aquitard has been pierced by a drainage ditch. To determine the appropriate risk category for each point, ditch depths (DD) from the GIS topography map and aquitard depths (AD) from GPR interpretations were compared. The value of 23 cm was used in the determination because this was the average error in the DD measurement and approximated the average error in the GPR interpretations, which was 25 cm.

Risk of ditch having pierced top of aquitard	Formula for determination*
Very low	AD - DD - 46cm
Low	AD - DD - 23cm
Moderate	AD - DD
High	AD - DD + 23cm
Very high	AD - DD + 46cm

*A point falls into risk category if the formula for that category results in a negative value and formula for subsequent categories do not. Risk considered "Very high" if only the "Very high" formula results in a negative value.

Table 4. Results of comparison between GPR survey and coring survey to determine depth of clayey aquitards along all ditches in Juniper Bay. Values are based on proposals by two anonymous consulting firms.

Survey Type	Days to Complete	Cost ($)	Productivity increase with GPR (%)	Cost decrease with GPR (%)
GPR	15	20,488	NA	NA
Coring - 15m spacing	257	391,512	1613	1811
Coring - 60m spacing	68	103,634	353	406
Coring - 300m spacing	16	24,555	7	20

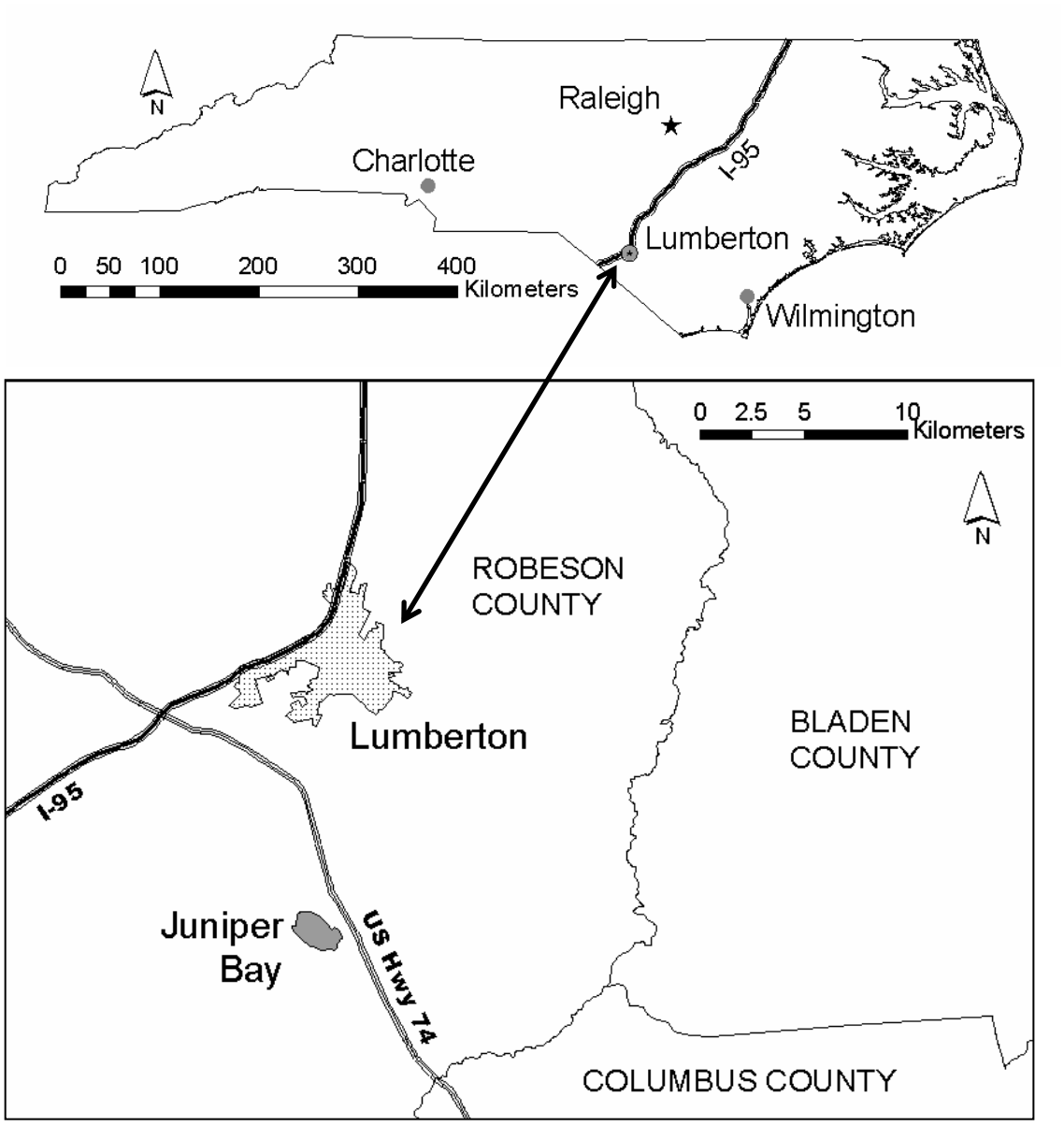

Figure 1. Map of North Carolina and Lumberton area showing location of the Juniper Bay study site. Arrow shows the location of Lumberton on both large and small scale maps.

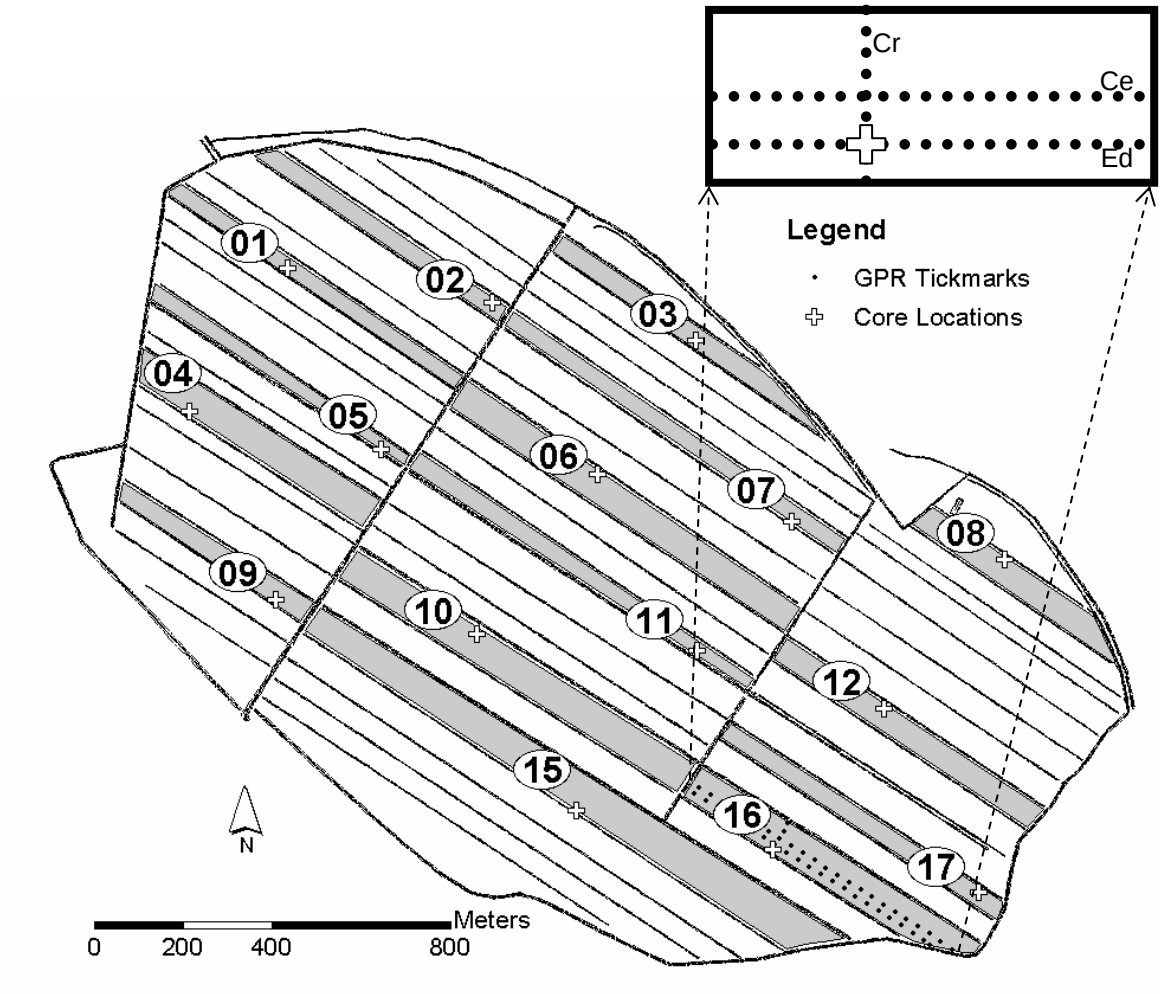

Figure 2. Map of Juniper Bay showing fieldlets where GPR surveys were conducted highlighted in gray and numbered for identification. Location of cores for preliminary survey are shown with bold crosses. In fieldlet 16 and in the blowup diagram, an example of the orientation of the center (Ce), edge (Ed), and cross (Cr) GPR transects is shown along with the location of the core. Each dot represents a tickmark from the GPR transect, located every 30 m.

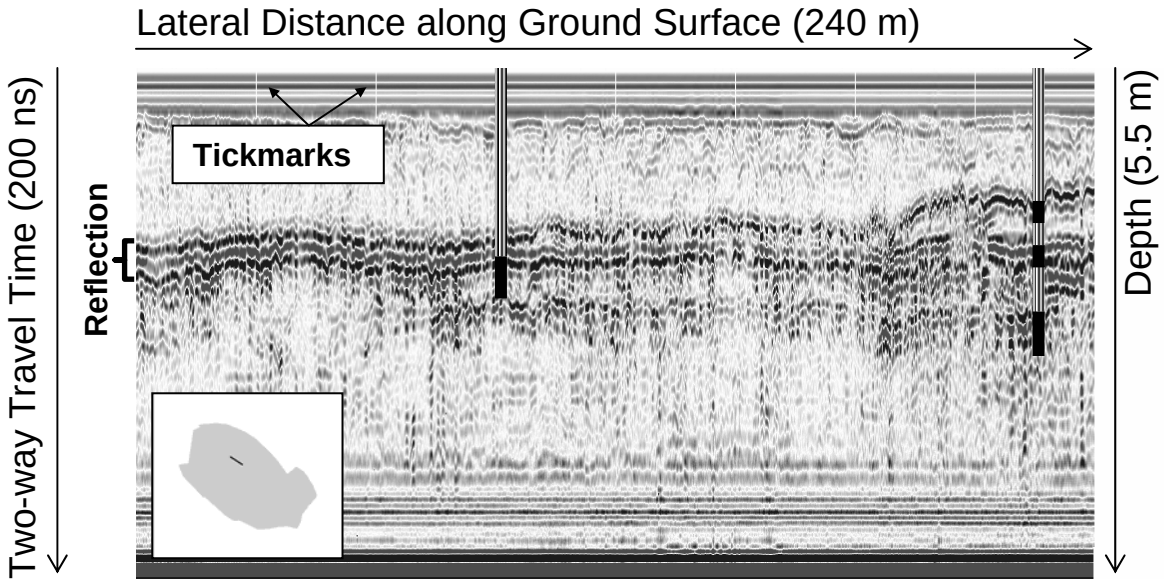

Figure 3. Example of GPR profile from survey at Juniper Bay. Horizontal axis depicts lateral distance along ground surface. Tickmarks were placed by GPR operator in the field and correspond to the location of survey flags every 30 m. Vertical axis originally depicts two-way travel time (left side) and after calibration depicts depth (right side). Multiple bright lines indicate a GPR reflection and are expected to represent a clayey aquitard. A single reflection can be seen on the left side of this profile, and this reflection diverges into multiple, overlying reflections toward the right side. The reflection pattern was confirmed by coring. Vertical bars along the profile represent core locations. Black areas of bars indicate clayey texture, and vertically cross-hatched areas of bars indicate sandy texture. The location of this profile within Juniper Bay is indicated by the black line on the diagram in the bottom left corner.

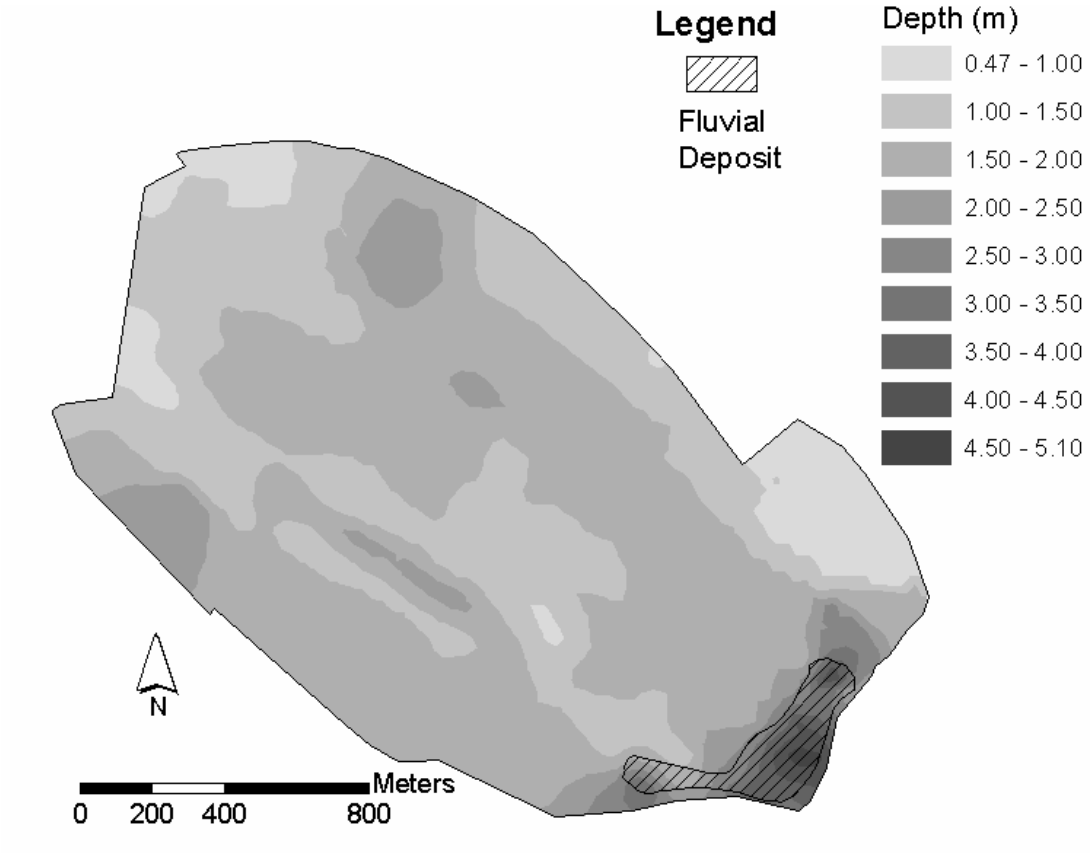

Figure 4. Interpolation map of depth to shallowest aquitard within Juniper Bay, based on GPR interpretation and created with ArcGIS - Geostatistical Analyst. Semivariogram used for interpolation had range of 1000 m, sill of 0.409 m^2, and nugget of 0.079 m^2. Map also displays the location and extent of GPR anomaly in southeast corner that appeared to be a fluvial deposit.

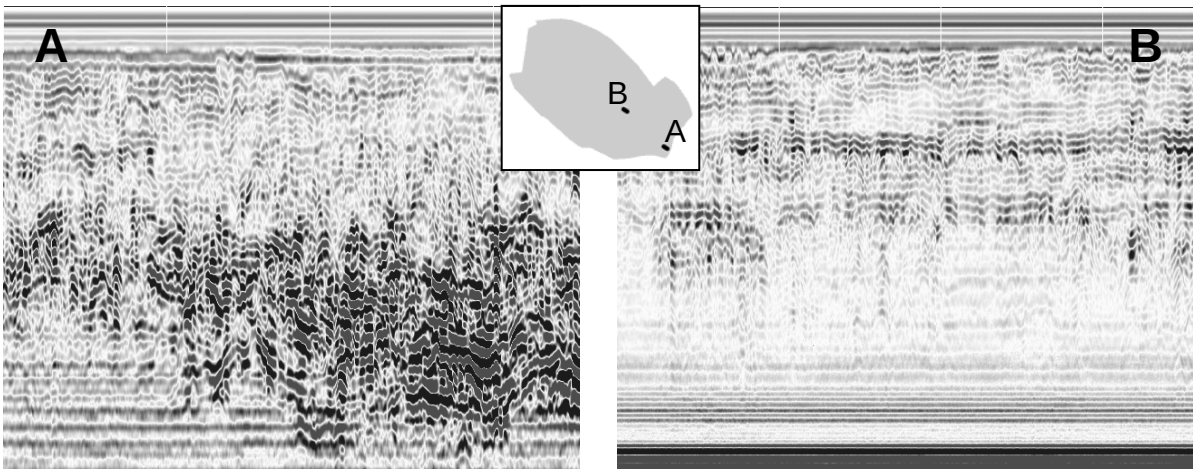

Figure 5. GPR profiles from Juniper Bay illustrating two different radar facies. Profile (A) is from the anomalous area in the southeast of Juniper Bay that appears to be a fluvial deposit. The reflections are intense and chaotic in this profile. Profile (B) is typical of the remainder of Juniper bay and appears to be a lacustrine deposit. The brighter reflections are continuous, sub-parallel, and nearly horizontal. These bright reflections bound areas of the profile that are pale and lack prominent reflections.

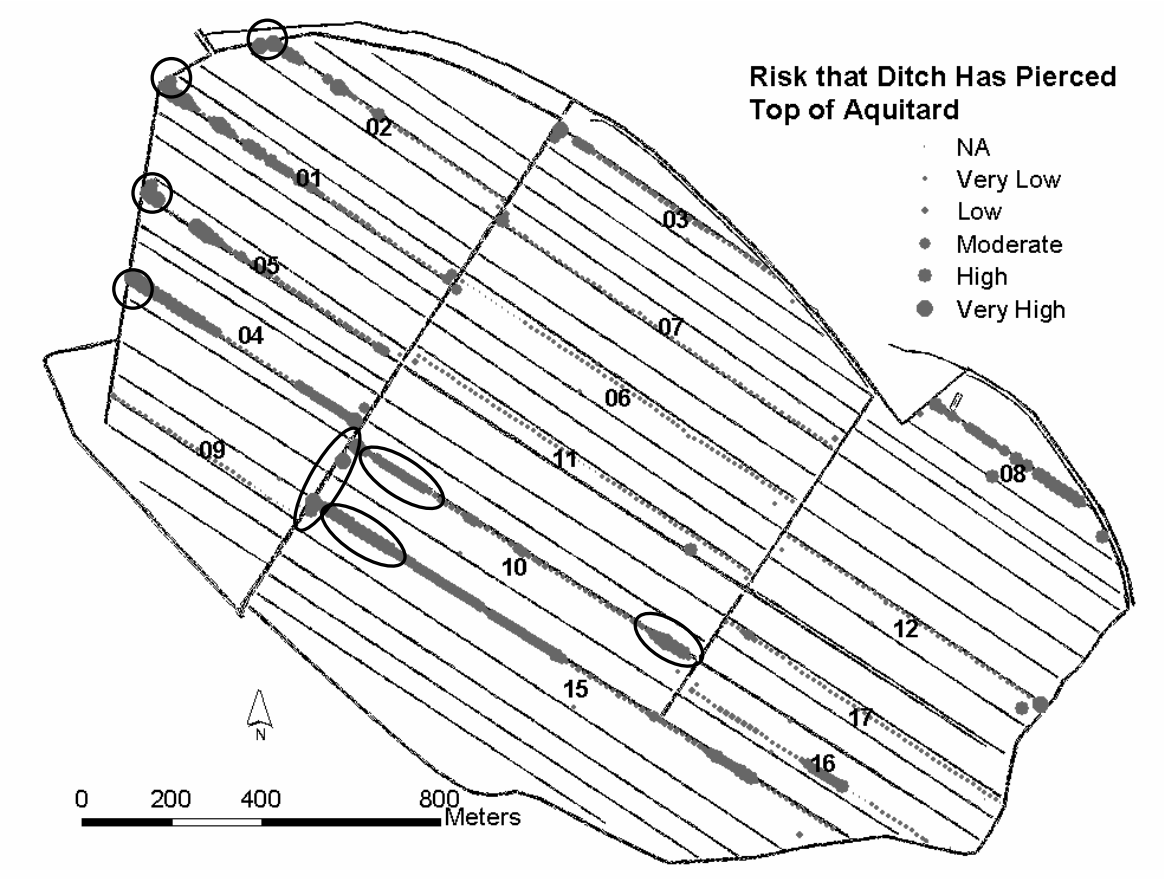

Figure 6. Map of Juniper Bay displaying the risk that the top of an aquitard has been pierced by a drainage ditch. Size of points are based upon the classification scheme presented in Table 3. Each point represents an observation point where the depth to a clayey aquitard was determined via GPR interpretation. Explanation of ranking scheme is given in Table 3. Identification numbers of fieldlets are shown, as in Figure 2. Ditches within ovals and circles are suspected to have pierced entirely through aquitards based on confirmation with coring records.

APPENDICES

APPENDIX A

Additional Interpolation Map Based on Coring

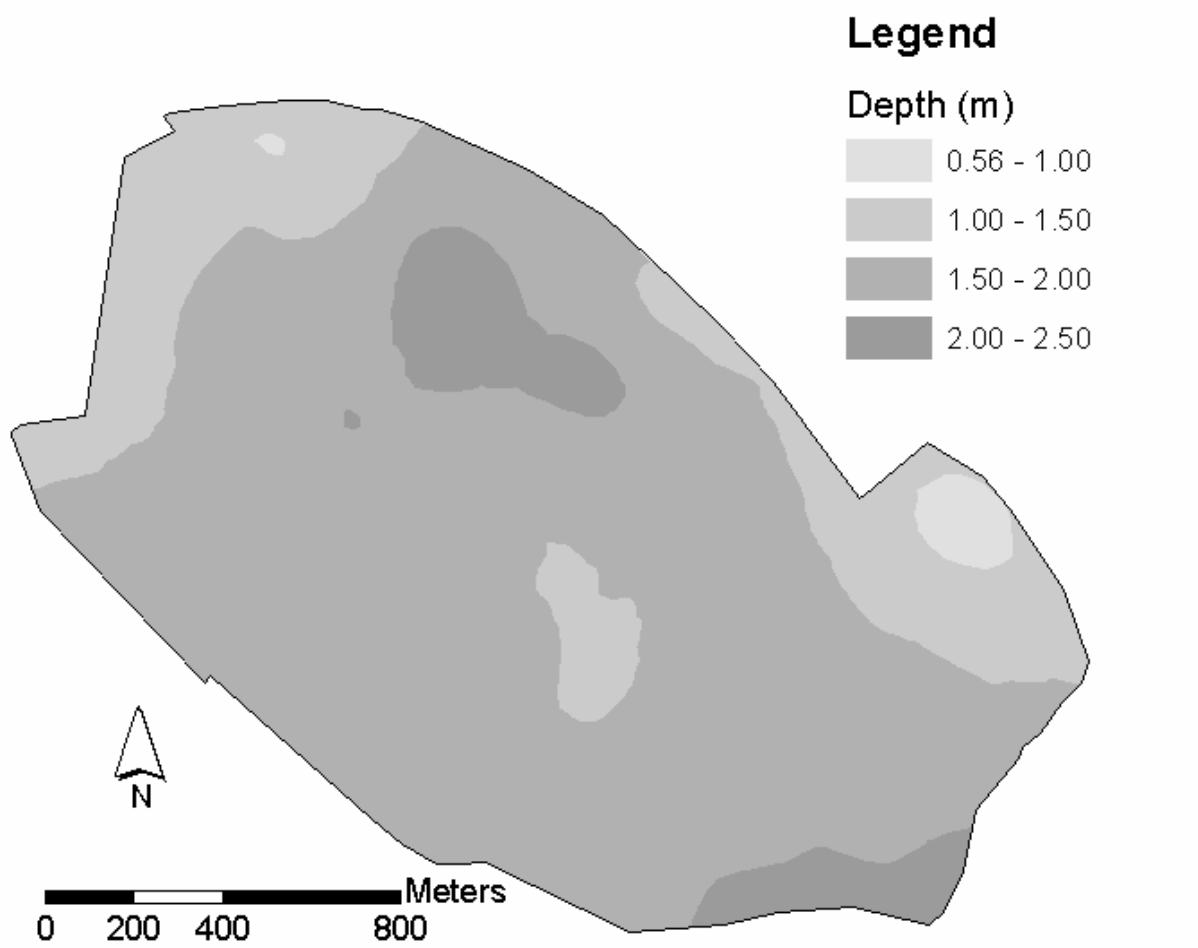

Figure A. Interpolation map of depth to shallowest aquitard within Juniper Bay, based on coring and created with ArcGIS - Geostatistical Analyst. Semivariogram used for interpolation had range of 777 m, sill of 0.264 m^2, and nugget of 0.115 m^2.

APPENDIX B

Information on Soil Texture above and below Interfaces Detected by GPR

Table B1. Summary statistics based on all texture data collected in Juniper Bay. Based on these percentages the average soil texture was a sandy loam.

Separate	% Sand	% Silt	% Clay
Average	69.27	11.93	18.90
Minimum	10.86	0.00	2.50
Maximum	95.00	48.74	62.98

Table B2. Summary statitistics for layers above and below an interface. Based on these percentages the average soil texture above and below an interface was loamy sand and sandy clay loam, respectively.

	Separate	% Sand	% Silt	% Clay
ABOVE	Average	83.99	6.25	10.03
	Minimum	62.77	0.00	2.50
	Maximum	95.00	25.00	17.50
BELOW	Average	59.37	15.07	25.57
	Minimum	19.48	0.00	8.25
	Maximum	89.33	38.09	56.40

Table B3. Summary statitistics for difference between layers above and below an interface. A positive value indicates an increase from above to below. A negative value indicates a decrease from above to below.

	Difference % Sand	Difference % Silt	Difference % Clay
Average	-24.62	8.82	15.54
Minimum	-68.95	-23.40	2.91
Maximum	-2.50	28.87	44.34

Table B4. Summary statitistics for difference between layers above and below interfaces in fieldlet 12 only. A positive value indicates an increase from above to below. A negative value indicates a decrease from above to below.

	Difference % Sand	Difference % Silt	Difference % Clay
Average	-28.35	9.94	18.41
Minimum	-40.83	4.24	4.25
Maximum	-13.35	17.13	26.41